Addis Ababa University

School of Graduate Studies

Faculty of Technology

Chemical Engineering Department

TWO DIMENSIONAL CONSERVATIVE CONTAMINANT TRANSPORT MODELING OF THE AKAKI WELLFIELD

By

Jemal Seid

November-2009

Addis Ababa-Ethiopia

Addis Ababa University

School Of Graduate Studies

Faculty of Technology

Chemical Engineering Department

TWO DIMENSIONAL CONSERVATIVE CONTAMINANT TRANSPORT MODELING OF THE AKAKI WELLFIELD

By

Jemal Seid

Approved by Board of Examiners

_____	_____	_____
Chairman, Department Graduation Committee	Signature	Date
_____	_____	_____
Advisor	Signature	Date
_____	_____	_____
Examiner	Signature	Date

Declaration

I, the under signed, declare that this thesis is my own work and that all sources of material used for the thesis have been dully acknowledged.

_____ _____

Jemal Seid Date

This is to certify that the above declaration made by the candidate is correct to the best of my knowledge.

_____ _____

Advisor Date

Two-Dimensional Conservative Contaminant Transport Modeling of the Akaki Wellfield

By: Jemal Seid

A Thesis Submitted to the School of Graduate Studies of Addis Ababa University in Partial Fulfillment of the Requirements for the Degree of Master of Science in Environmental Engineering

Nov, 2009

Acknowledgements

I am deeply grateful to Addis Ababa Water & Sewerage Authority (AAWSA) staff members Ato Yirga Tadesse and Ato Zeleke Teferi who provided & helped me with the necessary information, data, as well as laboratory set up, with out which the accomplishment of this thesis work would be unsuccessful.

Acknowledgements are also due to my advisor Ato Teshome Worku who arranged me in reaching the relevant institutions through official letters & guided me on how to proceed through out my work. I thank also the Chemical Engineering Department of faculty of technology for facilitating this process.

Gratitude also goes to W/t Esete Berhanu who had taken part in writing the manuscripts of parts of this thesis work.

Jemal S.

Addis Ababa, Ethiopia.

Abstract

This thesis work focuses on non-reactive solute transport modeling of the akaki wellfield for two selected groundwater contaminants (chloride & fluoride) for the 25 operating boreholes administered by Addis Ababa Water & Sewerage Authority (AAWSA). The work is conducted based on laboratory analysis of groundwater samples from selected boreholes and based on historical data of the wellfield boreholes.

The widespread use of chemical products, coupled with the disposal of large volumes of waste materials, poses the potential for widely distributed groundwater contamination. Because such contaminations can pose a serious threat to public health, prediction of the degree of contamination by appropriate numerical modeling tools is vital to aware the end user from possible risks. *Mathematical models solved numerically are the subject of this thesis work focusing on conservative solute transport in the Akaki well field.*

Chloride & fluoride ions predictive modeling of the wellfield for the next ten years (2007-2017) is made first by calibrating the model input parameters using the available historical solute concentration data for selected boreholes at various periods. For calibration purpose, initial solute concentration was taken as 3 mg/l for chloride and 0.51 mg/l for fluoride and MATLAB simulation of chloride & fluoride ion concentration is done.

The simulation results show that while chloride concentrations in the wellfield get increased; fluoride, however, is getting decreasing through out all of the boreholes in the wellfield. This is in agreement with the actual observed pattern of solute load of the wellfield revealing chloride is being introduced in to the wellfield by one or more mechanisms somewhere in the vicinity of the akaki river catchment (ARC) while fluoride is not.

Keywords: *aquifers, breakthrough curves, initial conditions, boundary conditions, calibration, prediction, conservative contaminant transport, hydraulic conductivity, porosity.*

Table of Contents

List of Tables

List of Figures

Acronyms & Abbreviations

AAU:	Addis Ababa University
AAWSA:	Addis Ababa Water and Sewerage Authority
ARC:	Akaki River Catchment
ASL:	Above Sea Level
AWF:	Akaki Well Field
BAR:	Big Akaki River
BC:	Boundary Conditions
BH:	Bore Hole
CC:	Conservative Contaminant
Cend:	Concentration at the end of June 2017
Fig:	Figure
LAR:	Little Akaki River
MATLAB:	Matrix Laboratory
PMWIN:	Processing Modflow
SSM:	Steady-State Models
WHO:	World Health Organization
WSS:	Water Supply and Sanitation

1. Introduction

Provision of safe and sufficient water supply and adequate sanitation services are indispensable components in the sustainable development of Ethiopia's urban and rural socio-economic well-being. At present, most of the population does not have adequate and safe access to water supply and sanitation (WSS) facilities. As a result, over 70% of the contagious diseases in the country are water borne/based diseases. Source of most of these diseases could be traced back to inadequate WSS facilities. Providing access to clean and adequate WSS facilities and improving the performance of this sub-sector directly reduces the morbidity and mortality rates of the population.

More than 25 towns and cities in Ethiopia are obtaining their potable water from groundwater source (boreholes). Few of the major groundwater based towns and cities are shown in Table 1.1 below.

Table 1.1 Towns & Cities in Ethiopia Supplied from Groundwater [10]

Towns	Major Rocks
Addis Ababa (Partially)	Volcanic Rocks
Combolcha	Alluvial Deposits
Debre Zeit	Volcanic Rocks
Mojo	Volcanic Rocks
Mekele	Dolerites within Mesozoic Sedimentary Rocks
Dire Dawa	Mesozoic Sandstones
Debre Markos	Volcanic Rocks
Dessie	Alluvial Deposits
Gonder	Volcanic Rocks
Bichena	Volcanic Rocks
Assaita	Volcanic Rocks
Butajira	Alluvial Deposits & Volcanic Rocks
Welkite	Volcanic Rocks
Harar (Dire Jara)	Mesozoic Sedimentary rocks alluvial deposits and Volcanic Rocks
Logia & Semera	Alluvial Sediments

The reliable assessment of hazards or risks arising from groundwater contamination problems and the design of efficient and effective techniques to mitigate them require the

capability to predict the behavior of chemical contaminants in flowing groundwater. *Reliable and quantitative predictions of contaminant movement can be made only if we understand the processes controlling transport, hydrodynamic dispersion, and chemical, physical, and biological reactions that affect soluble concentrations in the ground*.

The widespread use of chemical products, coupled with the disposal of large volumes of waste materials, poses the potential for widely distributed groundwater contamination. New instances of groundwater contamination are continually being recognized. Hazardous chemicals, e.g., pesticides, herbicides, and solvents, are used ubiquitously in everyday life. These and a host of other chemicals are in widespread use in urban, industrial, and agricultural settings. Whether intentionally disposed of, accidentally spilled, or applied to the ground for agricultural reasons, some of these chemicals can eventually reach the groundwater and contaminate it. Because of the volumes of toxic wastes and because of their stability in groundwater, such contamination can pose a serious threat to public health.

Groundwater is the subsurface transporting agent for dissolved chemicals including contaminants. Materials dissolved from the wastes may be transported from the burial or disposal site by groundwater flow, with the result that the quality of water from wells is reduced by the contaminated groundwater. In addition, natural discharges of an aquifer, such as at springs and seeps, can return a contaminant to the surface. Because of the slow rates of groundwater movement and natural flushing of aquifers, when areas are contaminated, they commonly remain so for decades or longer. The major geophysical inputs to the problems of waste disposal and groundwater contamination deal with the chemistry and rates and directions of contaminant transport.

Groundwater & contaminant transport modeling is one of the main tools used in the hydrogeological sciences for the assessment of the resource potential and prediction of future impact under different circumstances/stresses. Its predictive capacity makes it the most useful tool for planning, design, implementation and management of the groundwater resources. Although it has been widely used by developed countries

since the 1970's, its importance and application was not well understood in Ethiopia until the 1990's. This conservative contaminant transport modeling study of the Akaki well field is first of its kind and is aimed at predicting potential contaminant concentration of selected species at the available wells in the Akaki area supplying water for the city of Addis Ababa.

1.1 Background

Akaki well field is situated to the southeast of Akaki town about 22 km south of the centre of Addis Ababa (shown in Fig 1.1). The name Akaki is taken from the sub-city situated close to the well field and from the name of the river that drains Addis Ababa City. The well field covers an area of about 16-km^2 and comprises 25 production wells and four monitoring wells (See Fig 1.2). All the 25 production wells are situated to the south of the main Addis Ababa -Djibouti highway.

The aquifers in the well field area are mainly from *young volcanic rocks* largely made of scoria, and fractured vesicular basalts with little to no weathering. The aquifer is largely due to processes related to lava flow and tectonic fractures. The aquifer to the north of the well field mainly covering the city of Addis Ababa and in the mountains north of the city are largely due to weathered and fractured volcanic rock with minor sediments deposited between different series of lava flows.

The main groundwater movement is *from north to south in the central and northern part* of the Akaki River Catchment (ARC) and *towards the southeast direction in the lower part of the Catchment*. The potentiometer surface indicates that the groundwater is in connection with Akaki River about 5 km to the north of the well field. The base flow of Akaki River and its tributaries is mainly contributed from the groundwater. The recharge to the groundwater that takes place within Akaki River Catchment is considered contributing to the base flow.

Out of the 25 wells available in the area, 11 boreholes were planned for first phase

development (for a production of about 72,000m^3) and the remaining 14 were planned for the second phase development for about 50,000 m^3/day, in total 125,000 m^3/day. However, before implementing the project, Addis Ababa Water and Sewerage Authority (AAWSA) decided to conduct *groundwater modeling* for assessing the potential of the aquifer and predict the sustainable pumping rate from the aquifer. Therefore, Akaki groundwater was modeled using *Processing Modflow (PMWIN)* software developed by W.-H. Chiang & W. Kinzelbach. The first modeling was done in year 2000. Phase I boreholes commenced pumping following the recommendation from the modeling result. The year 2000 model result was revised in year 2002 by taking into account additional investigation results and the results from pumping of Phase I boreholes.

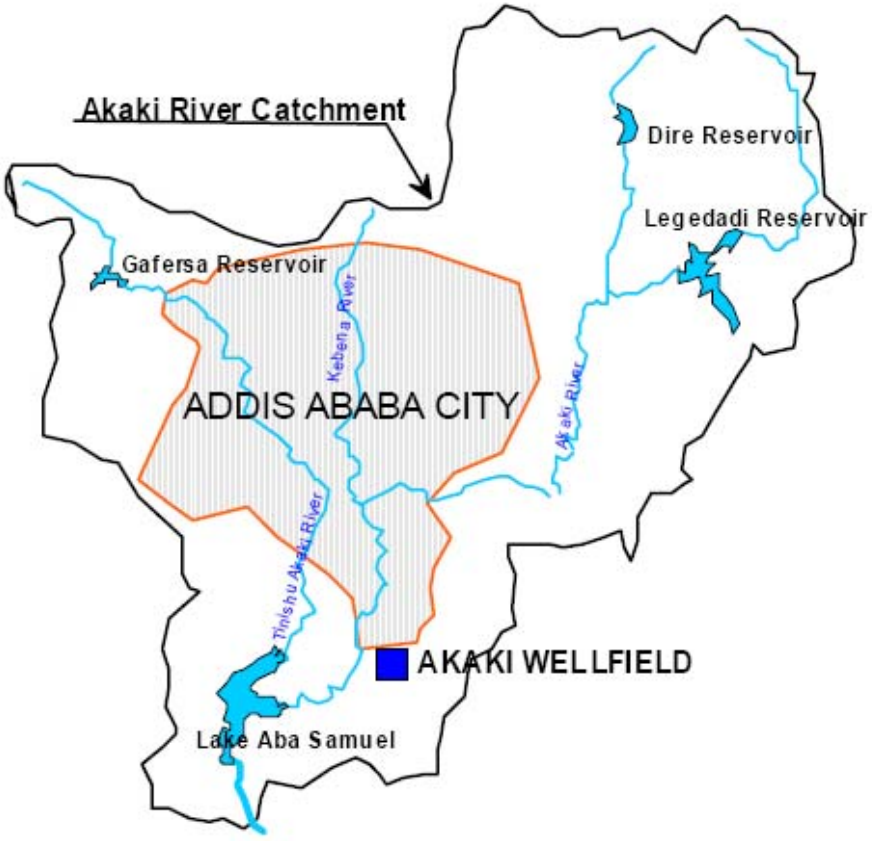

Fig 1.1 Location of Akaki Well Field

The well field based on test pumping data and recharge estimation was initially expected to yield about 125,000 m^3/day. However, groundwater modeling results indicated its

potential abstraction rate is in the order of 30, 000 m^3/day.

Akaki well field is a good example for the application of groundwater models in groundwater resources development and management. Groundwater modeling is a good tool to estimate the resource and predict impacts for development of large abstractions, such as cities, towns' water supply and groundwater based irrigation schemes. It also helps to avoid unnecessary investment on the resource.

Fig 1.2 Akaki Well Field Site

1.2 Problem Statement

The widespread use of chemical products, coupled with the disposal of large volumes of waste materials, poses the potential for widely distributed groundwater contamination. Hazardous chemicals, e.g., pesticides, herbicides, and solvents, are used ubiquitously in everyday life. These and a host of other chemicals are in widespread use in urban, industrial, and agricultural settings.

Figures 1.3 & 1.4 show contaminated Akaki & Kebena Rivers respectively which are feeders to the Akaki well field posing serious risk for the city water supply.

Fig 1.3 Chemically Polluted Little Akaki River

Fig 1.4 Organic Pollution in Kebena River

Because such contaminations can pose a serious threat to public health, *prediction of the degree of contamination by appropriate numerical modeling tools will be vital to aware the end user from possible risks.*

The challenges are:

(1) To prevent the introduction of contaminants in an aquifer,

(2) To predict their movement if they are introduced, and

(3) To remove them, to the extent possible, to protect the biosphere effectively.

The largest potential source of contamination of groundwater is the disposal of solid and liquid wastes. Waste disposal is not the only source of groundwater contamination. Additional sources include septic systems, agriculture, accidental leaks and spills, mining, highway de-icing, artificial recharge, underground injection, and saltwater encroachment.

Among the impacts from groundwater contamination includes:

Impacts from industrial effluents:

1. Disposal of sulphide containing chemicals could increase soil acidity that can facilitate mobilization of heavy metals that causes cancer and abortion.
2. Disposal of lime containing effluents increases soil alkalinity that in turn binds heavy

metals into soil by reducing agricultural production.

3. Drastically change the quality of both surface and groundwater.

Bacterial effect:

Bacterial pathogens cause some of the well-known and most feared infectious diseases such as cholera, typhoid, and dysentery. The symptoms tend to be severe and the control of such pathogens was the original target in sanitary improvement. For the detected bacteria the main source is human and animal faeces. Table 1.2 shows bacterial population of the Akaki well field.

Table 1.2 Bacterial Population of the Well Field. [17]

BH Date	Tot. Coliform/100ml	E. Coli/100ml
BH6 23-12-04	16	16
EP4 23-12-04	1	1
BH6 13-01-04	89	89
BH14 23-12-04	1	1
BH12 23-12-04	1	1

Several ground-burial disposal practices and repositories have been in use for many years and have been shown to cause minimal or no groundwater contamination. However, some waste-disposal practices have resulted in irreversible contamination of groundwater.

Restoration of contaminated aquifers can be extremely expensive. This may involve drilling many wells and pumping vast quantities of groundwater. The pumped water can often be treated, to reduce the concentration of contaminants, and re-injected into the aquifer.

1.3 Objective of the Study

1.3.1 General Objective

The purpose for the initial groundwater modeling program (in my previous study during project work) was to better understand how groundwater flow in the site area related to

regional groundwater flow and to understand the resulting potential for dissolved phase contaminant transport in the groundwater flow regime.

With additional site characterization work done after the initial modeling, the purpose of this 2-D model is to refine our understanding of groundwater flow and contaminant transport in the site vicinity. *The general objective of this study is, thus, to present a prediction model aimed at quantifying a selected contaminant concentration in the groundwater system of the Akaki well field.*

1.3.2 Specific Objective

The specific objective included incorporating the additional site characterization data generated since completion of the initial model to describe a two dimensional spatial & temporal simulation of a selected conservative contaminant transport in the groundwater system of the Akaki well field.

The selected conservative contaminants for this study are the stable halogen ions; chloride and fluoride. Because these ions are the first to reach a given groundwater regime in case of contamination (attributed to their conservative nature), they can be used for pollution indicators. *Prediction of concentration of these ions at the various boreholes of the well field is to be made using a software package MATLAB* so that issue of a possibility of well field contamination (if any) could be raised for decision making on well field mitigation or remediation program.

1.4 Scope & Limitations of the Study

This study of contaminant transport modeling of the Akaki well field is subject to the following conditions:

- ✓ A conservative (no reactive) contaminant (CC) is selected for modeling.
- ✓ Advective, dispersive & adsorptive contaminant transport processes are considered.
- ✓ Data collection is an essential part of modeling the behavior of a site. Collecting

the data required by existing models is difficult and expensive.

- ✓ Usually, difficulty arises in comparing the results of modeling to results obtained in the field.
- ✓ Lack of adequate historical data.

1.5 Significance of the Study

Mathematical models have a potentially useful role to play in arriving at a decision on the remedial action to be taken at a contaminated site. Where there is a need for a quantitative estimate of the threat to public health resulting from a particular course of action, of the estimated cost and time of clean-up for a particular remediation strategy, or of the results of other actions to be taken at a contaminated site, *mathematical models have a greater potential to provide the needed information than any other approach to the problem.*

The model will predict concentrations of conservative ions of chloride & fluoride in the wellfield for the coming 10 years (up to 2017 E.C). Based on the standard concentrations of these ions set for human health, the predicted concentrations of these ions, distributed spatially, could be used to signal the potential of contamination of the wellfield and its vulnerability.

2. Literature Review

2.1 Groundwater and Aquifers

Groundwater is contained in geological formations, called *aquifers,* which are sufficiently permeable to transmit and yield water. Sands and gravels, which are found in alluvial deposits, dunes, coastal plains, and glacial deposits, are the most common aquifer materials. The more porous the material, the higher yielding it is as an aquifer material. Sandstone, limestone with solution channels, and other karst formations are also good aquifer materials. In general, igneous and metamorphic rocks do not make good aquifers unless they are sufficiently fractured and porous. [22]

The two main types are *confined aquifers* and *unconfined aquifers.* A confined aquifer is a layer of water-bearing material overlaid by a relatively impervious material. If the confining layer is essentially impermeable, it is called an *aquiclude.* If it is permeable enough to transmit water vertically from or to the confined aquifer, but not in a horizontal direction, it is called an *aquitard.* An aquifer bound by one or two aquitards is called a *leaky* or *semi confined aquifer.*

Confined aquifers are completely filled with groundwater under greater-than-atmospheric pressure and therefore do not have a *free water table.* The pressure condition in a confined aquifer is characterized by a *piezometric surface,* which is the surface obtained by connecting equilibrium water levels in tubes or piezometers penetrating the confined layer.

An unconfined aquifer is a layer of water-bearing material without a confining layer at the top of the groundwater, called the *groundwater table,* where the pressure is equal to atmospheric pressure. The groundwater table, sometimes called the *free* or *phreatic surface,* is free to rise or fall. The groundwater table height corresponds to the equilibrium water level in a well penetrating the aquifer. Above the water table is the vadose zone, where water pressures are less than atmospheric pressure. The soil in the vadose zone is partially saturated, and the air is usually continuous down to the unconfined aquifer.

Physical Properties of Water

The density of a material is defined as the mass per unit volume. The density (ρ) of water varies with temperature, pressure, and the concentration of dissolved materials and is about 1000 kg/m^3. Multiplying ρ by the acceleration of gravity (g) gives the specific weight (γ) as $\gamma = \rho g$. For water, $\gamma \approx 9.8$ kN/m^3.

Some of the physical properties of water are defined as follows:

DYNAMIC VISCOSITY (μ)—The ratio of shear stress (τ_{yx}) in x direction, acting on an x–y plane to velocity gradient (dv_x/dy); $\tau_{yx} = \mu\, dv_x/dy$. For water, $\mu = 10^{-3}$ kg/m^2 s.

KINEMATIC VISCOSITY (ν)—Related to μ by $\nu = \mu/\rho$. Its value is about 10^{-6} m^2/s for water.

COMPRESSIBILITY (β)—The ratio of change in density caused by change in pressure to the original density:

$\beta = (1/\rho)\,(d\rho/dp) = (-1/v)\,(dv/dp)$

$\beta \approx 0.5 \times 10^{-9}$ m^2/N, for water. [22]

Physical Properties of Aquifers

As stated before, an aquifer serves as an underground storage reservoir for water. It also acts as a conduit through which water is transmitted and flows from a higher level to a lower level of energy. An aquifer is characterized by the three physical properties: *hydraulic conductivity, transmissivity, and storativity.*

Hydraulic Conductivity

Hydraulic conductivity, analogous to electric or thermal conductivity, is a physical measure of how readily an aquifer material (soil) transmits water through it. Mathematically, it is the proportionality between the rate of flow and the energy gradient causing that flow as expressed in the following equation. Therefore, it depends on the properties of the aquifer material (porous medium) and the fluid flowing through it.

$$K = k(\frac{\gamma}{\mu}) \qquad (2.1.1)$$

where:

K = hydraulic conductivity (called the coefficient of permeability in soil mechanics)

k = intrinsic permeability

γ = specific weight of fluid

μ = dynamic viscosity of fluid

For a given fluid under a constant temperature and pressure, the hydraulic conductivity is a function of the properties of the aquifer material, that is, how permeable the soil is.

Transmissivity

Transmissivity is the physical measure of the ability of an aquifer of a known dimension to transmit water through it. In an aquifer of uniform thickness d, the transmissivity T is expressed as

$$T = \overline{K}d \tag{2.1.2}$$

where

$\overline{K}$ represents an average hydraulic conductivity.

Storativity

Storativity, also known as the *coefficient of storage* or *specific yield,* is the volume of water yielded or released per unit horizontal area per unit drop of the water table in an unconfined aquifer or per unit drop of the piezometric surface in a confined aquifer. Storativity S is expressed as

$$S = (\frac{1}{A})(\frac{dQ}{dq}) \tag{2.1.3}$$

where:

dQ = volume of water released or restored

$d\phi$ = change of water table or piezometric surface

Thus, if an unconfined aquifer releases 2 m^3 water as a result of dropping the water table by 2m over a horizontal area of 10 m^2, the storativity is 0.1 or 10%.

2.2 Groundwater Flow

The flow of water through a body of soil is a complex phenomenon. A body of soil constitutes a solid matrix and pores. For simplicity, assume that all pores are interconnected and the soil body has a uniform distribution of phases throughout. To find the law governing groundwater flow, the phenomenon is described in terms of average velocities, average flow paths, average flow discharge, and pressure distribution across a given area of soil.

The theory of groundwater flow originates with *Henry Darcy* who published the results of his experimental work in 1856. He found that the total discharge Q was proportional to cross-sectional area A, inversely proportional to the length Δs, and proportional to the head difference $\phi_1 - \phi_2$ as expressed mathematically in the form:

$$Q = KA\frac{(\phi_1 - \phi_2)}{\Delta S} \tag{2.2.1}$$

where K is the proportionality constant representing hydraulic conductivity. This equation is known as Darcy's equation. The quantity Q/A is called *specific discharge* q. If $\phi_1 - \phi_2 = \Delta\phi$ and $\Delta s \rightarrow 0$, Equation 2.2.1 becomes:

$$Q = -K(\frac{d\phi}{dS}) \tag{2.2.2}$$

This equation states that the specific discharge is directly proportional to the derivative of the head in the direction of flow (*hydraulic gradient*). The specific discharge is also known as *Darcy's velocity*. Note that q is not the actual flow velocity (seepage velocity) because the flow is limited to pore space only. The seepage velocity v is then

$$V = \frac{Q}{nA} = \frac{q}{n} \tag{2.2.3}$$

where n is the porosity of the soil. Note that v is always larger than q. [22]

Intrinsic Permeability

The hydraulic conductivity K is a material constant, and it depends not only on the type of soil but also on the type of fluid (dynamic viscosity, μ) percolating through it. The hydraulic conductivity K is expressed as in equation (2.1.1).

$$K = k(\frac{\gamma}{\mu}) \tag{2.2.4}$$

where k is called the *intrinsic permeability* and is now a property of the soil only.

Values of hydraulic conductivity can be obtained from empirical formulas, laboratory experiments, or field tests. Table 2.1 gives the typical values for various aquifer materials.

Table 2.1 The Order of Magnitude of the Permeability of Natural Soils. [22]

Type of Soil	k (m^2)	K (m/s)
Clay	10^{-17} to 10^{-15}	10^{-10} to 10^{-8}
Silt	10^{-15} to 10^{-13}	10^{-8} to 10^{-6}
Sand	10^{-12} to 10^{-10}	10^{-5} to 10^{-3}
Gravel	10^{-9} to 10^{-8}	10^{-2} to 10^{-1}

Validity of Darcy's Law

Darcy's law is restricted to a specific discharge less than a certain critical value and is valid only within a laminar flow condition, which is expressed by Reynolds number Re defined as:

$$\mathrm{Re} = \frac{qD_{\rho}}{\mu} \tag{2.2.5}$$

Experiments have shown the range of validity of Darcy's law to be $\mathrm{Re} \leq 1 \sim 10$

In practice, the specific discharge is always small enough for Darcy's law to be applicable. Only cases of flow through coarse materials, such as gravel, deviate from Darcy's law. Darcy's law is not valid for flow through extremely fine-grained soils, such as colloidal clays.

Generalization of Darcy's Law

In practice, flow is seldom one dimensional, and the magnitude of the hydraulic gradient is usually unknown. The simple form, Equation 2.2.1, of Darcy's law is not suitable for solving problems. A generalized form must be used, assuming the hydraulic conductivity K to be the same in all directions (isotropic soil), as:

$$q_x = -K(\frac{\partial \phi}{\partial x}) \quad (2.2.6\ (a))$$

$$q_y = -K(\frac{\partial \phi}{\partial y}) \quad (2.2.6\ (b))$$

$$q_z = -K(\frac{\partial \phi}{\partial z}) \quad (2.2.6\ (c))$$

Equation of Continuity

Darcy's law furnishes three equations of motion for four unknowns (q_x, q_y, q_z, and ϕ). A fourth equation notes that the flow phenomenon must satisfy the fundamental physical principle of conservation of mass. When an elementary block of soil is filled with water no mass can be gained or lost regardless of the pattern of flow.

The conservation principal requires that the sum of the three quantities (the mass flow) is zero, hence when divided by $\Delta x \,.\, \Delta y \,.\, \Delta z$, and for constant density:

$$\frac{\partial q_x}{\partial x} + \frac{\partial q_y}{\partial y} + \frac{\partial q_z}{\partial z} = 0 \quad (2.2.7)$$

Equation 2.2.7 is the *equation of continuity*.

Fundamental Equations

Darcy's law and the continuity equation provide four equations for the four unknowns. Substituting Darcy's law Equation 2.2.6 into the equation of continuity Equation 2.2.7 yield:

$$\frac{\partial^2 \phi}{\partial x^2} + \frac{\partial^2 \phi}{\partial y^2} + \frac{\partial^2 \phi}{\partial z^2} = 0 \quad \text{or } \nabla^2 \phi = 0 \quad (2.2.8)$$

Which is the *Laplace's equation* in three dimensions. [22]

2.3 Sources of Groundwater Pollution

A groundwater contaminant is defined by most regulatory agencies as any physical, chemical, biological, or radiological substance or matter in groundwater. The contaminants can be introduced in the groundwater by naturally occurring activities, such as natural leaching of the soil and mixing with other groundwater sources having different chemistry. They are also introduced by planned human activities, such as waste disposal, mining, and agricultural operations.

Almost every major industrial and agricultural site has in the past disposed of its wastes on site, often in an inconspicuous location on the property. Every municipality has had to dispose of its waste at selected locations within its proximity. Accidental spills of toxic chemicals have also occurred, often without particular attention to or concern for the consequences—some practices of cleaning a toxic spill involve flushing it with water until it disappears into the ground. Past waste-disposal practices and dealing with spills have not always considered the potential for groundwater contamination.

Groundwater contamination, as shown in Figure 2.1, may be localized or spread over a large area, depending on the nature and source of the pollutant and on the nature of the groundwater system. A problem of growing concern is the cumulative impact of contamination of a regional aquifer from non-point sources (i.e., those that lack a well-defined single point of origin), such as those created by intensive use of fertilizers, herbicides, and pesticides. In addition, small point sources-such as numerous domestic septic tanks or small accidental spills from both agricultural and industrial source-threaten the quality of regional aquifers.

Septic tanks are a frequently used method for disposal of sewage. Where they are properly sited, such as in sparsely populated areas and in soils with good drainage above the water table, septic tanks generally pose little or no hazard. [18]

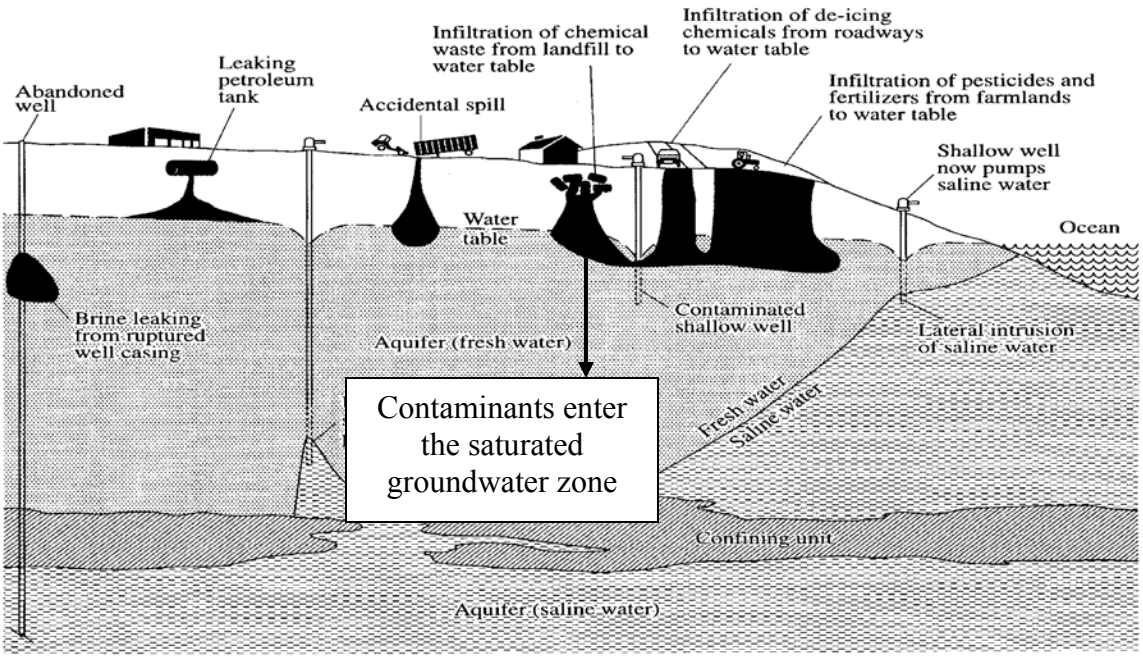

Fig 2.1 Schematic representation of contaminant plumes possibly associated with various types of waste disposal.

All too frequently, however, they are installed with drain fields that are too small and intersect nearby groundwater supply wells. In such situations, sewage often contaminates wells in the area or moves to the land surface, or both. Even where septic systems are well drained, they may eventually pollute the groundwater.

Sewage-disposal activities are introducing viruses into a variety of groundwater sources; but the persistence and movement of these viruses has only recently become the subject of scientific inquiry, and the extent to which such viruses in groundwater pose a hazard to public health is still largely unknown.

Saltwater encroachment associated with over drafting of aquifers or natural leaching from natural occurring deposits are natural sources of groundwater pollution. Most concern over groundwater contamination has centered on pollution associated with human activities. Human groundwater contamination can be related to waste disposal (private sewage disposal systems, land disposal of solid waste, municipal wastewater, wastewater

impoundments, land spreading of sludge, brine disposal from the petroleum industry, mine wastes, deep-well disposal of liquid wastes, animal feedlot wastes, radioactive wastes) or not directly related to waste disposal (accidents, certain agricultural activities, mining, highway deicing, acid rain, improper well construction and maintenance, road salt). A list of potential groundwater contamination sources is shown in Table 2.2.

Large quantities of organic compounds are manufactured and used by industries, agriculture and municipalities. These man-made organic compounds are of most concern. The organic compounds occur in nature and may come from natural sources as well as from human activities. In many locations groundwater has been contaminated by chemicals for many decades, though this form of pollution was not recognized as serious environmental problem until the 1980s.

A brief description of contamination sources follows.

1) Natural Phenomena: groundwater contains some impurities, even if it is unaffected by human activities. The types and concentrations of natural impurities depend on the nature of the geological material through which the groundwater moves and the quality of the recharge water. Groundwater moving through sedimentary rocks and soils may pick up a wide range of compounds such as magnesium, calcium, and chlorides**.** Some aquifers have high natural concentration of dissolved constituents such as arsenic**,** boron, and selenium**.** The effect of these natural sources of contamination on groundwater quality depends on the type of contaminant and its concentrations.

2) Agricultural Activities: Pesticides, fertilizers, herbicides and animal waste are agricultural sources of groundwater contamination. The agricultural contamination sources are varied and numerous: spillage of fertilizers and pesticides during handling, runoff from the loading and washing of pesticide sprayers or other application equipment, using chemicals uphill from or within a few hundred feet of a well. Agricultural land that lacks sufficient drainage is considered by many farmers to be lost income land. So they may install drain tiles or drainage wells to make the land more productive. The drainage

well then serves as a direct conduit to groundwater for agricultural wastes which are washed down with the runoff. Storage of agricultural chemicals near conduits to groundwater, such as open and abandoned wells, sink holes, or surface depressions where ponded water is likely to accumulate. Contamination may also occur when chemicals are stored in uncovered areas, unprotected from wind and rain, or are stored in locations where the groundwater flows from the direction of the chemical storage to the well.

Table 2.2 Potential Groundwater Contamination Sources. [18]

Place of origin	Potential groundwater contamination source			
	Municipal	Industrial	Agricultural	Individual
At or near the land surface	air pollution municipal waste land spreading salt for de-icing streets streets & parking lots	air pollution chemicals: storage & spills fuels: storage & spills mine tailing piles	air pollution chemical spills fertilizers livestock waste storage facilities & land spreading pesticides	air pollution, fertilizers, homes cleaners, detergents, motor oil, paints, pesticides.
Below the land surface	landfills leaky sewer lines	pipelines underground storage tanks	underground storage tanks wells: poorly constructed or abandoned	septic systems wells: poorly constructed or abandoned

Fertilizers are the primary cause of groundwater contamination beneath agricultural lands. Both inorganic (chemically manufactured) and organic (from animal or human waste) fertilizers applied to agricultural lands provide nutrients such as nitrogen, phosphorous, and potassium that fertilize the land and stimulate plant growth. A portion of these nutrients usually leaches through the soil and reaches the groundwater table. Phosphate and potassium fertilizers are readily adsorbed on soil particles and seldom constitute a pollution problem. However, only a portion of nitrogen is adsorbed by soil or

used by plants, and the rest is dissolved in water to form nitrates in a process called *nitrification.* Nitrates are mobile in groundwater and have potential to harm infant human beings and livestock if consumed on a regular basis [22].

3) Industrial Wastes: Manufacturing and service industries have high demands for cooling water, processing water and water for cleaning purposes. Groundwater pollution occurs when used water is returned to the hydrological cycle. Modern economic activity requires transportation and storage of material used in manufacturing, processing, and construction. Along the way, some of this material can be lost through spillage, leakage, or improper handling. The disposal of wastes associated with the above activities contributes to another source of groundwater contamination. Some businesses, usually without access to sewer systems, rely on shallow underground disposal. They use cesspools or dry holes, or send the wastewater into septic tanks. Any of these forms of disposal can lead to contamination of underground sources of drinking water. Dry holes and cesspools introduce wastes directly into the ground. Septic systems cannot treat industrial wastes. Wastewater disposal practices of certain types of businesses, such as automobile service stations, dry cleaners, electrical component or machine manufacturers, photo processors, and metal platters or fabricators are of particular concern because the waste they generate is likely to contain toxic chemicals. Other industrial sources of contamination include cleaning off holding tanks or spraying equipment on the open ground, disposing of waste in septic systems or dry wells, and storing hazardous materials in uncovered areas or in areas that do not have pads with drains or catchment basins. Underground and above ground storage tanks holding petroleum products, acids, solvents and chemicals can develop leaks from corrosion, defects, improper installation, or mechanical failure of the pipes and fittings. Mining of fuel and non-fuel minerals can create many opportunities for groundwater contamination. The problems stem from the mining process itself, disposal of wastes, and processing of the ores and the wastes it creates.

In terms of industrial liquid waste, surface impoundments and injection wells are probably the largest contributors to groundwater contamination. As legislation to protect surface water resources has become more stringent, the use of surface impoundments and injection wells has become an attractive wastewater effluent disposal option for many industries. However, leakage of contaminants through the bottom of a surface impoundment or migration of fluids from an injection well into a hydrologically connected usable aquifer can cause groundwater contamination [22]. The extent and severity of groundwater contamination from these sources is further complicated by the fact that, in addition to being hazardous, many of the organic and inorganic chemicals in industrial wastewater effluent and sludge are persistent.

4) Residential Wastes: Residential wastewater systems can be a source of many categories of contaminants, including bacteria, viruses, nitrates from human waste, and organic compounds. Injection wells used for domestic wastewater disposal (septic systems, cesspools, drainage wells for storm water runoff, groundwater recharge wells) are of particular concern to groundwater quality if located close to drinking water wells. Improperly storing or disposing of household chemicals such as paints, synthetic detergents, solvents, oils, medicines, disinfectants, pool chemicals, pesticides, batteries, gasoline and diesel fuel can lead to groundwater contamination. When stored in garages or basements with floor drains, spills and flooding may introduce such contaminants into the groundwater. When thrown in the household trash, the products will eventually be carried into the groundwater because community landfills are not equipped to handle hazardous materials. Similarly, wastes dumped or buried in the ground can contaminate the soil and leach into the groundwater.

With regard to municipal liquid waste, land application of sewage effluent and sludge is perhaps the largest contributor to groundwater contamination. Treated wastewater and sludge have been applied to land for many years to recharge groundwater and provide nutrients that fertilize the land and stimulate plant growth [22]. However, land application of sewage effluent can introduce bacteria, viruses, and organic and inorganic chemicals into groundwater.

Another major municipal source of groundwater contamination is urban runoff from roadway deicing. In many urban areas, large quantities of salts and deicing additives are applied to roads during the winter months. These salts and additives facilitate the melting of ice and snow; however, they can percolate with the water into the ground and cause groundwater contamination of shallow aquifers [22]. In addition, the high solubility of these salts in water and the relatively high mobility of the resulting contaminants such as chloride ions in groundwater can cause the zone of contamination to expand [22].

The land disposal of municipal solid waste is another potential cause of groundwater contamination. Buried waste is subject to leaching by percolating rain water and surface water or by groundwater contact with the fill. The generated leachate can contain high levels of BOD, COD, nitrate, chloride, alkalinity, trace elements, and even toxic constituents (in industrial waste landfill) that can degrade the quality of groundwater [22]. In addition, the biochemical decomposition of the organic matter in waste generates gases such as methane, carbon dioxide, ammonia, and hydrogen sulfide that can migrate through the unsaturated zone into adjacent terrains and cause potential hazards such as methane explosions [22].

5) Storage and Transport of Commercial Materials: Groundwater contamination from the storage and transport of commercial materials results from leaking storage tanks and spills.

STORAGE TANKS: Underground and aboveground storage tanks and transmission pipelines are another cause of groundwater pollution. Among all underground storage tanks and pipelines, gasoline and home oil fuel tanks probably contribute the most to groundwater contamination. These tanks and pipelines are subject to corrosion and structural failures with subsequent leaks that introduce a variety of contaminants into groundwater. Leakage is particularly frequent from bare steel tanks that are not protected against corrosion. Even if a leakage is small, it can pose a significant threat to groundwater quality.

Gasoline and petroleum products contain hydrocarbon components such as benzene, toluene, and xylene that are highly soluble and mobile in groundwater and can be hazardous to humans if consumed. One gallon of gasoline is enough to render one million gallons of groundwater unusable based on U.S. Environmental Protection Agency (EPA) drinking water standards. In addition, vapors and immiscible compounds continue to feed groundwater with contaminants as precipitation moves into and through the subsurface or as the groundwater table fluctuates.

SPILLS: Spills and discharges on the ground of chemical products can migrate downward and contaminate groundwater. Spills and discharges vary from casual activities at industrial sites, such as leaks from pipes and valves, to accidents involving aboveground storage tanks, railroad cars, and trucks. The discharged chemicals are usually entrained by storm water runoff and transported to the subsurface where they reach the groundwater and degrade its quality.

6) Mining Operations: Groundwater can be contaminated by the drainage from mines and by oil and gas mining operations.

MINES: Drainage of both active and abandoned surface and underground mines can produce a variety of groundwater pollution problems. Rainwater, particularly acid rain, overexposed surface mines, and mine tailings produce highly mineralized runoff frequently referred to as *acid mine drainage.* This runoff can percolate into the ground and degrade the quality of groundwater. In addition, water seepage through underground mines can leach toxic metals from exposed ores and raw materials and introduce them to groundwater. Oxidation and leaching connected with coal mining produce high iron and sulfate concentrations and low pH in groundwater [22].

OIL AND GAS: Oil and gas mining operations can also cause groundwater contamination. These operations generate a substantial amount of wastewater, often referred to as *brine.* The brine is usually disposed of in surface impoundments or injected in deep wells. Therefore, it can reach groundwater, and its constituents, such as ammonia,

boron, calcium, dissolved solids, sodium, sulfate, and trace metals, can subsequently degrade the quality of groundwater [22].

7) Other Activities: Inter-aquifer exchange and saltwater intrusion are two other human activities that cause groundwater contamination.

INTERAQUIFER EXCHANGE: In inter-aquifer exchange, two aquifers are hydraulically connected. Contamination occurs when contaminants are transferred from a contaminated aquifer to a clean aquifer. Inter-aquifer exchange is common when a deep well penetrates more than one aquifer to provide increased yield or when an improperly cased or abandoned well serves as a direct connection between two aquifers of different potential heads and different water quality. The hydraulic connection (well or fractures) can allow contaminants from aquifers with the greatest hydraulic head to move to aquifers of less hydraulic head [22].

SALTWATER INTRUSION: *Saltwater intrusion*, in which saline water displaces or mixes with fresh groundwater, is another source of groundwater contamination. Saltwater intrusion is usually caused when the hydrodynamic balance between the fresh water and the saline water is disturbed, such as when fresh groundwater is over-pumped in coastal aquifers. Saltwater intrusion can also occur when the natural barriers that separate fresh and saline water are destroyed, such as in the construction of coastal drainage canals that enable tidal water to advance inland and percolate into a freshwater aquifer [22].

2.4 Contaminant Transport Processes in Groundwater

When a contaminant is introduced in groundwater, it spreads and moves with the groundwater as a result of:

(1) *Advection* which is caused by the flow of groundwater,

(2) *Dispersion* which is caused by mechanical mixing and molecular diffusion, and

(3) *Retardation* which is caused by adsorption.

Transport mechanisms usually concerned with movement in the saturated zone, however, in many cases the unsaturated zone must not be ignored.

Dissolved contaminants principal transport mechanisms are detailed below:

- ✓ Advection
- ✓ Diffusion
- ✓ Dispersion
- ✓ Sorption
- ✓ Chemical/biological transformation

Advection

A contaminant moves with the flow of groundwater according to Darcy's law (equation 2.2.1). Transport of solute by the bulk movement of the solvent (groundwater). Therefore, when only advection is considered, a contaminant moves with the groundwater flow at the same rate as water, and no diminution of concentration is observed. In reality, however, the movement of the contaminant is also influenced by dispersion and retardation.

Dispersion

Dispersion is the spreading of the plume that occurs along and across the main flow direction due to aquifer heterogeneities at both the small scale (pore scale) and at the macroscale (regional scale). Dispersion tends to increase the plume uniformity as it travels downstream. Factors that contribute to dispersion include: faster flow at the center of the pores than at the edges, some pathways are longer than others, the flow velocity is larger in smaller pores than in larger ones. This is known as *mechanical dispersion*.

Hydrodynamic dispersion is the result of two processes, molecular diffusion and mechanical mixing or mechanical dispersion. *Molecular diffusion* is the process whereby ionic or molecular constituents move under the influence of their kinetic activity in the direction of their concentration gradients. Under this process, constituents move from regions of higher concentration to regions of lower concentration; the greater the difference, the greater the diffusion rate. [22]

Molecular diffusion can be expressed by *Fick's law* as:

$$F = -D_f \left(\frac{dc}{dx}\right) \tag{2.4.1}$$

where:

F: mass flux per unit area per unit time

D_f: diffusion coefficient

C: contaminant concentration

dc/dx: concentration gradient

Fick's law was derived for chemicals in unobstructed water solutions. When this law is applied to porous media, the diffusion coefficient should be smaller because the ions follow longer paths between solid particles and because of adsorption. This application yields an apparent diffusion coefficient D* represented by:

$$D^* = w \times D_f \tag{2.4.2}$$

where w is an empirical coefficient less than 1. Values of w are suggested by Robinson & Stokes for various ions (contaminants).

Mechanical mixing, as defined above, is the result of velocity variations within the porous medium. The velocity is greater in the center of the pore space between particles than at the edges. As a result, the contaminant spreads gradually to occupy an ever-increasing portion of the flow field. Mechanical mixing dispersion can occur both in the longitudinal direction of the flow as well as in the transverse direction. According to Bachmat and Bear, the mechanical mixing component of dispersion can be assumed proportional to the seepage velocity as:

$$D_{xx} = a_L \frac{v_x^2}{v} + a_T \frac{v_y^2}{v} \quad (2.4.3(a))$$

$$D_{yy} = a_L \frac{v_y^2}{v} + a_T \frac{v_x^2}{v} \quad (2.4.3(b))$$

where:

D_{xx}: mechanical mixing component of dispersion in x-direction

D_{yy}: mechanical mixing component of dispersion in y-direction

a_L: longitudinal dispersivity

a_T: transversal dispersivity

v: average linear pore water velocity with x & y components v_x & v_y.

The hydrodynamic dispersion coefficients are now calculated as:

$$D_x = D_{xx} + D^* \quad (2.4.4(a))$$

$$D_y = D_{yy} + D^* \quad (2.4.4(b))$$

For one dimensional contaminant transport, the term D_T is ignored because the transverse dispersion movement of contaminants is negligible as compared with the longitudinal dispersion movement of contaminants in the direction of the groundwater flow.

Dispersion in porous material refers to the spreading of a stream or discrete volume of contaminants as it flows through the subsurface. For example, if a spot of dye is injected into porous material through which groundwater is flowing, the spot will enlarge in size as it moves down-gradient.

Dispersion causes mixing with uncontaminated groundwater, and hence dispersion is a mechanism for dilution. Moreover, dispersion causes the contaminant to spread over a greater volume of aquifer than would be predicted solely from an analysis of groundwater velocity vectors. This spreading effect will be of particular concern when toxic or hazardous wastes are involved. Dispersion is chiefly of importance in predicting transport away from point sources of contamination but is also influential in the spread of non-

point-source contaminants, although of lesser importance. Contaminants introduced into the subsurface from non-point sources will be spread over a relatively large area because of the nature of the loading pattern. In this case, dispersion merely causes a relatively large zone of contaminated water to acquire some rough fringes. Dispersion is of interest because it causes contaminants to arrive at a discharge point (e.g., a stream or a water well) prior to the arrival time calculated from the average groundwater velocity. The accelerated arrival of contaminants at a discharge point is a characteristic feature of dispersion that is due to the fact that some parts of the contaminant plume move faster than the average groundwater velocity. [22]

Figure 2.3 below shows how dispersion can cause some of the contaminant to move faster than the average groundwater velocity and some of the contaminant to move slower than the average groundwater velocity. The front of the contaminant plume is no longer sharp but rather smeared. Therefore, when dispersion is also considered, the contaminant actually moves ahead of what would have been predicted by advection only.

Sorption

Sorption refers to the exchange of molecules and ions between the solid phase and the liquid phase. It includes adsorption and desorption. *Adsorption* is the attachment of molecules and ions from the solute to the rock material. Adsorption produces a decrease of the concentration of the solute or, equivalently, causes a *retardation* of the contaminant transport compared to the water movement. *Desorption* is the release of molecules and ions from the solid phase to the solute.

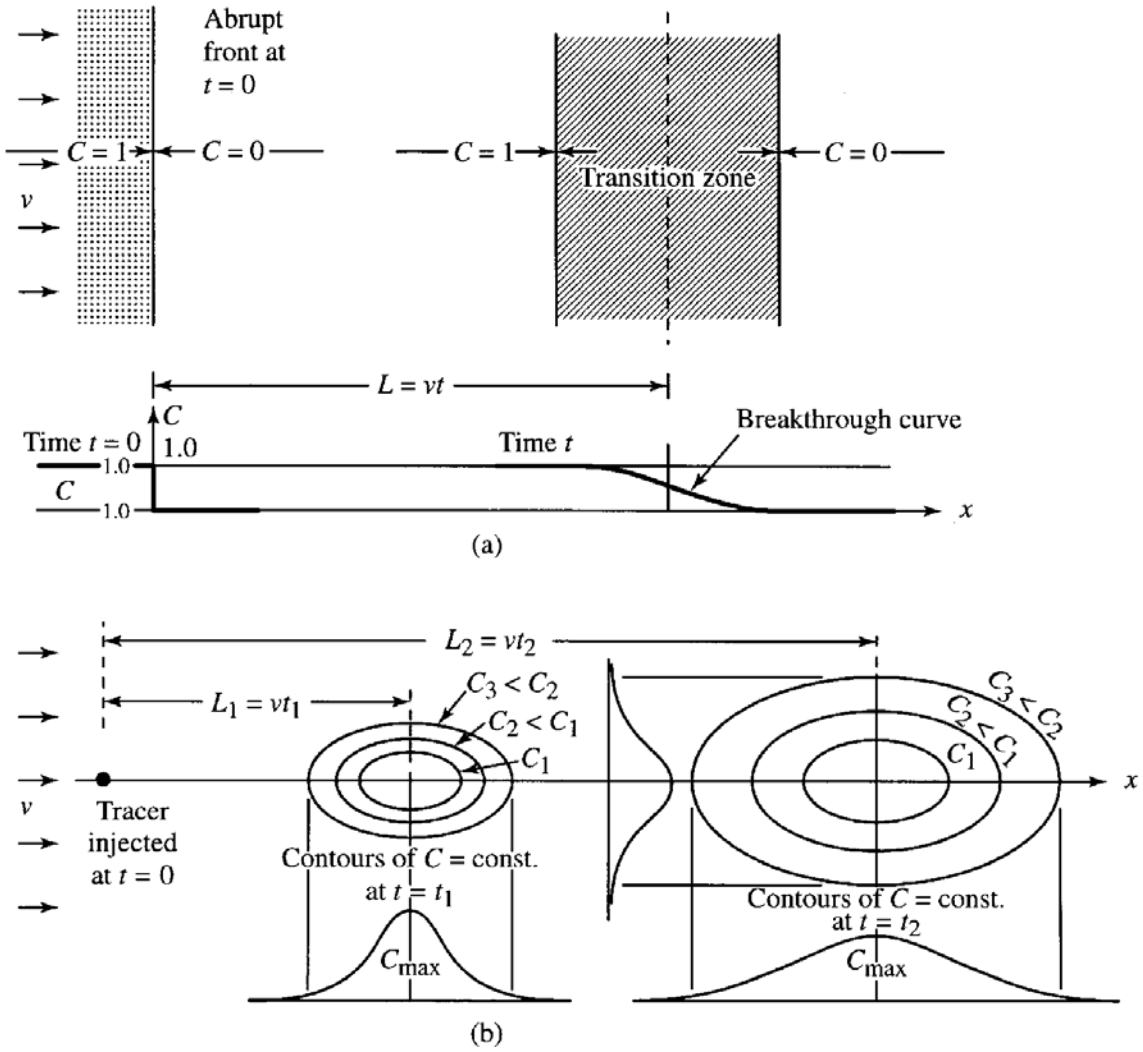

Fig. 2.3 Longitudinal and Transverse Spreading due to Mechanical Dispersion.

The relationship between the solute concentration in the adsorbed phase and in the water phase is called a *sorption isotherm*. The simplest expression is the *linear isotherm*

$$C_a = K_d \times C \tag{2.4.5}$$

where C_a is the sorbed concentration as mass of contaminant per mass of dry rock matrix [dimensionless], C is the dissolved concentration in mass of contaminant per volume of water [M/L^3] and K_d is the *distribution coefficient* [L^3/M]. This expression implies that there is an *equilibrium* between the adsorbed concentration and the dissolved concentration. This can be assumed when the adsorption process is fast compared to the advection of contaminant.

The adsorption causes retardation in the migration of contaminants compared to the advection. The contaminant transport gets more retarded as the fraction adsorbed increases. This effect can be described by a *retardation factor*, R_a, which for a linear isotherm, is:

$$R_a = 1 + K_d(\frac{\rho_d}{n}) \tag{2.4.6}$$

Where K_d is the distribution or adsorption coefficient described previously. The values ρ_d and n are the bulk density and porosity of the soil. The velocity of the contaminant in groundwater can be calculated as follows:

$$v_c = \frac{v}{R} \tag{2.4.7}$$

Where v_c is the velocity of the contaminant movement in groundwater, v is the groundwater velocity, and R is the retardation factor. A high retardation factor, i.e., high adsorption coefficient, significantly retards the movement of the contaminant in groundwater.

Chemical and Biological Transformations: This process represents transformation of contaminant into other compounds including degradation by bacterial activity, radioactive decay and chemical reactions. In this case it is important to consider reaction kinetics, radioactive & organic half lives. Bacterias are also involved in the degradation of contaminants in the unsaturated zone of groundwater, helping in lessening of groundwater contamination specially in the case of organic contaminants.

This study of contaminant transport modeling is limited to two-dimensional modeling analysis with no reaction (conservative) contaminant (Cl^- & F^-) to describe the transport of contaminants in groundwater.

In a homogeneous, isotropic medium having a unidirectional steady-state flow with seepage velocity v, the solute mass conservation statement may be expressed as:

$$\frac{\partial C}{\partial t} = (\frac{\partial}{\partial x})(D_{ij}\frac{\partial C}{\partial x}) + (\frac{\partial}{\partial y})(D_{ij}\frac{\partial C}{\partial y}) - (\frac{\partial}{\partial x})(v_x \times C) - (\frac{\partial}{\partial y})(v_y \times C) \tag{2.4.8}$$

For a uniform flow field, after rearranging terms, equation 2.4.8 may be rewritten as:

$$\frac{\partial C}{\partial t} = D_x(\frac{\partial^2 C}{\partial x^2}) + D_y(\frac{\partial^2 C}{\partial y^2}) - v_x(\frac{\partial C}{\partial x}) - v_y(\frac{\partial C}{\partial y}) \qquad (2.4.9)$$

This is the equation governing 2-D transport of conservative contaminants.

Where:

C: Contaminant concentration

v_x & v_y: x- & y- components of the seepage or average pore water velocity

D_x: Dispersion coefficient in x-direction

D_y: Dispersion coefficient in y-direction

The first term on the right hand side of equation 2.4.9 represents the longitudinal dispersive contaminant transport process, the second term represents the transversal dispersive contaminant transport process, the third & fourth terms represent the advective contaminant transport process in x- & y- direction respectively.

2.5 Background on Akaki Well Field

I. Location & Physiography

Akaki well field is located 23 km south-east of Addis Ababa, in the *lower part of Akaki river catchment.* The area of the well field is *16 sq. km*. The Akaki river catchment includes the jurisdiction of the city of Addis Ababa and the surrounding Oromiya Region and covers about 1,600km^2. The Catchment is dominated by undulated topographic surface with elevation ranging from 1800mals at the mouth of the river to over 3100 meter above sea level (masl) in the Entoto mountain ranges over a distance of 65 km. The well field has more or less flat terrain with ground elevation ranging between 2050-2100 masl. The Akaki river catchment is bounded by Mt. Furi (2839 masl) in the south-west, Mt. Yerer (3100 masl) in the east, Mt. Wochecha in the north-west and of course the Entoto ranges in the north. Some Prominent volcanic peaks in the well field include Grara Bushu (2,346 masl) in the north-east, Mt. Guji (2475 masl) in the east and Mt. Bilbilo (2,380 mals) in the south &south-east.

II. Climate

The Climate of Addis Ababa is Woina Dega type [20]. The Rainfall has unimodal pattern, one distinct rainy and dry season. The dry season is October through may and the wet one is from June to September being the highest rainfall peak in August. The long-term mean annual rainfall observed at Addis Ababa Observatory is 1254 mm. Addis Ababa Observatory is the only gauging station, which has the long-term monitoring in the catchment since the turn of the century except a gap between 1941-1945.

The maximum temperature of Addis Ababa ranges between 20^0c (in wet season) to 25^0c (in dry season), while the minimum falls between 7 - 12^0c in the year. This indicates that daily variation of temperature is highly pronounced.

Wind speed is generally moderate, ranging between 0.5 to 0.9 m/s. The average daily sunshine hours are 9.5 hours in November & December, and far low, 3 hours, in July and August.

Pan-evaporation records at Addis Ababa Observatory showed that the average monthly pan-evaporation during dry season (November) is about 180 mm and in west season (July) falls to 75 mm.

III. Hydrology

Akaki River Catchment is mainly drained by two rivers; the *Big Akaki river*, draining the eastern part and *Little Akaki river*, draining the western portion of the catchment. Both the rivers emerge from Entoto Ranges flowing to south-east and after 95 km join the Awash river near Dodota. The Big Akaki and Little Akaki joins at Aba-Samuel Lake, man made reservoir just downstream of Akaki well field, about 84 km up-stream of the confluence with Awash River.

Since 1981, the Big Akaki River is gauged at Addis -Debrezeit road bridge, commanding a catchment area of 885km^2. The station is equipped with an automatic hydrometric record and seven staff gauges to measure manually. The mean annual discharge (from

1981-1998) of the Big Akaki at this point is 9,517 1/s or 10.75 l/s/km^2 which is equivalent to say to annual yield of 339 mm.

The discharge records reveal that 82% of the annual run-off is generated in July, August and September only, emphasizing that the groundwater contribution to the river is minimum compared to the run-off generated in the west season. An increasing trend of low flow with time is observed on the hydrograph; which is attributed to the waste water contribution from the city of Addis. The increase in the low flow of the Big Akaki as a result of the contribution of waste effluent ranges from 0.5 m^3/day in early 1980's to 1 m^3/d - 1.4 m^3/d in late 80's [20]. The low flow of Akaki river (both Big & small) excluding the waste water effluent is estimate to range between 600-1000 l/s.

IV. Groundwater Recharge Estimation

Semi-distributed Water Balance model was developed to estimate the groundwater recharge of the catchment. The model consider three parameters; maximum moisture holding capacity of the unsaturated zone, fraction of soil moisture that percolate to recharge the groundwater and the base-flow recession coefficient. The Akaki catchment is divided to nine sub- catchments based on topography in order to account the spatial variation of input variables and catchment characteristics. Catchment characteristics such as depth to water level, soil permeability, land-use and other parameter values have been established, and accounts for transfer of water from one sub-catchment to another through the hydrological process is made. Taking into consideration of the aerial average monthly rainfall and the potential evapotranspiration for each sub-catchment the model produces monthly runoff at the out let of the catchment and the groundwater recharge. Thus in Akaki river catchment, the mean annual recharge to the groundwater is about 51 mm which occurs from June to September, mainly happens in July and August.

V. Geology and Geo-structures

The geology of Akaki river catchment briefly look as follows: The north and north eastern area (the Entoto mountain, the northern and north eastern Addis Ababa) is covered with trachytes, rhyolites, basalts and several episodes of pyroclastic materials of

older volcanism occur on the upper part and foothill sides of Entoto ridge. Overlying these, younger basaltic rocks (Addis Ababa Basalt) are found covering the central and southern part of the city. Outcrops of ignimbrites north of Bole area (Eastern Addis) and Lideta area (Central Addis) have been observed underlying the Addis Ababa basalt. Younger volcanic of trachy-basalt, trachytes, ignimbrites and tuff belonging to the wochecha, Furi and Yerer volcanoes are recognized overlying un-conformably on the Addis Ababa basalt in the western, south-western and eastern part of the catchment. Akaki (including the well field), Dukem and Debrezeit area are covered with olivine basalt, scoria, scoriaceous basalts and vesicular basalts. In the upper part, in some places, intercalation of tuffs, sand and gravels are also recognized. In north-east, east and in smaller extent in the western part of Debre Zeit, outcrops of trachytes, rhyolitic ignimbrites and tuffs are recognized covering the area.

The overburden covering the bed rocks includes soils, lacustrine & alluvial deposits. Thick insitu soil type cover is found in the centeral, south-eastern, north- eastern, western (kolfie & Keraniyo) and in northern (Gullelie) part of the catchment. The lacustrine covers Bole, Lideta, Mekanisa, Akaki-Aba Samuel area and Dukem-Debre Zeit area. Some alluvial deposit also occur along Big & small Akaki rivers in the southern and south-western part of Addis and minor deposit also occur along Kebena river in the area north-west of Bole.

The Akaki catchment lies at the upper shoulder of the Main Ethiopia Rift System. Therefore, it is highly affected by rift tectonics, which is manifested by numerous faults of the rift trend (NE-SW), and faults and lineaments of E-W, N-W and NE-SE trend. The density of faults increases towards the south-eastern part of the catchment area (where the well field lies) to the direction of the rift floor. In the well field area, some of the cinder cones are aligned along the major NE-SW trending faults which presupposed to be erupted through these faulting processes. [20]

VI. Hydrogeology

The Occurrence of groundwater in Akaki catchment is associated mainly to the volcanic rocks and minor alluvial aquifers do exist along the banks of both Big (BAR) and Little Akaki rivers (LAR). These Volcanic aquifers have primary porosities like vesicles and joints and secondary porosities like faults, fractures & fissures produced as a result of tectonic activities and weathered zones. In the volcanic rocks groundwater circulation and occurrence is associated with these porosities while in the alluvial aquifers, it is in the interstitial spaces in between the sediments.

The geometry of the aquifer systems in the catchment area is highly variable, discontinuous and not well defined. In most area, the volcanic aquifers show semi-confined to unconfined nature which in few area (kerchelie and kality), confined aquifers are penetrated. Correlation of the lith-hydrostratigrahic units is very difficult and yet not established.

The Potentiometric surface indicates that the groundwater is in connection with the surface water of Big & Little Akaki rivers north of Akaki bridge. Thus the base flow of the rivers is contributed from the groundwater. The recharge to the groundwater which takes place within the Akaki catchment to the north of Akaki bridge is considered contributing to the base flow.

The piezometric surface constructed from groundwater points inventory made during previous projects showed that the general groundwater flow direction is from north to south in the upper &central part and towards south & south-east in the lower parts of the catchment area.

The aquifers in the well field are scoriae deposits, fractured & jointed scoriaceous basalts, vesicular basalts and basalts. These aquifers in most cases are interlayered and overlay one another. As observed from the geological logs, the occurrence of thicker beds is real. The vertical and horizontal inhomogenity of the aquifer system is obviously seen on the fence diagram of the well field.

As a result of the variability and complex nature of the volcanic aquifers in the catchment area, the hydraulic properties of the aquifers is also highly variable resulting extremely variable discharges (yields) of boreholes even in close distances unless otherwise it lies on the same fracture/fault zone. However, in Akaki well field variation in hydraulic properties of the aquifer and the yields of boreholes is not so much pronounced.

The transmissivity (T-value) and storativity (S-value) calculated from pumping tests in the well field reveal that it ranges between 1834 m^2/d to 105,408 m^2/day and from 0.0065 (0.6%) to 0.016 (2%) respectively. In the area north of Aba Samuel to Lafto area, the T-values range between 19-117 m^2/d and the S-values are estimated to range between 0.05 - 0.0001. In Dukem area T-values range between 61-153 m^2/d. In north of Akaki well field and kality area T-values range from 2.8 - 6,099 m^2/d. Central part of Addis do have 0.3 - 5,760 m^2/d while the northern part of the catchment (Entoto, Gulele and Tatek) have 0.3 - 1,092 m^2/day. The western catchment areas (woletie Suk - Alem Gena area) have T-values ranging between 9.9 – 95 m^2/day and the S-values between 0.0004 to 0.013 [20].

From this distribution of hydraulic characteristics of the aquifers, it is clear that aquifer parameters are lower in the upper & western part of the catchment area, relatively higher in the central, southern and south-eastern part and extremely high at Akaki well field and gets lower in the Dukem area south-east of the well field. [20]

VII. Groundwater Quality

The groundwater quality in Akaki River Catchment is more or less similar and good quality water for domestic & industrial uses except the hot (thermal) water in Fluha - Grand Palace - Hilton area where the water is highly mineralized (high TDS). Generally the analytical result showed that all ions in the samples are under the WHO recommended permissible limit for drinking water.

Some wells in the town (specially shallow wells along river banks) show higher Nitrate and chloride concentration which obviously would be due to contamination with waste water from domestic and industrial effluents.

The water group is Ca-Mg bicarbonate type. It is obvious that Ca and Mg is from the weathering and decomposition of the basalts which avail the leaching of ions from (pyroxene, Olivine & plagioclases) and the bicarbonates are from hydration of CO_2 gas from the atmosphere and oxidation of the organic matter in the soil.

VIII. Conceptual Model of the Study Area

Based on the above discussed physiographic, geological, hydrogeological & hydrological conditions, the conceptual model of the area is constructed as outlined below:

- ✓ The model area encompasses the twenty five (25) well fields in the Akaki area and extends to south & south-east up to the confluence with Awash river and the central part of Dukem Plain.
- ✓ The source of recharge for all surface and groundwater is the precipitation which only occurs in the catchment area.
- ✓ The piezometric surface of the groundwater follows the topographic gradient from north to south in the upper catchment and to south and south-east in the lower part, in Akaki & Dukem area.
- ✓ As a result of the non-uniformity, highly variable and complex geological setting which reflects similar hydrogeological conditions, it is not possible to define different model layers. On the other hand, the continuous topographically controlled piezometric surface of the groundwater in the region, and the first instance to simulate flow in such type of complex hydrogeological conditions initiate to consider the aquifer as a single layer system. In addition, the fact that the study is for long term contaminant prediction, the effect of multi-layer system on the out put is negligible. Therefore, considering the upper most aquifer system as a single layered aquifer system would produce valid results.

2.6 Groundwater Pollution Monitoring Parameters: Focus on Pollutants

Groundwater pollution threatens many valuable water resources. The consequences are often more serious than for surface water due to the relatively long subsurface residence times. Also, groundwater pollution may go undetected for years, while remediation is

difficult and costly, or sometimes even impossible. For the lazy person, groundwater is an elusive entity shrouded in mystery and generally out of sight and out of mind. Any attempt to evaluate groundwater pollution, requires an understanding of the particular aquifer system, its recharge and pollution pathways.

Groundwater pollution occurs widely from a variety of anthropogenic sources. These include point sources such as waste disposal facilities, industrial pollution, wastewater treatment works, on site sanitation, cemeteries and many others. Diffuse pollution includes agricultural practices, atmospheric fallout and other sources. Changes in land use, such as the clearing of vegetation, over abstraction of groundwater, or excavation below the water table, can also contribute significantly to groundwater pollution [5].

A large number of inorganic, organic and microbiological pollutants have been detected in groundwater because of polluting activities. The chemical and hydrological changes caused by such activities can also mobilize groundwater constituents that were originally present in the aquifer. With such a cocktail of pollutants that may occur at a contaminated site, the question arises: Which parameters should be monitored for pollution detection, and at what frequency? Should inorganic and organic chemical constituents, physical variables, isotopes, and other parameters be included?

For certain practices, such as waste management, monitoring procedures and parameters are prescribed by the authorities. The system of issuing permits or licenses provides a certain degree of flexibility for stipulating the analytical parameters to be monitored but the question remains whether these are the most effective in detecting pollution. Experience has shown that a site-specific approach is often needed, rather than a generalized procedure for a certain type of activity.

Here in Addis Ababa, the key activity that can potentially pollute the groundwater is sewage treatment & disposal. Focus on monitoring parameters of Addis Ababa groundwater pollution that arise from such activity is discussed below.

In a study of a groundwater pollution plume caused by sewage infiltration, Barber developed approaches for screening and detailed investigation of the pollution. For the initial detection of the pollution plume, the parameters used were chloride, boron, EC, and dissolved organic carbon (DOC). Chloride (and bromide) are conservative ions, i.e. they do not enter into redox reactions, adsorb significantly onto mineral surfaces, form complexes with other ions, or undergo transformations that remove the ions from solution. Similarly, boron does not undergo redox transformations, biological degradation, precipitation or significant sorption. The conservative ions are the first species to break through when a plume moves through a porous medium and so should be the first to be detected at the edges of the moving plume. In contrast, other non-conservative parameters, such as nitrate, sulphate, bicarbonate, phosphate, ammonium, calcium, magnesium and potassium, undergo chemical reactions in solution, are adsorbed onto the aquifer material or are biologically transformed. These move slower than the conservative species and are usually found at a later time or closer to the pollution source. The major source of boron in sewage is sodium perborate used as bleach in detergent powders and the boron concentration in the final effluent typically varies between 0.3 and 1.5 mg/l. Natural groundwater in the USA study area had a boron concentration <20 to 50 µg/l while contaminated groundwater had 90 to 530 µg/l [5]. When checked for boron, Cape Town sewage was found to have relatively high boron concentrations in sewage sludge [5], but no recent data were available for this parameter for the final effluent from the various treatment plants. The concentrations of pollutants in sewage sludge are controlled in terms of regulations issued in 1991 and later guidelines jointly issued by several government departments [5].

Primary and secondary sewage treatment reduces the DOC (i.e. the “bulk” organic parameter) of the effluent by 80 to 90%. The selective removal of more easily biodegradable compounds in these processes yields treated effluent containing relatively recalcitrant and mobile organic compounds [5]. However, during infiltration, DOC is further reduced in the unsaturated zone by biodegradation and sorption to the sediments. The bulk parameter DOC itself gives no indication as to the nature of the organic compounds and, as a first step, Barber subjected the wide range of compounds to

extraction to obtain hydrophobic and hydrophilic fractions. Each of these was then further subdivided into acid, neutral and basic fractions. In addition, methylene-blueactive substances were determined as well as volatile halogenated organic compounds (VOX). VOX compounds, particularly the chlorinated species, are amongst the most commonly detected organic pollutants in groundwater [5].

Most aquifers are vulnerable and the range of potential pollutants in groundwater is vast. Inorganic constituents are many, but organic chemicals are increasing by the thousands each year. The Chemical Abstract Service registry now contains records for more than 22 million organic and inorganic substances [5]. Certainly, not all of these will occur in measurable quantities in groundwater, but the large number of potential pollutants indicates the problem of detecting and identifying chemical compounds in the environment.

The various approaches described in the literature vary but for a first screening there seems to be agreement that the common inorganic constituents can give a clear indication of pollution in the aquifer. EC measurements, which can easily be performed in the field, are extremely useful in identifying changes in salinity that accompany most inorganic pollution events. Provided the general direction of groundwater flow is known, it could be possible to confirm the occurrence of pollution at the particular point source. The additional analysis of parameters such as boron and a “bulk” organic parameter such as DOC will provide further proof of the pollution event. In the case of a pure organic spill, e.g. solvents, it may be necessary to use soil-gas sampling or redox measurements as screening tools. Analysis of chemical oxygen demand (COD) is often prescribed in regulations and permit conditions, presumably as a (organic?) “pollution indicator” parameter. This can be useful, provided it is realized that the oxygen demand also relates to natural inorganic constituents existing in reduced form in (deeper parts of) the aquifer. At low values (i.e. <<50 mg/l, and certainly at <10 mg/l) the COD determination is not necessarily accurate. Then the dissolved organic carbon (DOC) provides a more accurate indication of (organic) constituents in the water.

Groundwater quality monitoring can have large cost implications, both with respect to sampling and analysis. Although this paper does not investigate these costs, groundwater quality monitoring decisions has to take it into consideration in one way or another. On the one hand, aquifers should be protected practically at all costs as the cleanup after pollution events have huge cost implications. On the other hand, the cost has to be economically justifiable. Not all aquifers are that valuable due to salinity, poor yield or other factors. Therefore, the monitoring needs, including the parameters to be analyzed, should be linked to the present groundwater use or more generally to the aquifer potential. The economic value of the aquifer should be determined on a rational basis, e.g. using an aquifer system management classification, such as that developed by Parsons (1995), followed by a calculation of the cost involved should the aquifer be lost.
Identifying and quantifying groundwater pollution needs an aquifer specific, site specific and pollutant specific approach in a joint effort by hydrogeologists and pollution monitoring experts. In this approach, the conceptual hydrogeology, the monitoring network and the parameters for monitoring will be defined. However, "bulk parameters" such as electrical conductivity and dissolved organic carbon are extremely useful tools for delineating pollution plumes. Electrical conductivity in particular, can easily be determined in the field and in the majority of cases will give a reliable indication of the extent of the problem.

For determining the background values, groundwater quality monitoring at a hazardous waste facility, initially requires analysis of the full list of frequently occurring characteristic pollutants, as well as all additional priority pollutants and organic compounds with a high migration potential. At the same time, the common cations and anions should be included and used for delineating pollution plumes. Unless specific hazardous substances are detected, the common constituents can be analyzed more regularly than the special pollutants. Until pollution is detected, the list of determinands can be shortened significantly by only analyzing for key constituents such as EC, boron, sodium, chloride and potassium. In the case of non-hazardous waste facilities, the common constituents may form the bulk of the analyses, and this would significantly reduce the monitoring costs.

For detecting sewage pollution, boron, chloride and electrical conductivity are the key indicators with regard to inorganic compounds and dissolved organic carbon for organic compounds. When the dissolved organic carbon concentration is high, or if it persists in time and space, it should be subdivided into hydrophilic and hydrophobic fractions for further study of the organic components.

For reasons detailed above, *this conservative contaminant transport modeling of the Akaki well field uses chloride ion as its groundwater quality monitoring parameter* which is conservative & fast moving with the contaminant plume.

3. Materials & Methods

3.1 Research Materials

To conduct the laboratory tasks required for the validation of the model in this thesis work, the following chemicals & apparatus are used.

Chemicals: Mercuric Nitrite, Diphenyl Carbazone (serving as Chloride capsules), Fluoride capsules, Nitric Acid.

Apparatus: Plastic containers for groundwater samples, Pipette, volumetric flask.

Laboratory Procedure

a) Groundwater samples are collected from ten boreholes of the wellfield; namely: BH04, BH07, BH10, BH14, BH16, BH20, BH23, BH24, BH25 and BH26 during the month of July 2009 in plastic containers.

b) Each sample in the plastic containers is then transferred to 100 ml volumetric flask in Addis Ababa Water & Sewerage Authority (AAWSA) laboratory.

c) The sample is then mixed with one capsule of diphenyl carbazone.

d) 2 ml mercuric nitrite solution is introduced to the mixture using a pipette to form a precipitate of mercuric salt.

e) Nitric acid is then added to fix the PH of the resulting mixture around 4 and to make the chloride color sharply visible.

Following the above procedures, the results of the laboratory analysis are tabulate in Table 3.13 in later sections.

3.2 Modeling Features

Groundwater model is a device that approximates a field situation. There are two approaches; a *physical model* which more or less represents the action on field conditions like a laboratory sand tanks to simulate groundwater flow directly. The other is the *mathematical model*, which simulate groundwater flow indirectly by means of governing equations that are thought to represent the physical process of the system. It considers the

equation governing heads or contaminant flows along boundary of the system (boundary condition) and for time dependant conditions, equations describing initial heads or concentration distribution (initial condition) of the system. Mathematical models can be solved analytically or numerically. *Mathematical models solved numerically are the subject of this thesis work focusing on conservative solute transport in the Akaki well field.*

The Purpose of groundwater contaminant transport model is based on three main objectives:

1. **Predictive**: Used for prediction of the future of the consequences of proposed works, i.e. say drawdown, discharge, etc. This requires calibration.
2. **Interpretative**: Used for gaining insight into the controlling parameters in a site-specific settings or as a frame work for assembling and organizing field data and formulating ideas, about system dynamics. It does not necessarily require calibration. Example: Regional Aquifer system Analysis.
3. **Generic:** Used to analyze flow in hypothetical hydrological systems. It is also helpful in formulating regional regulation guidelines and screening tools to identify regions suitable or unsuitable for some proposed action. It does necessarily require calibration. Example: Model used to study lake-ground water interaction.

Conservative contaminant transport modeling of the Akaki well field helps predict solute concentration of a given groundwater constituent (Cl^- & F^-) some time ahead to be able to know the risk associated with the predicted solute concentration and to decide on whether a groundwater remediation measure is necessary.

Groundwater modeling is one of the excellent tools to organize and synthesize field data of hydrogeological assessment. Models require adequate and reliable data to produce useful results. Otherwise inadequate and poor quality data input results unreliable output which would be "*garbage in garbage out*".

If the purpose of investigation requires groundwater modeling, like other assessment methodologies, it has its own steps or protocol to follow. *A modeling protocol includes code selection (MATLAB, in this study), model design, calibration, calibration sensitivity analysis, verification, prediction, prediction sensitivity analysis and post-audit*. Each of these steps builds support in demonstrating that a given site specific model is capable of producing meaningful results, that is, the model is valid. The steps of modeling protocol for application in groundwater contaminant transport model are shown below in Fig 3.1.

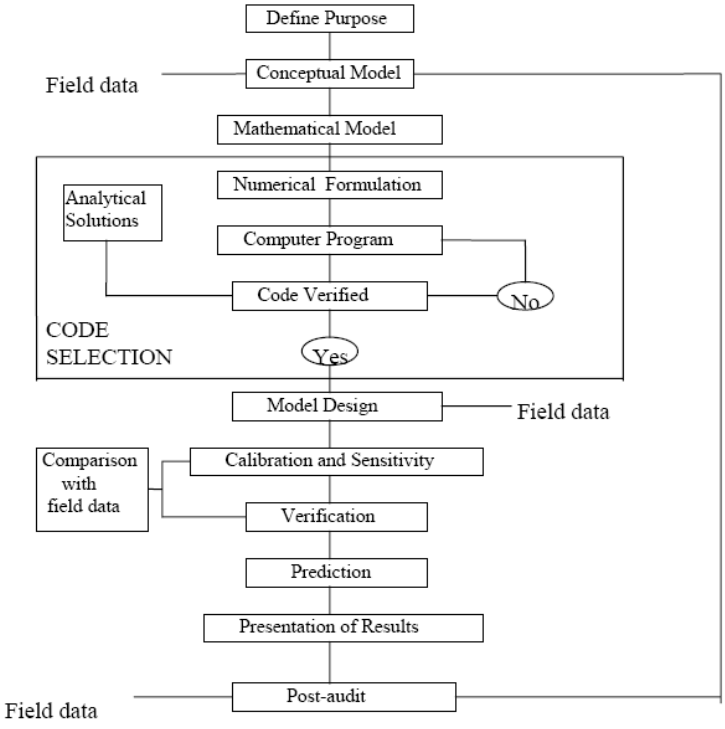

Fig 3.1 Modeling Protocol Flow Diagram

3.2.1 Numerical Solution Technique Scheme of the Selected Model

When mass-balanced equation are specified with derivatives in more than one dimension, such as time, and one or more spatial dimension for dynamic models or more than one spatial dimension for steady-state models (SSM), the system is then described by partial differential equations. Consider the equation for two-dimensional advective-dispersive transport of a conservative solute with no reaction:

$$\frac{\partial C}{\partial t} = -v_x \frac{\partial C}{\partial x} - v_y \frac{\partial C}{\partial y} + D_x \frac{\partial^2 C}{\partial x^2} + D_y \frac{\partial^2 C}{\partial y^2} \qquad (3.1)$$

In this application concentration variations are considered over time and in the x and y direction, that is, C=C(x,y,t). While analytical solutions to this equation are available when u, D_x, and D_y are constant over time and space, numerical methods are required when these parameters vary temporally and/or spatially. The methods involve discretized calculations over both the temporal and spatial dimensions. The most common method for implementing this type of solution, finite difference method is described in this section.

Finite Difference Method

The finite difference method solves the mass-balance equation(s) by forcing them to be satisfied at a set of discrete points in space. Figure 3.2 below illustrates a two-dimensional grid that might be used to solve Eq.(3.1). Nodes in the x direction are indexed by i, while nodes in the y direction are indexed by j, with C(i,j,t) indicating the concentration at grid point i,j at time t. The key step in the finite difference method is to express the derivatives for concentration at each point i,j as appropriate difference between concentrations at adjacent nodes. For example, for the first (advection) term of the rhs of Eq.(3.1), the first derivative of C(i,j,t) with respect to x is needed and could be expressed using either:

$$\frac{\partial C(i,j,t)}{\partial x} = \frac{C(i+1,j,t) - C(i,j,t)}{\Delta x} \tag{3.2}$$

or

$$\frac{\partial C(i,j,t)}{\partial x} = \frac{C(i,j,t) - C(i-1,j,t)}{\Delta x} \tag{3.3}$$

Where Δx is the difference between nodes in the x direction. Equation (3.2) uses *forward differencing* for the advection term. It approximates the derivatives at point i,j using the difference between the concentration one node downstream of the point (in the direction of advection) and C(i,j,t). Alternatively Eq.(3.3) uses *backward differencing* since the first derivative is computed by taking the difference between C(i,j,t) and the concentration at the node one step upstream. Neither approach is expected to provide an especially accurate estimate of the concentration derivative at point i,j especially if its value is changing rapidly as a function of x. [2]

For this study the central differencing scheme is used for the x- & y- advection terms as in equations [3.4] & [3.5].

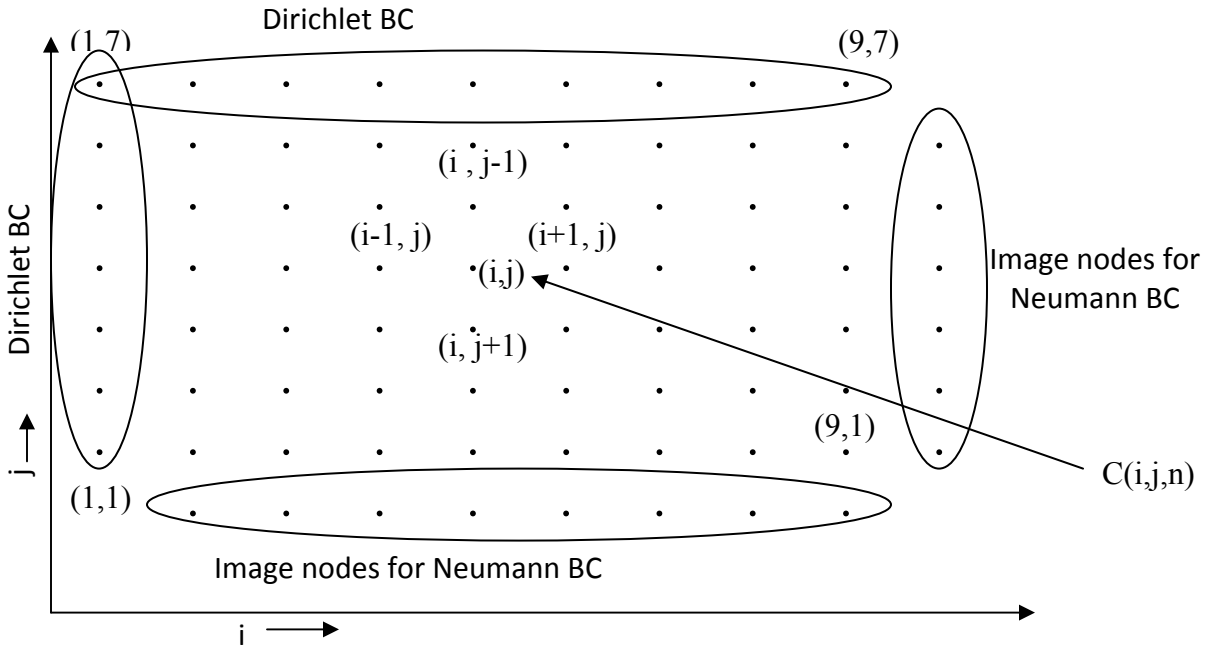

Fig. 3.2 Finite difference grid of Akaki wellfield with 9 x 7 node system

A third alternative is achieved by taking the average of the forward and backward differencing equation. Thus, the 1st term on rhs of equation [3.1] can be written as:

$$\frac{\partial C(i,j,t)}{\partial x} = \frac{forward + backward}{2} = \frac{C(i+1,j,t) - C(i-1,j,t)}{2\Delta x} \qquad (3.4)$$

Similarly, for the y- component of the advective term, the 2nd term is written as:

$$\frac{\partial C(i,j,t)}{\partial y} = \frac{C(i,j+1,t) - C(i,j-1,t)}{2\Delta y} \qquad (3.5)$$

This approach, referred to as *central differencing* for the advection term, does not even use the value of the concentration at point i,j; rather, it calculates the derivative by drawing a straight line between the concentrations immediately up-and downstream of the target location.

As with the finite cell method, the same terminology- backward, forward or central differencing-was used to describe the weighting of concentrations passing with the advective flow across the interface of two cells. There is a clear parallel between the

finite cell method, where concentrations are averaged over volumetric compartments and mass transport occurs between them, and the finite difference method in which mass-balance equations are satisfied and concentrations computed at points in space. In the latter, the points are still thought to be representative of the spatial domain around them, that is, the degree of spatial representation is still limited by the coarseness of the grid. Likewise, many of the same issues that arise with respect to accuracy, stability and numerical dispersion in the finite cell method apply to the finite difference method, especially with regard to the use of backward, forward, or central differencing. These issues are addressed in more detail below. First, equations for the remaining derivatives in Eq.(3.1) are developed.

The dispersion terms in Eq.(3.1) require a differencing expression for second derivatives. Recognizing that the second derivative describes the rate of change in the first derivative with distance, it can be computed by taking the difference between the forward difference estimate of the first derivative (which best describes the value of the first derivative midway between node i,j and node i+1, j) and the back ward difference estimate (for the point mid way between node i,j and node i-1,j), and dividing by the distance between these points, Δx:

$$\frac{\partial^2 C(i,j,t)}{\partial x^2} = \frac{\partial(\frac{\partial C}{\partial x})}{\partial x} = \frac{\left[\frac{C(i+1,j,t)-C(i,j,t)}{\Delta x}\right]-\left[\frac{C(i,j,t)-C(i-1,j,t)}{\Delta x}\right]}{\Delta x}$$

$$= \frac{C(i+1,j,t)-2C(i,j,t)+C(i-1,j,t)}{(\Delta x)^2} \qquad (3.6)$$

A similar expression describes the second derivative for the dispersion term in the y direction:

$$\frac{\partial^2 C(i,j,t)}{\partial y^2} = \frac{C(i,j+1,t)-2C(i,j,t)+C(i,j-1,t)}{(\Delta y)^2} \qquad (3.7)$$

The second derivative in each case is estimated by adding the concentrations at the adjacent nodes and subtracting twice the concentration at the target node, and then dividing by the square of the internode distance.

The final derivative that must be specified for dynamic solution of Eq.(3.1) is the time derivative. Indexing discrete points in time by t=1, 2, …n, n+1, … , where n is the current time in the simulation, the time derivative is first expressed using a simple Euler expression (forward differencing in time):

$$\frac{\partial C(i,j,n)}{\partial t} = \frac{C(i,j,n+1) - C(i,j,n)}{\Delta t} \tag{3.8}$$

Rearranging to solve for C(i,j,n+1):

$$C(i,j,n+1) = C(i,j,n) + \frac{\partial C(i,j,n)}{\partial t}\Delta t \tag{3.9}$$

Finally, substituting for the terms on the right hand side of Eq. (3.1), including the central difference expressions for the advection term, the following equation is obtained:

$$C(i,j,n+1) = C(i,j,n) + \Delta t\left\{-v_x\left[\frac{C(i+1,j,n)-C(i-1,j,n)}{2\Delta x}\right] - v_y\left[\frac{C(i,j+1,n)-C(i,j-1,n)}{2\Delta y}\right]\right.$$
$$\left. + D_x\left[\frac{C(i+1,j,n)-2C(i,j,n)+C(i-1,j,n)}{(\Delta x^2)}\right] + D_y\left[\frac{C(i,j+1,n)-2C(i,j,n)+C(i,j-1,n)}{(\Delta y)^2}\right]\right\} \tag{3.10}$$

Equation (3.10) is explicit, that is, C(i,j,n+1) at node i,j at time step n+1 is computed solely from values of c available at the current time n, at node i,j and the four surrounding nodes. While relatively easy to implement, explicit solutions may exhibit problems with stability. This is the basic equation used in this thesis study for numerically approximating solute concentrations in the boreholes of the akaki wellfield. Though not used for this study, a fully implicit & partial implicit methods are discussed below.

The stability criteria for the various terms in equation 3.10 are given by:

$$\Delta t \le \frac{1}{|v_x|/\Delta x + |v_y|/\Delta y}$$ for the advective term, and

$$\Delta t \le \frac{0.5}{D_x/(\Delta x^2) + D_y/(\Delta y^2)}$$ for the dispersive term

A fully implicit solution defines all terms in the time derivatives, $\partial C/\partial t$, using concentrations (and model inputs and parameters) at time n+1. The fully implicit equivalent of Eq.(3.10) is given by:

$$C(i,j,n+1)=C(i,j,n)+\Delta t\left\{-v_x\left[\frac{C(i+1,j,n+1)-C(i-1,j,n+1)}{2\Delta x}\right]-v_y\left[\frac{C(i,j+1,n+1)-C(i,j-1,n+1)}{2\Delta y}\right]\right.$$
$$\left.+D_x\left[\frac{C(i+1,j,n+1)-2C(i,j,n+1)+C(i-1,j,n+1)}{(\Delta x^2)}\right]+D_y\left[\frac{C(i,j+1,n+1)-2C(i,j,n+1)+C(i,j-1,n+1)}{(\Delta y)^2}\right]\right\} \quad (3.11)$$

If model inputs u, D_x, D_y, and k vary with time, their values at time n+1 would also be used in Eq.(3.10).

A partially implicit solution defines the time derivative as a weighted average of values computed using concentrations (and model inputs) at times n and n+1:

$$C(i,j,n+1)=C(i,j,n)+\Delta t\left\{\alpha\frac{\partial C}{\partial t}\Big|_{n+1}+(1-\alpha)\frac{\partial C}{\partial t}\Big|_{n}\right\} \quad (3.12)$$

The case where α =0 corresponds to the explicit method, α=1 to the fully implicit method, and 0 < α <1 to a partially implicit solution. The special case in which α =0.5 is known as the Crank-Nicolson method. The partially implicit solution corresponding to the explicit Eq.(3.10) and the fully implicit Eq.(3.11) is

$$C(i,j,n+1)=C(i,j,n)+\Delta t\alpha\left\{-v_x\left[\frac{C(i+1,j,n+1)-C(i-1,j,n+1)}{2\Delta x}\right]-v_y\left[\frac{C(i,j+1,n+1)-C(i,j-1,n+1)}{2\Delta y}\right]+\right.$$
$$\left.D_x\left[\frac{C(i+1,j,n+1)-2C(i,j,n+1)+C(i-1,j,n+1)}{(\Delta x^2)}\right]+D_y\left[\frac{C(i,j+1,n+1)-2C(i,j,n+1)+C(i,j-1,n+1)}{(\Delta y)^2}\right]\right\}+ \quad (3.13)$$
$$\Delta t(1-\alpha)\left\{-v_x\left[\frac{C(i+1,j,n+1)-C(i-1,j,n+1)}{2\Delta x}\right]-v_y\left[\frac{C(i,j+1,n+1)-C(i,j-1,n+1)}{2\Delta y}\right]+\right.$$
$$\left.D_x\left[\frac{C(i+1,j,n+1)-2C(i,j,n+1)+C(i-1,j,n+1)}{(\Delta x^2)}\right]+D_y\left[\frac{C(i,j+1,n+1)-2C(i,j,n+1)+C(i,j-1,n+1)}{(\Delta y)^2}\right]\right\}$$

Implicit or partially implicit solution methods are very effective at maintaining stability. However, they increase the computational burden significantly. For a system with N total nodes, a set of N simultaneous equation must be solved at each time step. First though, the remaining building blocks of the solution, the initial and boundary condition, must be specified.

Specifications of Initial and Boundary Conditions

With any of the finite difference solution methods thus far described, *initial conditions* are needed for the model state variables (e.g. Contaminant concentrations) at all modes at time t=0 in order to initiate the computations. In some problems these conditions are

unknown or highly uncertain, especially when the model is used for long-term simulations involving historic reconstruction. Even when the primary interest is in recent, current or future values predicted by the model, historic conditions, perhaps beginning many years earlier, may be needed to initiate the calculations. In some cases accurate selection of these initial conditions may not be necessary-the model equations may have a short enough "memory" that the initial conditions do not influence the solution. This is fortunate, especially if you have little information for specifying the initial conditions. For other problems, the initial conditions do matter, and they must be determined as part of the calibration or parameter estimation process. The only way toe tell is to try solving the equations with different initial conditions and see how the solutions differ.

Boundary conditions are required to specify the system state variables and /or their derivatives(e.g. concentration and mass flux conditions) at all system boundaries, whether a dynamic or a steady-state solution is implemented. Consider the set of boundary nodes identified in Figure 3.2. Along the left-hand side of the domain (where i=1),values of C(i-1,j) are off the grid and unavailable. How then can the backward or central differencing expressions for the first derivative or the expression for the second derivative be included in the mass-balance equation since these both include C(i-1,j,t) ? Similar problems arise with the identification of C(i,j-1,t) for nodes in the last (right-hand) column, and C(i,j+1,t) for nodes along the bottom row. A creative solution is needed for this dilemma. Three types of boundary conditions may apply:

Type 1, or *Dirichlet* boundary conditions: Here the model state variables are specified, for example, the concentrations along the boundary are known (at all times).

Type 2, or *Neumann* boundary conditions: the derivatives of the model state variables are known. In the case advective-dispersive transport, this involves specifications of the spatial derivative of the concentration normal to the boundary, either $\partial C/\partial x$, $\partial C/\partial y$, or $\partial C/\partial z$.

Type 3, *Cauchy*, or mixed boundary conditions: Linear combinations of the state variables and their derivatives are specified.

When the concentrations along a boundary are known, a Dirichlet boundary condition is used. Given the fluid flow rate,Q=uA, this is equivalent to specifying the advective flux across the boundary, =uAC, where A is the cross-sectional area associated with the grid point (normal to the boundary) A Neumann boundary condition is used to specify the dispersive flux across a boundary [-DA($\partial C/\partial x$)] , since it involves fixing the value of the derivative. The total (advective +dispersive) flux across a boundary, uAC-DA($\partial C/\partial x$), is specified using a mixed boundary condition.

To implement a Dirichlet boundary condition, the concentrations along the appropriate boundary row or column are set to their known values through out the calculation. To implement a Neumann or a mixed boundary condition, image nodes are added as an extra row or column beyond the grid boundary. Concentrations at these grid points are set equal to the values necessary to maintain the known flux (total or dispersive) across the boundary. The exact equation used depends up on the type of differencing used to represent the derivatives.

3.2.2 Model Domain, Grids and Boundary Conditions

The northern, western and eastern surface water catchment boundaries are taken as *no-flow boundary*. Since the groundwater leave out the catchment in *south-east* direction towards Dukem plain, *a constant-head boundary was established at 1800 masl*. This specified head boundary extends from north-east of Dukem down to the confluence of Akaki and Awash rivers.

The Model area is *16 km*^{2}. The model grid consists of *9 columns* and *7 rows* (see Fig 3.2). The grid spacing is *500 m* in both X and Y directions in the well field. The *well field* cells have *500 m* uniform spacing. Figure 3.3 below shows the model domain selected for the solute transport study in the Akaki well field area showing the relative arrangement of the 25 boreholes managed by the Addis Ababa Water and Sewerage Authority (AAWSA). The model (study) area is the area encompassed in the rectangular shaped vicinity.

Discretization of the model area is made based on the relative location of the 25 boreholes in the wellfield (see table 3.1). The wellfield lies on 16 Km^2 area of land with around 4 km dimension in X- & 3 km in Y- direction. The borehole with the lowest X-grid coordinate (BH 05b) lies on the western boundary while that with the highest X-grid coordinate (BH 03a) lies on the eastern boundary. Similarly, the borehole with the lowest Y-grid coordinate (BH 01) lies on the southern boundary while that with the highest Y-grid coordinate (BH 03a) lies on the northern boundary.

As mentioned earlier the wellfield is situated with in the drainage basin of the streams of Dengora & Keta which join to form the Sakelo, which in turn flows to the Akaki river. The surface catchment area is bounded eastwards and southwards by a topographic limit: Volcanoes Mt. Furi, Mt. Yerer, Gara Bashu, Mt. Guji & Mt. Bilbilo. Northwards and westwards, the wellfield is bounded by the Akaki river. The boreholes are located approximately 500 m apart both in the x- & y-direction and because of this the discrete length in both directions (dx & dy) is taken as 500 m.

Chloride concentrations at the western boundary of the model area are observed to be time varying concentrations of *2, 1.3, 1.5, & 1.2 mg/l* for calibration period and *4 & 13 mg/l* for prediction period. Fluoride concentrations at the same boundary are time varying concentrations of *0.85, 0.49, 0.66, 0.29 & 0.51 mg/l* for calibration period and *0.82, 0.34 & 0.2 mg/l* for prediction period through out a large span of time (around ten years). Similarly, chloride concentrations at the northern boundary of the model area are observed to be time varying concentrations of *1.5, 2, 0.7, 2.5, 1.1 & 4 mg/l* for calibration period and *7.5 & 17 mg/l* for prediction period. Fluoride concentrations at this boundary are time varying concentrations of *0.75, 0.61, 0.49, 0.38, 0.31, 0.4 & 0.55 mg/l* for calibration period and *0.4 & 0.19 mg/l* for prediction period through out a large span of time (around ten years).

The eastern & southern boundaries of the wellfield, on the other hand, are set with a Newman type boundary condition as the solute gets uniformly distributed along the far end of the flow field.

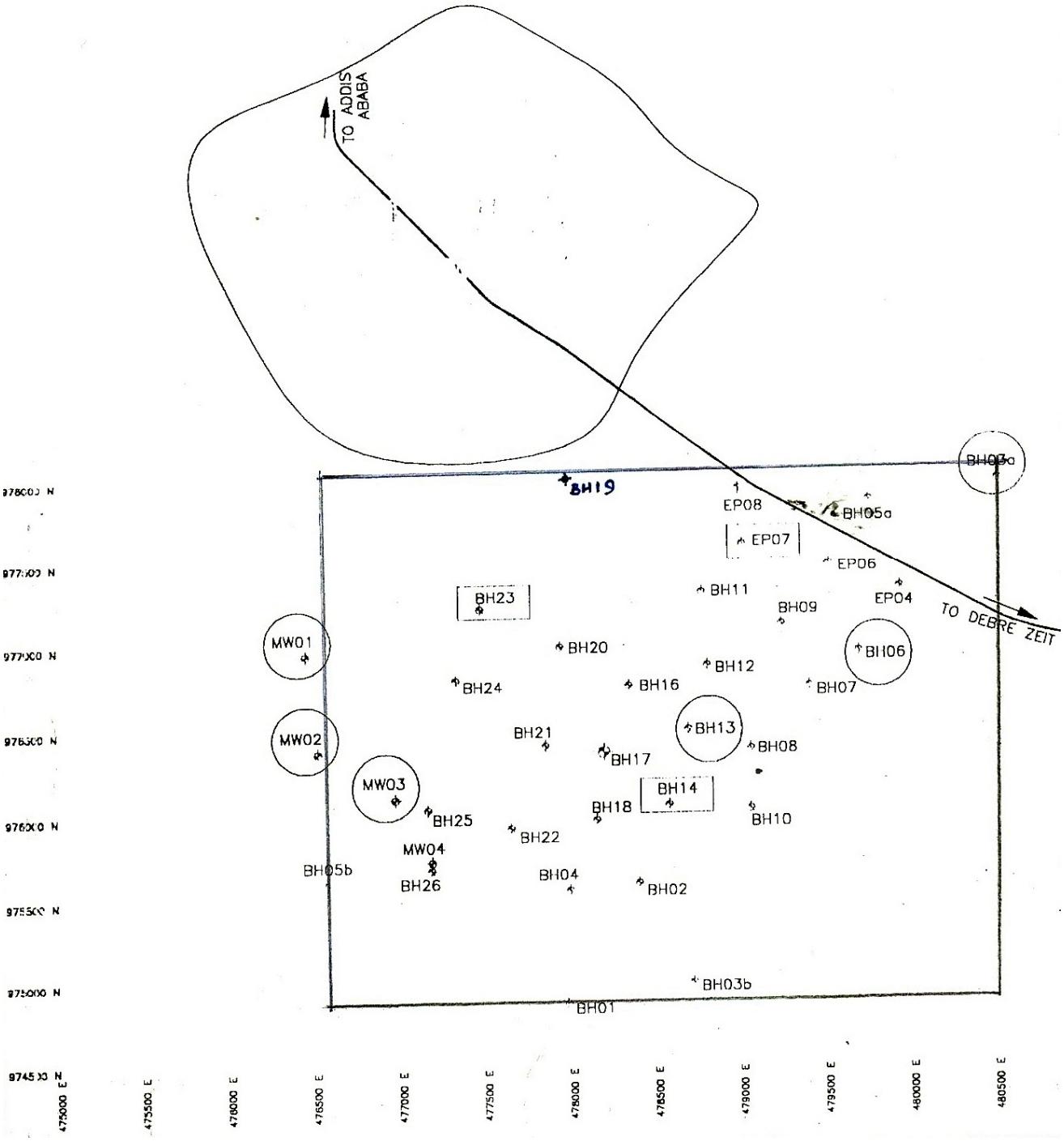

Legend:

◯ : Monitoring Wells for Water Quality

▭ : Monitoring Wells for Groundwater level

Fig 3.3 Model Area of the Akaki Well field.

Table 3.1 Discretization Scheme of the Well field.

Borehole Name	Rel X	Rel Y	(for dx=dy=500)	
			X(Col)	Y(Row)
Borehole BH01	1398	0	3.796	1
Borehole BH03	1825	730	4.65	2.46
Borehole BH03a	3943	3115	8.886	7.23
Borehole BH03b	2139	118	5.278	1.236
Borehole BH04	1418	693	3.836	2.386
Borehole BH05b	0	748	1	2.496
Borehole BH06	3122	2077	7.244	5.154
Borehole BH07	2831	1876	6.662	4.752
Borehole BH08	2487	1511	5.974	4.022
Borehole BH09	2672	2245	6.344	5.49
Borehole BH10	2484	1161	5.968	3.322
Borehole BH11	2206	2448	5.412	5.896
Borehole BH12	2234	2008	5.468	5.016
Borehole BH14	2006	1192	5.012	3.384
Borehole BH16	1773	1893	4.546	4.786
Borehole BH17	1625	1502	4.25	4.004
Borehole BH18	1580	1107	4.16	3.214
Borehole BH19	1445	2623	3.89	6.246
Borehole BH20	1371	2126	3.742	5.252
Borehole BH21	1282	1543	3.564	4.086
Borehole BH22	1077	1064	3.154	3.128
Borehole BH23	903	2357	2.806	5.714
Borehole BH24	756	1934	2.512	4.868
Borehole BH25-2	588	1179	2.176	3.358
Borehole BH26	607	821	2.214	2.642

Table 3.1 (above) shows the discretization scheme of the 25 boreholes in the wellfield scale-1:30). The 2nd & 3rd columns lists the relative X- & Y- coordinates of the boreholes with reference to the model area respectively while, the 4th & 5th columns lists nodal assignments to each borehole for a discrete length of 500 m in both directions.

3.2.3 Input Parameters to the Model & Calibration Data

Initial hydrogeologic data's for modeling the contaminant transport are listed below through Table 3.2 to 3.4, while manipulated data (based on these original data) are presented from Table 3.5 through to Table 3.7. Though, water level data varies with time,

other hydrogeologic data remain constant. For groundwater velocity calculations recent water level data are incorporated and details of the analysis are presented in section 3.3 of solute transport modeling.

Table 3.2 shows water levels at various boreholes of Akaki Well Field with two dimensional spatial description of each borehole by use of the global positioning system. These data will be used later in Table 3.6, after being interpolated, to calculate the hydraulic gradient of the area to be modeled and hence average groundwater velocity. Table 3.3 & Table 3.4 present transmissivity & aquifer lithology data respectively for selected boreholes to serve as initial data for hydraulic conductivity calculations shown in Table 3.5.

Table 3.2 Water Level Data for the 25 Boreholes in the Akaki Well Field. [20]

X(m)	Y(m)	Z, water level (m) ASL	BH owner/location Name
477972	974859	2019.6	Water III Borehole BH01
478399	975589	2019.7	Water III Borehole BH03
480517	977974	2028.7	Water III Borehole BH03a
478713	974977	2019.7	Water III Borehole BH3b
477992	975552	2019.2	Water III Borehole BH04
476574	975607	2019.5	Water III Borehole BH05b
479696	976936	2019.6	Water III Borehole BH06
479405	976735	2019.4	Water III Borehole BH07
479061	976370	2019.4	Water III Borehole BH08
479246	977104	2019.3	Water III Borehole BH09
479058	976020	2019.6	Water III Borehole BH10
478780	977307	2019.5	Water III Borehole BH11
478808	976867	2019.2	Water III Borehole BH12
478580	976051	2019.6	Water III Borehole BH14
478347	976752	2019.6	Water III Borehole BH16
478199	976361	2019.5	Water III Borehole BH17
478154	975966	2019.6	Water III Borehole BH18
478019	977482	2019.5	Water III Borehole BH19
477945	976985	2019.5	Water III Borehole BH20
477856	976402	2019.4	Water III Borehole BH21
477651	975923	2019.6	Water III Borehole BH22
477477	977216	2020.6	Water III Borehole BH23
477330	976793	2018.6	Water III Borehole BH24
477162	976038	2019.7	Water III Borehole BH25-2
477181	975680	2019.6	Water III Borehole BH26

Table 3.3 Transmissivity Data for Selected Boreholes of the Akaki Well Field. [20]

Code	Well Location name	X	Y	Water level (mASL)	Transmissivity (m^2/day)
270	Borehole BH03b	478713	974977	2019.7	15552
274	Borehole BH04	477992	975552	2019.2	9100.8
275	Borehole BH05b	476574	975607	2019.5	11923.2
276	Borehole BH06	479696	976936	2019.6	105408
277	Borehole BH07	479405	976735	2019.4	43700
278	Borehole BH08	479061	976370	2019.4	49600
282	Borehole BH12	478808	976867	2019.2	28100
284	Borehole BH14	478580	976051	2019.6	25600
286	Borehole BH17	478199	976361	2019.5	55738
289	Borehole BH20	477945	976985	2019.5	2272.32
292	Borehole BH23	477477	977216	2020.6	10791.36
293	Borehole BH24	477330	976793	2018.6	4631.04
294	Borehole BH25-2	477162	976038	2019.7	43372.8
295	Borehole BH26	477181	975680	2019.6	98800

Based on previous groundwater modeling study, porosity of the aquifers in the Akaki Wellfield is known to be around 0.35, and this value is taken as initial parameter to be calibrated later to match the observed solute concentrations in the various boreholes. The longitudinal (α_L) and transversal dispersivity (α_T) of the aquifers in the boreholes are taken initially as 1 m & 0.1 m respectively, which are again to be calibrated to match the observed values.

The transmissivity & aquifer lithology data listed below are used to calculate the hydraulic conductivity of each borehole in the wellfield. The governing empirical equation relating transmissivity, aquifer thickness, and hydraulic conductivity was discussed in previous chapter, section 2.1 and equation (2.1.2) was used for this computation. After calculation of hydraulic conductivity for each borehole in the study area, the average hydraulic conductivity of the model area is approximated by interpolation. A tabulation of this is shown in Table 3.5 later. Note that aquifer thickness and transmissivity of some of the boreholes in the wellfield are missing and calculations are made based on the available data.

Table 3.4 Aquifer Lithology Data for the 25 Boreholes in the Akaki Well Field. [20]

well code	Well Name	Location	Grid UTM E longitude X	Grid UTM N latitude Y	Elevation (mASL)	Depth (m)	Aquifer Thickness(m)
270	BH01	AWF	**477,972.857**	**974,859.574**	**2078.493**	133	27
271	BH02	AWF	**478,399.737**	**975,589.689**	**2072.49**	122	22
272	BH-03a (Abandoned)	AWF	**480,517.697**	**977,974.648**	**2100.059**	169.53	72
273	BH-03b	AWF	**478,713.309**	**974,977.481**	**2083.074**	130	16
274	BH-04	AWF	**477,992.754**	**975,552.803**	**2067.5**	125.83	26
	BH-05a (Abandoned)	AWF	**479,762.535**	**977,855.751**	**2100.517**	168.9	39
275	BH-05b	AWF	**476,574.831**	**975,607.028**	**2070.291**	142	
276	BH-06	AWF	**479,696.660**	**976,936.535**	**2086.735**	145.53	47.3
277	BH-07	AWF	**479,405.708**	**976,735.015**	**2086.025**	151	51
278	BH-08	AWF	**479,061.557**	**976,370.799**	**2086.498**	144.18	45
279	BH-09	AWF	**479,246.528**	**977,104.643**	**2077.696**	146.38	34.8
280	BH-10	AWF	**479,058.958**	**976,020.107**	**2091.215**	130	43
281	BH-11-2	AWF	**478,780.537**	**977,307.579**	**2080.046**	138	45.5
282	BH-12	AWF	**478,808.328**	**976,867.470**	**2070.601**	152.4	49.5
283	BH-13	AWF	**478,694.864**	**976,490.552**	**2074.224**	149	76
284	BH-14	AWF	**478,580.608**	**976,051.679**	**2078.562**	130	43
285	BH-16	AWF	**478,347.234**	**976,752.673**	**2067.534**	148.56	52
286	BH-17	AWF	**478,199.176**	**976,361.674**	**2065.059**	144.18	34
287	BH-18	AWF	**478,154.375**	**975,966.371**	**2073.504**	140	51
288	BH-19	AWF	**478,019.429**	**977,482.170**	**2070.186**	150.15	58
289	BH-20	AWF	**477,945.037**	**976,985.086**	**2068.297**	148.6	56

Akaki phase II well code	Well Name given during drilling	Location	Grid UTM E longitude X	Grid UTM N latitude Y	Elevation Ground (mASL)	Depth (m)	Aquifer Thickness (m)
290	BH-21	AWF	**477,856.365**	**976,402.405**	**2063.592**	151	40
291	BH-22	AWF	**477,651.572**	**975,923.577**	**2066.757**	142	47
292	BH-23	AWF	**477,477.480**	**977,216.975**	**2064.292**	145	51
293	BH-24	AWF	**477,330.427**	**976,793.113**	**2061.604**	130	28
294	BH-25-2	AWF	**477,162.775**	**976,038.564**	**2060.817**	135	48
295	BH-26	AWF	**477,181.545**	**975,680.606**	**2070.129**	116.68	33

Hydraulic gradient calculations tabulated in Table 3.6 are made so by using the X- & Y-location coordinates of each borehole. The hydraulic gradient, therefore, has two components one in the X- direction, the other in Y-direction symbolized respectively as H_x & H_y. The hydraulic gradient between two boreholes having water level BH^1_z and BH^2_z is given as:

$$H_x = \frac{BH_z^1 - BH_z^2}{BH_x^1 - BH_x^2} \tag{3.13}$$

$$H_y = \frac{BH_z^1 - BH_z^2}{BH_y^1 - BH_y^2} \tag{3.14}$$

Where BH_x^1 & BH_x^2 are the X-coordinates of borehole 1 & 2 respectively,

BH_y^1 & BH_y^2 are the Y-coordinates of borehole 1 & 2 respectively,

H_x & H_y are the X- & Y- components of the hydraulic gradient vector respectively.

Table 3.5 Average Hydraulic Conductivity of the Aquifers in the Well Field. [20]

Borehole Name	Thickness (m)	Transmissivity, T (m^2/day)	Hydraulic Conductivity, K (m^2/day)	Hydraulic Conductivity, K (m^2/month)
Borehole BH01	27	NA		
Borehole BH02	22	NA		
Borehole BH03a	72	NA		
Borehole BH03b	16	15552		
Borehole BH04	26	9100.8		
Borehole BH05a	39	NA		
Borehole BH05b	NA	11923.2		
Borehole BH06	47.3	105408		
Borehole BH07	51	43700		
Borehole BH08	45	49600		
Borehole BH09	34.8	NA		
Borehole BH10	43	NA		
Borehole BH11	45.5	NA		
Borehole BH12	49.5	28100		
Borehole BH13	76	NA		
Borehole BH14	43	25600		
Borehole BH16	52	NA		
Borehole BH17	34	55738		
Borehole BH18	51	NA		
Borehole BH19	58	NA		
Borehole BH20	56	2272.32		
Borehole BH21	40	NA		
Borehole BH22	47	NA		
Borehole BH23	51	10791.36		
Borehole BH24	28	4631.04		
Borehole BH25-2	48	43372.8		
Borehole BH26	33	98800		
Total	1037.1	504589.52		
Average	**43.2125**	**36042.1086**	**834.0067**	**50040**

Using equations (3.13) and (3.14), hydraulic gradients between every consecutive pairs of boreholes are calculated to be later interpolated yielding the average hydraulic gradient of the study area as shown in Table 3.6. H_x & H_y are listed in columns 5 & 6 as horizontal & vertical hydraulic gradient respectively of the wellfield system chosen for the study.

Table 3.6 Average Hydraulic Gradient of the Wellfield. [20]

Borehole Name	X	Y	Water Level	Horizontal Gradient	Vertical Gradient
Water III Borehole BH01	477972	974859	2019.6		
Water III Borehole BH03	478399	975589	2019.7	0.000234	0.000137
Water III Borehole BH03a	480517	977974	2028.7	0.004249	0.003774
Water III Borehole BH03b	478713	974977	2019.7	0.004989	0.003003
Water III Borehole BH04	477992	975552	2019.2	0.000693	-0.00087
Water III Borehole BH05b	476574	975607	2019.5	-0.00021	0.005455
Water III Borehole BH06	479696	976936	2019.6	3.2E-05	7.52E-05
Water III Borehole BH07	479405	976735	2019.4	0.000687	0.000995
Water III Borehole BH08	479061	976370	2019.4	0	0
Water III Borehole BH09	479246	977104	2019.3	-0.00054	-0.00014
Water III Borehole BH10	479058	976020	2019.6	-0.0016	-0.00028
Water III Borehole BH11	478780	977307	2019.5	0.00036	-7.8E-05
Water III Borehole BH12	478808	976867	2019.2	-0.01071	0.000682
Water III Borehole BH14	478580	976051	2019.6	-0.00175	-0.00049
Water III Borehole BH16	478347	976752	2019.6	0	0
Water III Borehole BH17	478199	976361	2019.5	0.000676	0.000256
Water III Borehole BH18	478154	975966	2019.6	-0.00222	-0.00025
Water III Borehole BH19	478019	977482	2019.5	0.000741	-6.6E-05
Water III Borehole BH20	477945	976985	2019.5	0	0
Water III Borehole BH21	477856	976402	2019.4	0.001124	0.000172
Water III Borehole BH22	477651	975923	2019.6	-0.00098	-0.00042
Water III Borehole BH23	477477	977216	2020.6	-0.00575	0.000773
Water III Borehole BH24	477330	976793	2018.6	0.013605	0.004728
Water III Borehole BH25-2	477162	976038	2019.7	-0.00655	-0.00146
Water III Borehole BH26	477181	975680	2019.6	-0.00526	0.000279
				-0.00818	0.016301
Average Hydraulic Gradient Value				**-0.00033**	**0.000651**

Using the results of the tabulations made earlier, the background literature for AWF and the numerical findings, a host of input parameters are presented next.

Summary of the initial inputs to the calibrative model is shown below in Table 3.7. The values in the first four rows (shown italicized) are subject to calibration in the modeling process to be described later as calibrated parameters.

Table 3.7 Summary of Initial Input Parameters to the Calibration Model

Parameter	Initial Input Value
Hydraulic Conductivity, K[m/month]	*50040*
Effective Porosity, n	*0.35*
longitudinal dispersivity, α_L[m]	*0.1*
Transversal dispersivity, α_T[m]	*0.01*
Horizontal Hydraulic Gradient, H_x	-0.00033
Vertical Hydraulic Gradient, H_y	0.000651
Model area length, Lx[m]	4000
Model area width, Ly[m]	3000
Prediction time, tmax[months]	120
Discrete length, dx[m]	500
Discrete width, dy[m]	500
Discrete time, dt[month]	1

Solute concentration data for selected boreholes which are to be used for model calibration purpose is tabulated below. These concentration data were analyzed periodically some time in the past ten years. The initial solute concentration data of Cl^- ion was found to be *3 mg/l* and that for fluoride ion was *0.51 mg/l* in 1997 E.C around most of the boreholes in the wellfield and major ions concentration at other periods for selected boreholes & monitoring wells are shown below from Table 3.8 through to Table 3.11.

For wider understanding of the solute load of the wellfield, additional data on other non-conservative anions is included in Tables 3.8 through to Table 3.11. Still, a more comprehensive detail of cationic concentration, anionic concentration, physio-chemical, and bacteriological properties of raw water data from selected boreholes in the wellfield is attached in appendix B-1 through to appendix B-5 at the back sections of this paper.

Table 3.8 Major Anions Concentrations for Borehole 06. [20]

Major Anions	Unit	Analysis Period			
		Jun. 20-22, 97	Oct.10/04	May31/05	Oct.05/05
Cl, Chloride	mg/l	3	2	2	1
NO_2, Nitrite	mg/l	0.021	<0.026	Nil	<0.026
NO_3, Nitrate	mg/l	22.8	16.66	17.8	
F, Fluoride	mg/l	0.022	0.14	0.5	0.65
HCO_3, Bicarbonate	mg/l		272.1	232	292.8
CO_3, Carbonate	mg/l		Nil	21.6	Nil
SO_4, Sulfate	mg/l	12	1.1	18	6
PO_4, Phosphate	mg/l	0.184	<0.045	0.132	0.18

Table 3.9 Major Anions Concentrations for Borehole 07. [20]

Major Anions	Unit	Analysis Period			
		Jun/ 97	Oct/04	May/05	Oct/05
Cl, Chloride	mg/l	3	2		
NO_2, Nitrite	mg/l	0.021	0.031		
NO_3, Nitrate	mg/l	22.8	21		
F, Fluoride	mg/l	0.022	0.51		
HCO_3, Bicarbonate	mg/l				
CO_3, Carbonate	mg/l				
SO_4, Sulfate	mg/l	12	2.2		
PO_4, Phosphate	mg/l	0.184	0.186		

Anionic solute load data listed here are enough for this study subject to the scopes briefed in section 1.4 of chapter one.

Note that anionic solute data for borehole BH22 tabulated in Table 3.10 below has extra data for verification of the predictive model. The last three columns of this table are therefore helpful later in analyzing the validity of the model.

Table 3.10 Major Anions Concentrations for Borehole 22. [20]

Major Anions	Unit	Analysis Period								
		Jul/03	Aug/03	Oct/03	Nov/03	Dec/03	Jan/04	Aug/07	Jan/08	May/08
Chloride	mg/l	2	1.3	1.5	1.5	1.2	1.2	2.5	2.5	2.5
Nitrite	mg/l	<0.026	<0.021	<0.026	<0.026	<0.026	<0.026	Nil	Nil	0.01
Nitrate	mg/l	7.62	<0.026	16.83	20.38	17.72	15.95	3.6	3.6	3.6
Fluoride	mg/l	0.85	0.49	0.66	0.29	0.6	0.51	0.79	0.82	0.82
Bicarbonate	mg/l	255	253.8	256.2	297.7	273.3	287.9	275.7	278.2	280.6
Carbonate	mg/l							Nil		
Sulfate	mg/l	12.2	6.1	0.5	1.4	Nil	0.9	11.4		
Phosphate	mg/l	0.09	<0.045	<0.045	<0.045	<0.045	0.1	0.37		

Table 3.11 Major Anions Concentrations for Borehole EP 08. [20]

Major Anions	Unit	May-03	Jul-03	Aug.03	Oct.03	Nov.03	Dec.03	Jan.04	Jun.04
Cl, Chloride	mg/l	1.5	2	0.7	1.5	2.5	1.5	1.1	7
NO_2, Nitrite	mg/l	<0.026	<0.026	<0.026	<0.026	<0.026	0.026	0.3	Nil
NO_3, Nitrate	mg/l	23.04	21.8	20.38	18.16	24.37	20.38	19.94	18.61
F, Fluoride	mg/l	0.75	0.61	0.49	0.38	0.31	0.4	0.55	0.4
HCO_3, Bicarbonate	mg/l							268.4	305
CO_3, Carbonate	mg/l							Nil	Nil
SO_4, Sulfate	mg/l	21	12.9	14.5	1	3.3	1.2	1.3	0.9
PO_4, Phosphate	mg/l	<0.045	0.13	<0.045	<0.045	<0.045	<0.045	0.16	0.1

3.3 Data Analysis: Conservative Transport Modeling of Akaki Well Field

Chloride & fluoride ions predictive modeling of the wellfield for the next ten years (2007-2017) is made first by calibrating the model input parameters using the available solute concentration data for selected boreholes at various periods. For calibration purpose, initial solute concentration was taken as 3 mg/l for chloride and 0.51 mg/l for fluoride in 1997 E.C and MATLAB simulation of chloride & fluoride ion concentration is made for ten years up to 2007.

Conservative solute modeling in the wellfield helps detect early potential pollution threats in the study area. For this purpose, special monitoring wells are available upstream of the well field (namely, EP 07 & BH 23) and at the central part (BH 14). Due to the fact that conservative contaminants move faster than others do and are front runners in the contaminant plume, their predictive modeling is helpful in aiding decision making on the management & remediation strategy of the wellfield before any severe pollution occurs.

Two subsections below (3.3.1 & 3.3.2) focus on the stepwise processes of the predictive solute modeling.

3.3.1 Calibration & Sensitivity Analysis of Parameters

Model calibration for solute transport is made with initial input parameters listed in Table 3.7 in previous section 3.2.3. Tables 3.8 to 3.10 of anionic concentrations for boreholes BH 06 (7, 5), BH 07 (7, 5) and BH 22 (3, 3) are used for model calibration with which MATLAB concentration outputs are to be compared. *The aim of the calibration process is to tune the input parameters to the model so that the corresponding anionic concentration values of the boreholes from the code output gets matched, as much as possible, with the actual table-listed values.*

Boundary conditions for the chloride & fluoride calibrative models are set to known boundary boreholes concentrations (fixed value-Dirichlet), as obtained from field investigations, on the northern & western boundary of the system while Newman boundary condition (zero solute flux) is assigned to the remaining eastern & southern boundaries.

For the calibration process, input parameters are tuned with two separate calibration programs one for chloride concentration and another for fluoride concentration. This helps the calibration process to be more reliable as concentration values are compared for

both chloride and fluoride in the available calibration data period. i.e. from June '97 to June '07.

The calibration program is presented below in program 3.1 for chloride ion modeling, with little difference with that for fluoride modeling which is shown in appendices of this paper. Though two independent programs are used for calibration purpose, the input parameters are tuned to the same value which best fit the observed concentration values of both species to be modeled.

A trial of many runs was made to get the model outputs nearly in agreement with the actual observed concentrations of the species to be modeled for the three boreholes selected in the wellfield; namely, BH 06 (7, 5), BH 07 (7, 5) and BH 22 (3, 3). During the process, it was found that of the four varying inputs of the model, *porosity & hydraulic conductivity are sensitive* to the model while *longitudinal & transversal dispersivities of the wellfield are less sensitive* to the model. The calibration process is made, therefore, by varying porosity (n) & hydraulic conductivity (K) values while dispersivity values are held fixed and the calibrated input parameters to the predictive model are shown in table 3.12.

Program 3.1: Program for Calibration of Parameters Using Chloride Ion.

```
format short
disp('Enter the Porosity of the Aquifers in AWF, n');
n=input('n = ');
disp('Enter the Longitudinal Dispersivity, L (m)');
L=input('L = ');
disp('Enter the Transversal Dispersivity, T (m)');
T=input('T = ');
disp('Enter the Hydraulic Conductivity of the AWF Aquifer, K (m/month)');
K=input('K = ');
Lx=4000; Ly=3000; tmax=120; dx=500; dy=500; dt=0.25; Hx=-0.00033;
```

```
Hy=0.000652; vx=(-K/n)*Hx; vy=(-K/n)*Hy; v=sqrt(vx^2+vy^2);
Dx=(L*(vx^2/v))+(T*(vy^2/v));Dy=(L*(vy^2/v))+(T*(vx^2/v));
%Stability Criterion
if (dt > 1/((abs(vx)/dx)+(abs(vy)/dy))) | (dt > 0.5/((Dx/dx^2)+(Dy/dy^2)))
      warning('The Method is not stable',...
      'Try another values of dt, dx or dy');
   return
else
nx = (Lx/dx)+1;
ny = (Ly/dy)+1;
nt = (tmax/dt)+1;
   disp('The method is stable; MATLAB now calculates the nodal concentrations @ each
time step');
%Generating the Matrix C of Chloride Concentration
   C=zeros(nx,ny,nt);
%Initial Chloride Concentration Values for Interior Nodes (Based on AWF Initial Solute Data)
   for i=2:nx-1
      for j=2:ny-1
         C(1,j,1)=2;C(i,1,1)=3;C(i,j,1)=3;C(nx,j,1)=3;C(i,ny,1)=2;
      end
   end
  %Initial Chloride Concentration Values for Corner Nodes (Based on AWF Initial Solute Data)
  C(1,1,1)=0.5*(C(1,2,1)+C(2,1,1));
  C(nx,1,1)=0.5*(C(nx,2,1)+C(nx-1,1,1));
  C(1,ny,1)=0.5*(C(1,ny-1,1)+C(2,ny,1));
  C(nx,ny,1)=0.5*(C(nx,ny-1,1)+C(nx-1,ny,1));
%Time Iteration Loop
 for k=2:nt
   for i=2:nx-1
    for j=2:ny-1
```

```
%Describing Chloride Concentration @ the Four Boundaries & Interior Nodes
    C(1,j,2:74)=2;C(1,j,75)=1.3;C(1,j,76:77)=1.5;C(1,j,78)=1.5;C(1,j,79)=1.2;C(1,j,80:121)=1.2;
    C(nx,j,k)=C(nx,j,k-1)+(-vx*dt/(2*dx)).*(C(nx,j,k-1)-C(nx-1,j,k-1))+(-vy*dt/2*dy)).*(C(nx,j+1,k-1)-
C(nx,j-1,k-1))+(dt*Dx/dx^2).*(C(nx,j,k-1)-2.*C(nx,j,k-1)+C(nx-1,j,k-1))+(dt*Dy/dy^2).*(C(nx,j+1,k-1)-
2.*C(nx,j,k-1)+C(nx,j-1,k-1));
    C(i,1,k)=C(i,1,k-1)+(-vx*dt/(2*dx)).*(C(i+1,1,k-1)-C(i-1,1,k-1))+(-vy*dt/(2*dy)).*(C(i,2,k-1)-
C(i,1,k-1))+(dt*Dx/dx^2).*(C(i+1,1,k-1)-2.*C(i,1,k-1)+C(i-1,1,k-1))+(dt*Dy/dy^2).*(C(i,2,k-1)-
2.*C(i,1,k-1)+C(i,1,k-1));
C(i,ny,2:72)=1.5;C(i,ny,73:74)=2;C(i,ny,75)=0.7;C(i,ny,76:77)=1.5;C(i,ny,78)=2.5;C(i,ny,79)=1.5;C(i,ny,8
0:84)=1.1;C(i,ny,85:121)=4;
     C(i,j,k)=C(i,j,k-1)+(-vx*dt/(2*dx)).*(C(i+1,j,k-1)-C(i-1,j,k-1))+(-vy*dt/(2*dy)).*(C(i,j+1,k-
1)-C(i,j-1,k-1))+(dt*Dx/dx^2).*(C(i+1,j,k-1)-2.*C(i,j,k-1)+C(i-1,j,k-
1))+(dt*Dy/dy^2).*(C(i,j+1,k-1)-2.*C(i,j,k-1)+C(i,j-1,k-1));
   end
  end
%Describing Chloride Concentration @ the four corner nodes of the AWF study area
  C(1,1,k)=0.5*(C(1,2,k)+C(2,1,k));
  C(nx,1,k)=0.5*(C(nx,2,k)+C(nx-1,1,k));
  C(1,ny,k)=0.5*(C(1,ny-1,k)+C(2,ny,k));
  C(nx,ny,k)=0.5*(C(nx,ny-1,k)+C(nx-1,ny,k));
 Max=(nx-2)*(ny-2);
  for i=1:Max
   error(i)=1;
  end
 error; count=0;
 tol =1E-06;
%Count Iteration Loop
 while error>tol
   for i=2:nx-1
     forj=2:ny-1
Cnew(1,j,2:74)=2;Cnew(1,j,75)=1.3;Cnew(1,j,76:77)=1.5;Cnew(1,j,78)=1.5;Cnew(1,j,79)=1.2;Cnew(1,j,80
:121)=1.2;
```

```
Cnew(nx,j,k)=C(nx,j,k-1)+(-vx*dt/(2*dx)).*(C(nx,j,k-1)-C(nx-1,j,k-1))+(-vy*dt/2*dy)).*(C(nx,j+1,k-1)-
C(nx,j-1,k-1))+(dt*Dx/dx^2).*(C(nx,j,k-1)-2.*C(nx,j,k-1)+C(nx-1,j,k-1))+(dt*Dy/dy^2).*(C(nx,j+1,k-1)-
2.*C(nx,j,k-1)+C(nx,j-1,k-1));
Cnew(i,1,k)=C(i,1,k-1)+(-vx*dt/(2*dx)).*(C(i+1,1,k-1)-C(i-1,1,k-1))+(-vy*dt/(2*dy)).*(C(i,2,k-1)-C(i,1,k-
1))+(dt*Dx/dx^2).*(C(i+1,1,k-1)-2.*C(i,1,k-1)+C(i-1,1,k-1))+(dt*Dy/dy^2).*(C(i,2,k-1)-2.*C(i,1,k-
1)+C(i,1,k-1));
Cnew(i,ny,2:72)=1.5;Cnew(i,ny,73:74)=2;Cnew(i,ny,75)=0.7;Cnew(i,ny,76:77)=1.5;Cnew(i,ny,78)=2.5;Cn
ew(i,ny,79)=1.5;Cnew(i,ny,80:84)=1.1;Cnew(i,ny,85:121)=4;
Cnew(i,j,k)=C(i,j,k-1)+(-vx*dt/(2*dx)).*(C(i+1,j,k-1)-C(i-1,j,k-1))+(-vy*dt/(2*dy)).*(C(i,j+1,k-1)-C(i,j-
1,k-1))+(dt*Dx/dx^2).*(C(i+1,j,k-1)-2.*C(i,j,k-1)+C(i-1,j,k-1))+(dt*Dy/dy^2).*(C(i,j+1,k-1)-2.*C(i,j,k-
1)+C(i,j-1,k-1));
    end
   end
   Cnew(1,1,k)=0.5*(C(1,2,k)+C(2,1,k));
   Cnew(nx,1,k)=0.5*(C(nx,2,k)+C(nx-1,1,k));
   Cnew(1,ny,k)=0.5*(C(1,ny-1,k)+C(2,ny,k));
   Cnew(nx,ny,k)=0.5*(C(nx,ny-1,k)+C(nx-1,ny,k));
   for i=2:nx-1
      for j=2:ny-1
         error=abs((Cnew(i,j,k)-C(i,j,k))./Cnew(i,j,k));
         count=count+1;
         C(i,j,k)=Cnew(i,j,k);
      end
   end
   Cnew;
  end
 end
end
format short
 Cnew
```

3.3.2 Model Prediction and Validation

With calibrated input parameters to the predictive modeling now being evaluated (as in Table 3.12), prediction of both species (chloride & fluoride) is the next task to be carried out for the period selected. i.e. from June 2007 up to June 2017. The rationale behind the selection of this period is that:

- ✓ The initial period of prediction should be such that it is some time earlier than the current period to be able to validate the model with the recent available primary data from the results of laboratory analysis.
- ✓ A relatively moderate period of prediction (10 yrs) should be used as there are uncertainties in future groundwater circumstances in which sudden pollution around the nearby Addis – Debrezeit main road or toxic infiltration in to the wellfield may occur.

Table 3.12 Calibrated Input Parameters to the Predictive Model

Parameter	Initial Input Value
Hydraulic Conductivity, K[m/month]	*54500*
Effective Porosity, n	*0.33*
longitudinal dispersivity, α_L[m]	*1*
Transversal dispersivity, α_T[m]	*0.1*
Prediction time, tmax[months]	120
Discrete length, dx[m]	500
Discrete width, dy[m]	500
Discrete time, dt[month]	0.25

For prediction purpose, laboratory analysis of groundwater samples from ten selected boreholes of the wellfield, namely: BH04, BH07, BH10, BH14, BH16, BH20, BH23, BH24, BH25 and BH26 is made to make the predictive model valid for the current chloride & fluoride concentration values observed in the boreholes. The results of the

laboratory works, which are chloride & fluoride concentration values of the selected boreholes for the month of July 2009, to be used for model validation, are shown below in Table 3.13.

Table 3.13 Major Anions Concentrations at Selected Boreholes for July 2009 (k=101)

Major Anions	Unit	BH04	BH07	BH10	BH14	BH16	BH20	BH23	BH24	BH25	BH26
Cl^-	mg/l		9.5	9.5		11.0	14.0	14.5		10.5	
NO_2^-	mg/l	--	0.002	0.014	0.004	0.007	0.006	0.002	0.004	0.002	0.004
F^-	mg/l	0.47	0.26	0.25	--	0.41	0.43	0.58	0.24	0.54	0.2
NH_3^-	mg/l	--	0.015	0.005	0.003	--	--	--	0.036	--	--
SO_4^{2-}	mg/l	8.5	6.0	4.4	7.4	10.9	16.5	15	12.5	10.4	11.9
PO_4^{3-}	mg/l	0.529	0.445	0.42	0.396	0.407	0.37	0.352	0.441	0.344	0.389

As with model calibration, the predictive modeling is made for two groundwater species concentrations, chloride & fluoride concentrations, for reasons to be explained in the later section. The final time step outputs of the calibrative model are taken as initial values for the predictive modeling.

Boundary conditions for the predictive modeling (with similar profile as the calibrative model boundary type) are time varying, that is solute input to the system are changing with time. This is because:

1) Solute infiltration rate in to the groundwater system is higher in the summer than is in the dry season.

2) Solute release in to the study area is increasing from time to time attributable to the fact that artificial generation of the conservative ions is taking place somewhere in the vicinity of the Akaki river catchment.

The program for validated model of chloride prediction is presented below in program 3.2 while that for fluoride prediction is attached in the appendices.

Program 3.2 Program for Validated Chloride Prediction Model

```
% Fully Explicit Method for Chloride Prediction
format short
%Varying Input Strings
disp('Enter the Porosity of the Aquifers in AWF, n');
n=input('n = ');
disp('Enter the Longitudinal Dispersivity, L (m)');
L=input('L = ');
disp('Enter the Transversal Dispersivity, T (m)');
T=input('T = ');
disp('Enter the Hydraulic Conductivity of the AWF Aquifer, K (m/month)');
K=input('K = ');
%Discretization Scheme, Groundwater Velocity & Dispersion Coefficients
Lx=4000; Ly=3000; tmax=120; dx=500; dy=500; dt=0.25; Hx=-0.00033;
Hy=0.000652; vx=(-K/n)*Hx; vy=(-K/n)*Hy; v=sqrt(vx^2+vy^2);
Dx=(L*(vx^2/v))+(T*(vy^2/v));Dy=(L*(vy^2/v))+(T*(vx^2/v));
%Stability Criterion
if (dt > 1/((abs(vx)/dx)+(abs(vy)/dy))) | (dt > 0.5/((Dx/dx^2)+(Dy/dy^2)))
      warning('The Method is not stable',...
      'Try another values of dt, dx or dy');
      return
else
nx = (Lx/dx)+1;
ny = (Ly/dy)+1;
nt = (tmax/dt)+1;
   disp('The method is stable; MATLAB now calculates the nodal concentrations @ each
time step');
%Generating the Matrix C of Chloride Concentration
   C=zeros(nx,ny,nt);
%Initial Chloride Concentration Values for Interior Nodes in June 07
```

```
  for i=2:nx-1
     for j=2:ny-1
        C(1,j,1)=2;C(i,1,1)=2;C(i,j,1)=2.5;C(nx,j,1)=2;C(i,ny,1)=4;
     end
  end
%Initial Chloride Concentration Values for Corner Nodes in June 07
  C(1,1,1)=0.5*(C(1,2,1)+C(2,1,1));
  C(nx,1,1)=0.5*(C(nx,2,1)+C(nx-1,1,1));
  C(1,ny,1)=0.5*(C(1,ny-1,1)+C(2,ny,1));
  C(nx,ny,1)=0.5*(C(nx,ny-1,1)+C(nx-1,ny,1));
%Time Iteration Loop
for k=2:nt
   for i=2:nx-1
    for j=2:ny-1
%Describing Chloride Concentration @ the Four Boundaries
C(1,j,2:65)=4;C(1,j,66:481)=13;
C(nx,j,k)=C(nx,j,k-1)+(-vx*dt/(2*dx)).*(C(nx,j,k-1)-C(nx-1,j,k-1))+(-vy*dt/2*dy)).*(C(nx,j+1,k-1)-C(nx,j-
1,k-1))+(dt*Dx/dx^2).*(C(nx,j,k-1)-2.*C(nx,j,k-1)+C(nx-1,j,k-1))+(dt*Dy/dy^2).*(C(nx,j+1,k-1)-
2.*C(nx,j,k-1)+C(nx,j-1,k-1));
    C(i,1,k)=C(i,1,k-1)+(-vx*dt/(2*dx)).*(C(i+1,1,k-1)-C(i-1,1,k-1))+(-vy*dt/(2*dy)).*(C(i,2,k-1)-C(i,1,k-
1))+(dt*Dx/dx^2).*(C(i+1,1,k-1)-2.*C(i,1,k-1)+C(i-1,1,k-1))+(dt*Dy/dy^2).*(C(i,2,k-1)-2.*C(i,1,k-
1)+C(i,1,k-1));
C(i,ny,2:65)=7.5;C(i,ny,66:481)=17;
%Describing Chloride Concentration @ the Interior Nodes
C(i,j,k)=C(i,j,k-1)+(-vx*dt/(2*dx)).*(C(i+1,j,k-1)-C(i-1,j,k-1))+(-vy*dt/(2*dy)).*(C(i,j+1,k-1)-
C(i,j-1,k-1))+(dt*Dx/dx^2).*(C(i+1,j,k-1)-2.*C(i,j,k-1)+C(i-1,j,k-1))+(dt*Dy/dy^2).*(C(i,j+1,k-
1)-2.*C(i,j,k-1)+C(i,j-1,k-1));
    end
   end
```

```
%Describing Chloride Concentration @ the four corner nodes of the AWF study area
  C(1,1,k)=0.5*(C(1,2,k)+C(2,1,k));
  C(nx,1,k)=0.5*(C(nx,2,k)+C(nx-1,1,k));
  C(1,ny,k)=0.5*(C(1,ny-1,k)+C(2,ny,k));
  C(nx,ny,k)=0.5*(C(nx,ny-1,k)+C(nx-1,ny,k));
 end
end
format short
C

%Cl Conc Verifications for Boreholes BH07, BH10, BH16, BH20, BH22 & BH25
disp('C(:,:,9)');C(:,:,9),disp('C(:,:,29)');C(:,:,29),disp('C(:,:,45)');C(:,:,45),
disp('C(:,:,65)');C(:,:,65),disp('C(:,:,77)');C(:,:,77),disp('C(:,:,101)');C(:,:,101),

%Sketching the Spatial Concentration Distribution of Chloride @ the end of June 17
figure (1)
X=[0:dx:Lx];
Y=[0:dy:Ly];
D=C(:,:,nt);Cend=D'
surf(X,Y,Cend)
colormap hsv
colorbar
xlabel('X, East Length of the AWF in m')
ylabel('Y, North Length of the AWF in m')
zlabel('Cend, Conc in mg/l')
title('Concentration profile @ the end of June 2017')

%Plotting Chloride Concentration of Selected Boreholes Vs Prediction Time
figure (2)
%t=1:dt:nt
```

```
for t=1:nt
%C07=C(7,5,:)
   time(t)=((t-1)/4)+1;
   C07(t)=C(7,5,t);
end
plot(time,C07);
grid on
xlabel('t, Time in months')
ylabel('C07, Cl Conc Profile @ Borehole 07 in mg/l')
figure (3)
%t=1:dt:nt
for t=1:nt
%C10=C(6,3,:)
   time(t)=((t-1)/4)+1;
   C10(t)=C(6,3,t);
end
plot(time,C10);
grid on
xlabel('t, Time in months')
ylabel('C10, Cl Conc Profile @ Borehole 10 in mg/l')
figure (4)
%t=1:dt:nt
for t=1:nt
%C16=C(5,5,:)
   time(t)=((t-1)/4)+1;
   C16(t)=C(5,5,t);
end
plot(time,C16);
grid on
xlabel('t, Time in months')
```

```
ylabel('C16, Cl Conc Profile @ Borehole 16 in mg/l')
figure (5)
%t=1:dt:nt
for t=1:nt
%C20=C(4,5,:)
   time(t)=((t-1)/4)+1;
   C20(t)=C(4,5,t);
end
plot(time,C20);
grid on
xlabel('t, Time in months')
ylabel('C20, Cl Conc Profile @ Borehole 20 in mg/l')
figure (6)
%t=1:dt:nt
for t=1:nt
   time(t)=((t-1)/4)+1;
   C22(t)=C(3,3,t);
end
plot(time,C22);
grid on
xlabel('t, Time in Months')
ylabel('C22, Cl Conc Profile @ Borehole 22 in mg/l')
figure (7)
%t=1:dt:nt
for t=1:nt
%C25=C(2,3,:)
   time(t)=((t-1)/4)+1;
   C25(t)=C(2,3,t);
end
plot(time,C25);
```

```
grid on
xlabel('t, Time in months')
ylabel('C25, Cl Conc Profile @ Borehole 25 in mg/l')
figure (8)
%t=1:dt:nt
for t=1:nt
   time(t)=((t-1)/4)+1;
   C07(t)=C(7,5,t);C10(t)=C(6,3,t);C16(t)=C(5,5,t);
end
plot(time,C07,time,C10,time,C16);
grid on
xlabel('t, Time in Months')
ylabel('C, Cl Conc Profile @ Selected Boreholes in mg/l')
figure (9)
%t=1:dt:nt
for t=1:nt
   time(t)=((t-1)/4)+1;
   C20(t)=C(4,5,t);C22(t)=C(3,3,t);C25(t)=C(2,3,t);
end
plot(time,C20,time,C22,time,C25);
grid on
xlabel('t, Time in Months')
ylabel('C, Cl Conc Profile @ Selected Boreholes in mg/l')
```

In addition to the laboratory work results (Table 3.13), chloride and fluoride ion concentrations for the months of August 2007 (k=9, where k is the corresponding time step in the predictive modeling), January 2008 (k=29) and May 2008 (k=45) for borehole BH 22 are available inTtable 3.10 in previous section for model validation since these months are with in the prediction period. Table 3.14 below gives another tabulation of

past anionic concentrations of selected boreholes for the month of October 2008 (k=65) which will be valuable in the validation of the model.

Table 3.14 Major Anionic Concentrations at Selected Boreholes for October 2008 (k=65)

Major Anions	Unit	BH 04	BH 06	BH 14	BH 16	BH 23	BH 24
Cl, Chloride	mg/l	3.5	3.5	2.5	4.0	6.5	2.5
NO_2, Nitrite	mg/l	--	--	--	--	--	--
NO_3, Nitrate	mg/l	2.9	3.3	3	2.4	1.6	4.3
F, Fluoride	mg/l	0.18	0.34	0.21	0.33	--	--
HCO_3, Bicarbonate	mg/l	240	240	240	260	270	290
CO_3, Carbonate	mg/l	--	--	--	--	--	--
SO_4, Sulfate	mg/l	7.3	7.7	5.5	13.1	11.4	12.6

With analysis of data made so far for conservative ions (namely: Cl^- & F^-) transport in the Akaki wellfield, discussion of the findings of the modeling analysis is devoted to the next chapter.

4. Results and Discussions

This chapter will focus on the results of the findings of chloride and fluoride ions simulation. The first section (4.1) details chloride ion simulation results of the wellfield through out the prediction period with a brief discussion of the anion's spatial & temporal distribution. Section 4.2 is devoted to the results of fluoride ion simulation.

4.1 Chloride Ion Simulation Results

The simulation of chloride ion in the wellfield throughout the prediction period is validated using the available observed concentrations at selected boreholes (BH07, BH10, BH16, BH20, BH22, BH23, and BH25) and time steps (Jan.2008, Oct.2008, and Jul.2009). Table 4.1 below shows comparisons of the observed & computed chloride concentrations in the wellfield. It can be shown from the table that the *observed & computed values agree more or less to a reasonable degree* with an average of 13.66 % error. In terms of groundwater modeling these errors are low since solute transport modeling are subject to irregularities due to one or more of the following reasons:

- ✓ Setting boundary conditions of the study area over longer period of time span can not definitely be accurate as new settings are expected to appear with time.
- ✓ Hydrogeological basis used for the study couldn't exactly describe what actually is in the sub-surface system. As an explanation, heterogeneity of the aquifer's geological structure can significantly affect the simulation results which are based on uniform geology basis.
- ✓ *Climate change* can significantly influence groundwater flow to affect the results.

Table 4.1 Comparison of Observed and Computed Chloride Concentrations

Period	Observed Vs Computed	BH 04	BH 07	BH 14	BH 22	BH 23	BH 24
Jan. 2008 (k=29)	Observed Chloride (mg/l)				2.5		
	Computed Chloride(mg/l)				2.5		
Oct. 2008 (k=65)	Observed Chloride (mg/l)	3.5	4.0	2.5		6.5	2.5
	Computed Chloride(mg/l)	3.1	6.8	3.4		7.7	6.5
July. 2009 (k=101)	Observed Chloride (mg/l)	9.5	9.5	9.5		14.5	13.0
	Computed Chloride(mg/l)	5.1	11.6	7.0		15.5	11.3

Validated simulation of chloride ion in the wellfield show that chloride ion distribution through out the wellfield at the end of the prediction period (June 2017) varies between 12.86 mg/l to 18.01 mg/l as shown in Table 4.2 below. It is obvious to see from the table & Fig 4.1 that the farthest areas in the direction of the groundwater flow (i.e south-western parts of the wellfield) have relatively lower chloride concentrations. In general at any time, these parts have lower concentrations because for the solute to travel these areas it will take more time than for other areas of the wellfield and moreover, as these areas are bounded by no flow boundaries, solute transport mechanism is largely due to dispersion which hampers the overall solute movement. The concentration distribution also shows that chloride ion is getting higher in the wellfield than previous concentrations in early periods of prediction time - in agreement with the possible condition of solute generation in the akaki river catchment by man made activities. Among the reasons that might be responsible for this are:

- ✓ Chloride release from pit latrines in the vicinity of the Akaki river catchment.
- ✓ Dissociation of chloride salts in the catchment.

Though the WHO (World Health Organization) level of drinking water aesthetic quality for chloride is ***250 mg/l***, chloride concentrations may exceed this level in prolonged period of time. *The wellfield is, however, safe with respect to chloride in the ten year predictive period of 2007-2017.*

Table 4.2 Spatial Chloride Concentration Distribution at the End of June 2017

Y(m) \ X(m)	0	500	1000	1500	2000	2500	3000	3500	4000
0	12.99	12.98	13.26	15.03	16.34	16.02	17.46	16.65	17.01
500	13.00	12.86	14.44	16.36	16.79	16.83	17.34	16.67	17.38
1000	13.00	13.39	15.41	15.97	16.43	16.93	16.78	17.14	17.36
1500	13.00	13.68	16.11	16.51	17.20	17.34	17.84	17.70	17.14
2000	13.00	15.11	16.69	16.60	16.63	16.82	16.95	18.01	17.18
2500	13.00	16.40	16.62	17.01	17.43	17.43	17.38	17.27	17.41
3000	15.00	17.00	17.00	17.00	17.00	17.00	17.00	17.00	17.20

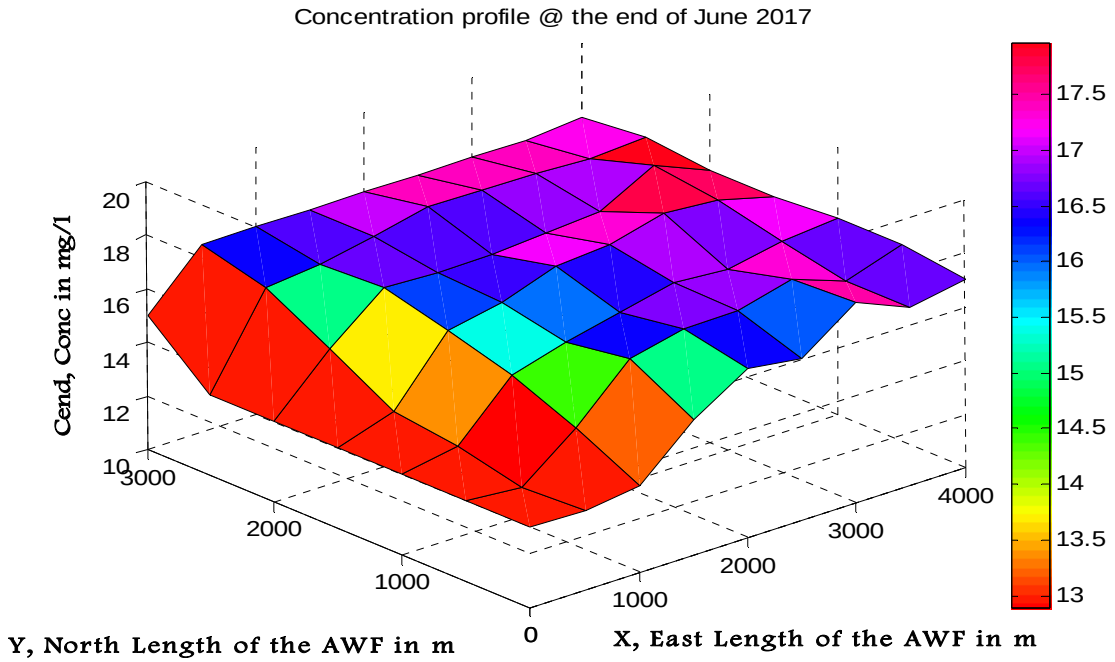

Fig 4.1 Chloride concentration Surface Plot of the Wellfield at the End of June 2017

The surface plot of the chloride distribution at the end of June 2017 in the wellfield is shown above in Fig 4.1.

Chloride breakthrough curves for each selected boreholes BH07, BH10, BH16, BH20, BH22 and BH25 are shown from Fig 4.2 through to Fig 4.7 while the first & last three borehole's superimposed curves are shown in Fig 4.8 & Fig 4.9 respectively.

From Fig 4.2 it can be seen that chloride concentration at borehole BH07 decreases at the early period of the prediction time later to increase uniformly through to nearly the 40th month prediction time. The uniform increase in chloride concentration (to about 18 mg/l) up to the 40th month period is because of an influx of chloride through the system's northern & western boundaries. After 40th month, the concentration gets decreased to almost 16.5 mg/l and then fluctuates between narrow ranges to show the influx chloride widely distributed to other boreholes. The slight ups and downs later around the end of the prediction time are certainly the periodic changes due to solute infiltration variations.

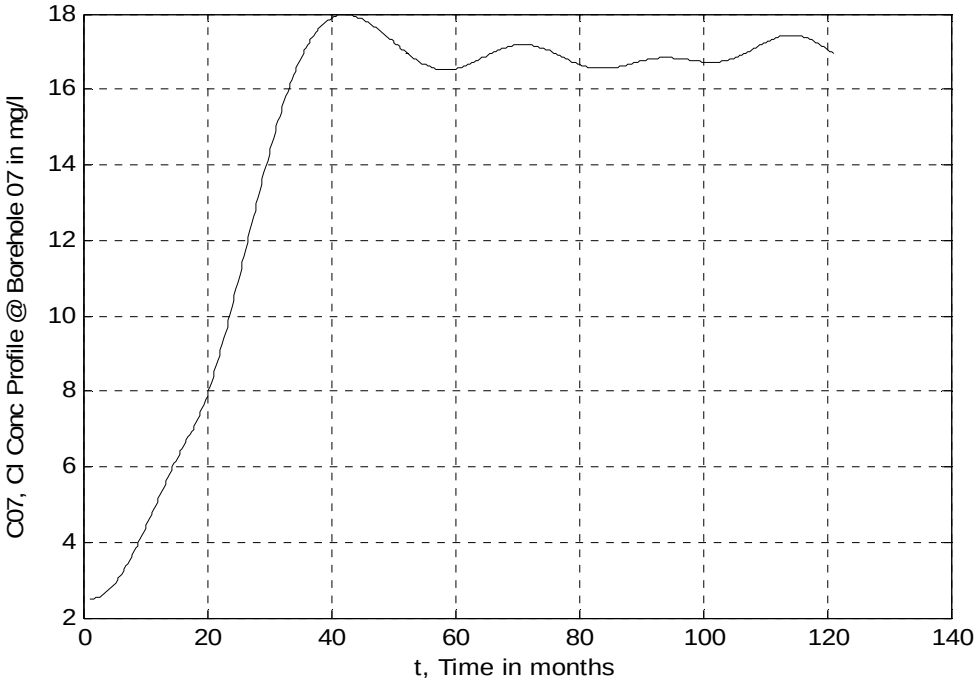

Fig 4.2 Chloride Breakthrough Curve for Borehole BH07

Figures 4.3 & 4.4 show chloride concentrations for boreholes BH10 & BH16 respectively where concentrations reach around 18 mg/l for BH10 at later times than that for BH07. A contaminant plume is expected to attain its peak at the center-borehole (BH16) after it causes contamination to downstream boreholes (BH10 & BH07). Peak chloride concentration of 18 mg/l is attained for borehole BH10 at relatively higher time than BH07 (around 80^{th} month) because BH10 is located downstream of BH07-thus solute reaches BH10 after it contaminates BH07. The peak chloride concentration for borehole BH16 is attained at a relatively lower time step (around 40^{th} month) than that for BH10 because BH16 is located nearer to the western & northern solute influx boundaries than BH10 before eventually the solute gets widely distributed throughout the far edge boreholes (BH10).

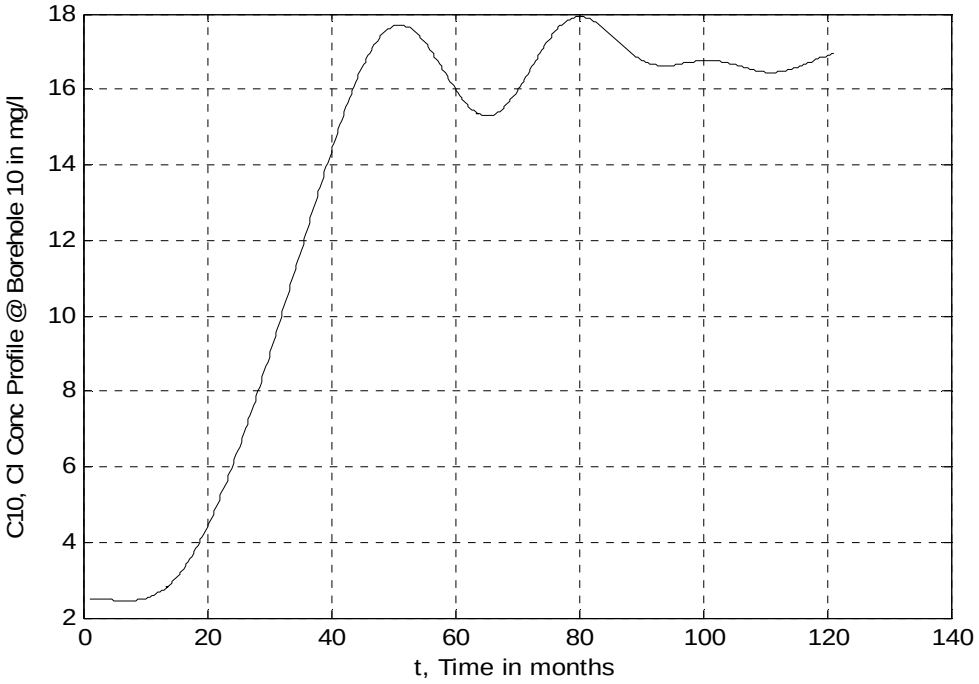

Fig 4.3 Chloride Breakthrough Curve for Borehole BH10

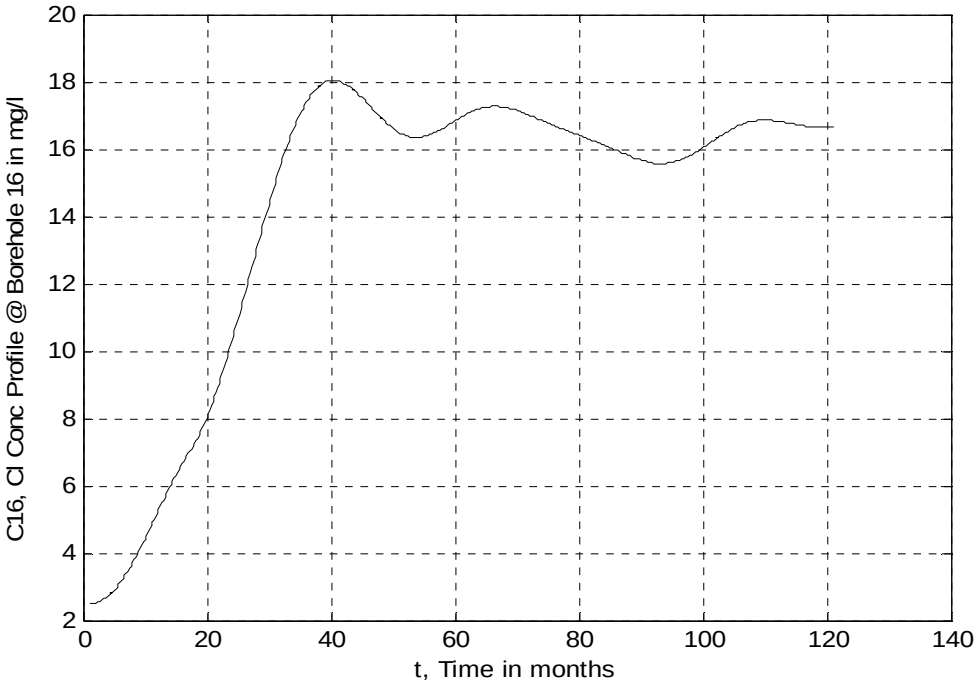

Fig 4.4 Chloride Breakthrough Curve for Borehole BH16

A look at the breakthrough curve on Fig 4.5 for borehole BH20 shows nearly similar pattern as that for borehole BH07 & BH16, primarily because all are located nearly at similar latitude where major groundwater flow is in the north-south direction.

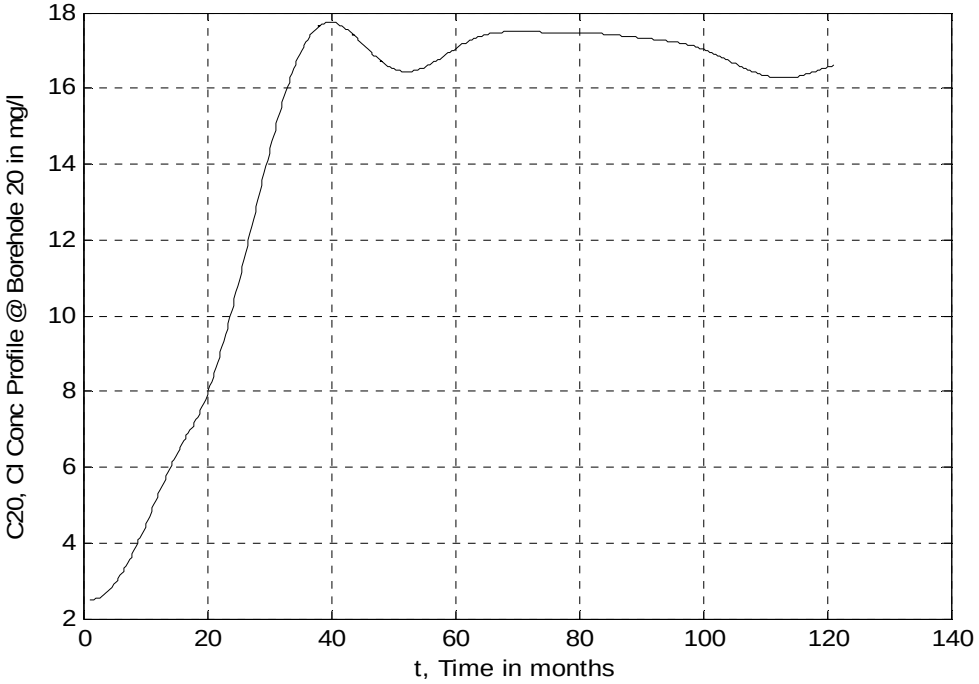

Fig 4.5 Chloride Breakthrough Curve for Borehole BH20

Chloride breakthrough curves for boreholes BH22 & BH25 shown in Figures 4.6 & 4.7 exhibit similar behaviors with nearly no fluctuations for chloride concentrations once local peak values are attained. During the uniform increase period, it can be seen that, at any given time, concentrations are higher at boreholes BH20 & BH25 than those at borehole BH22. This is because, again, the formers are in near distance to the solute influx boundaries than the latter. That is, BH25, the nearest borehole to the influx boundary, gets more solute (chloride) in a given time than BH20; BH20 in turn gets more solute in a given time than BH22 gets. However, after the solute gets distributed through out the wellfield boreholes, BH22 (nearer to the no-flow boundaries) attains higher chloride concentrations than BH25.

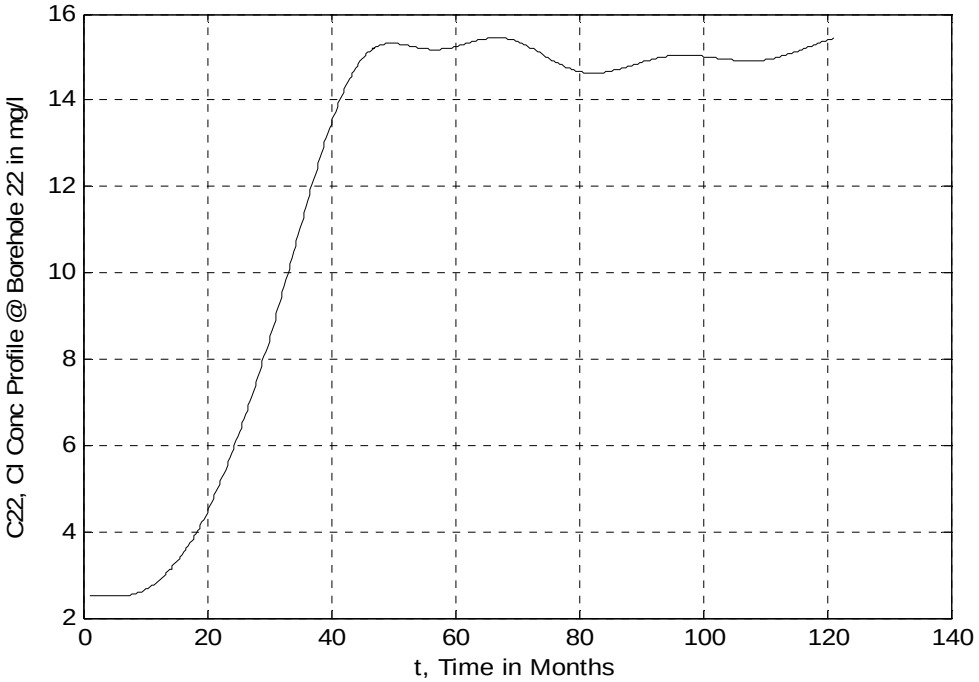

Fig 4.6 Chloride Breakthrough Curve for Borehole BH22

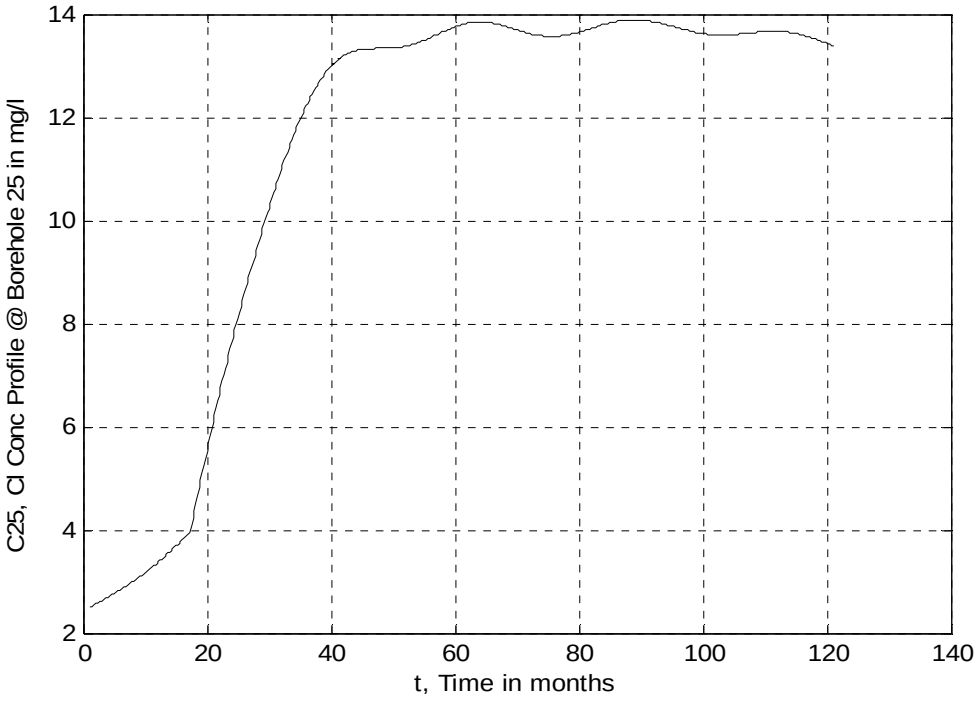

Fig 4.7 Chloride Breakthrough Curve for Borehole BH25

Figures 4.8 & 4.9 show simultaneous plots of chloride breakthrough curves for BH07-BH10- BH16 and BH20-BH22-BH25 respectively to see the relative characteristics of chloride concentrations at the boreholes.

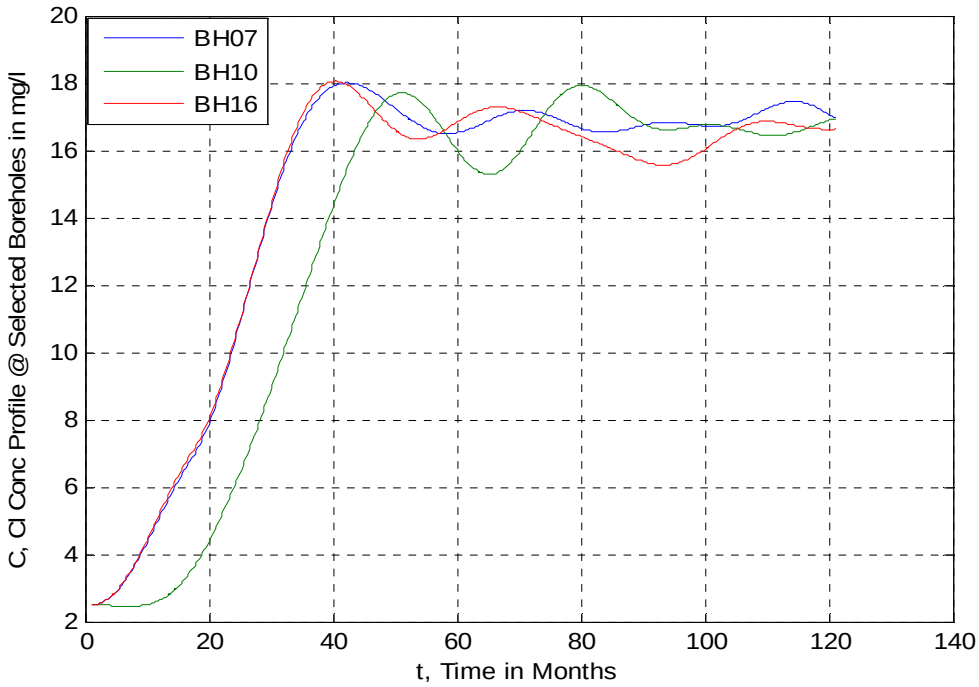

Fig 4.8 Superimposed Chloride Breakthrough Curves for Boreholes 07-10-16

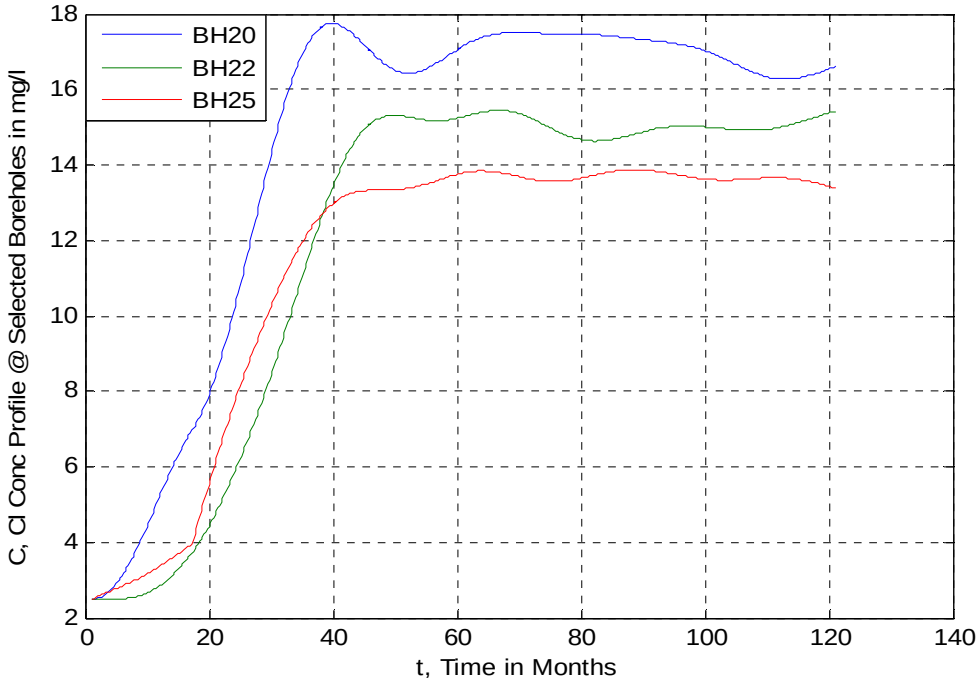

Fig 4.9 Superimposed Chloride Breakthrough Curves for Boreholes 20-22-25

4.2 Fluoride Ion Simulation Results

Discussion of fluoride ion simulation follows below in a similar fashion as with chloride simulation results. The results of the fluoride ion simulation are, once again, verified with the observed selected boreholes fluoride concentrations. For fluoride ion validation, as with chloride, the latest available fluoride laboratory data was on July. 2009 (k=101).

Tabulation of observed & computed fluoride concentrations is shown below in Table 4.3. Except for slight variations, it can be seen that computed fluoride concentrations fits to a reasonable match with the actual observed ones. Reasons for this slight fluoride variation in some boreholes are as indicated before for chloride in section 4.1.

Table 4.3 Comparison of Observed and Computed Fluoride Concentrations

Period	Observed Vs Computed	BH 04	BH 06	BH 07	BH 16	BH 22	BH 25	BH 26
Aug. 2007 (k=9)	Observed (mg/l)					0.79		
	Computed (mg/l)					0.40		
Jan. 2008 (k=29)	Observed (mg/l)					0.82		
	Computed (mg/l)					0.42		
Oct. 2008 (k=65)	Observed (mg/l)	0.18	0.34	nil	0.33		0.47	0.34
	Computed (mg/l)	0.45	0.39	0.39	0.39		0.55	0.55
July. 2009 (k=101)	Observed (mg/l)	0.47		0.26	0.41		0.54	0.20
	Computed (mg/l)	0.47		0.33	0.31		0.37	0.37

Distribution of fluoride concentration among the boreholes in the wellfield at the end of the prediction time (Jun. 2017) is shown in Table 4.4 with corresponding surface plot shown in Fig 4.10. It is obvious to see fluoride concentrations vary from the minimum 0.16 mg/l to the peak 0.21 mg/l at this time. In view of the fact that the WHO standard level of drinking water aesthetic quality for fluoride is *1.5 mg/l*, the wellfield can be regarded as *'adequately safe'*. As to be mentioned later, peak fluoride concentrations of around 0.62 mg/l are attained at the early times of the prediction period which are adequately below the WHO standard fluoride levels for drinking water aesthetic quality.

Table 4.4 Spatial Fluoride Concentration Distribution at the End of June 2017

Y(m) \ X(m)	0	500	1000	1500	2000	2500	3000	3500	4000
0	0.1958	0.1916	0.2104	0.1942	0.1838	0.2056	0.1769	0.2018	0.1960
500	0.2000	0.2021	0.2043	0.1902	0.1893	0.1991	0.1801	0.2006	0.1903
1000	0.2000	0.2058	0.1857	0.1961	0.1949	0.1868	0.1916	0.1796	0.1877
1500	0.2000	0.2099	0.1925	0.2091	0.1954	0.1967	0.1812	0.1685	0.1900
2000	0.2000	0.2002	0.1833	0.1825	0.1914	0.1834	0.2064	0.1726	0.1800
2500	0.2000	0.1853	0.1859	0.1754	0.1825	0.1747	0.1949	0.2070	0.1821
3000	0.1950	0.1900	0.1900	0.1900	0.1900	0.1900	0.1900	0.1900	0.1861

Yet, since the groundwater modeling of akaki wellfield had predicted (AAWSA report) sustainable supply of water from the boreholes until 2020, *the wellfield won't be faced with major fluoride contamination under normal conditions.*

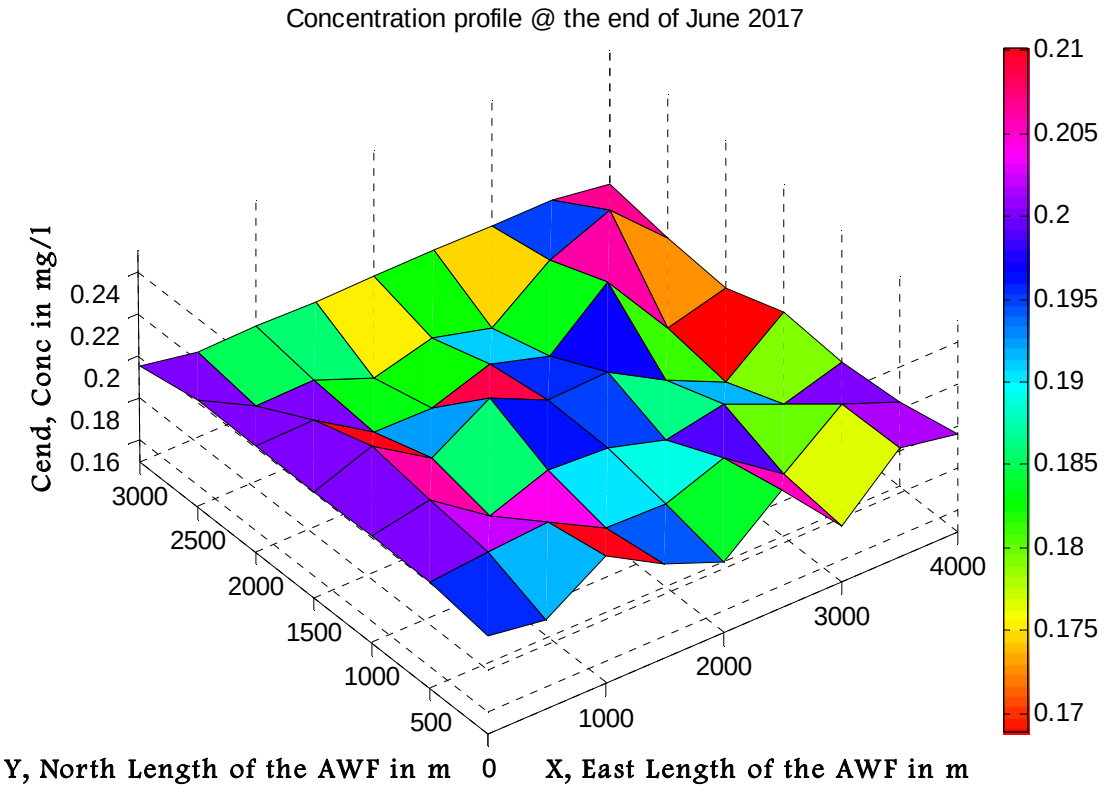

Fig 4.10 Predicted Fluoride concentration profile of Wellfield at the End of June 2017

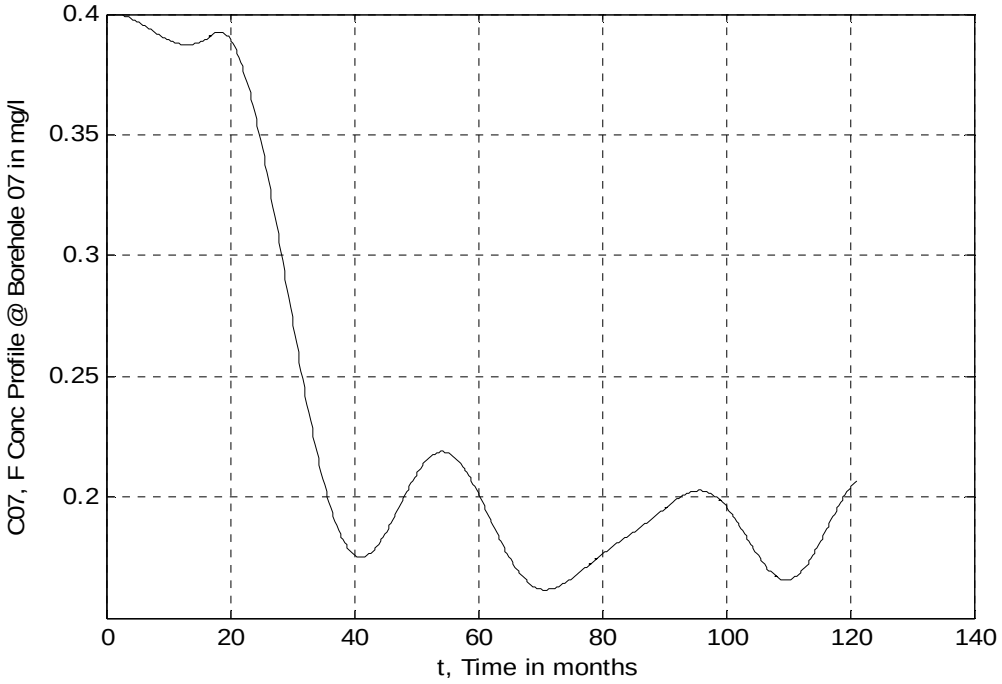

Fig 4.11 Fluoride Breakthrough Curve for Borehole BH07

Figure 4.11 shows fluoride breakthrough curve for borehole BH07 where fluoride concentration levels decrease steeply about 0.4 mg/l to 0.15 mg/l to indicate removal of fluoride through advective transport with groundwater flow with no further addition to the wellfield. The ups and downs at latter periods in the figure are indication of seasonal fluoride infiltration variations in the dry and wet seasons.

Fluoride breakthrough curve for BH10 (shown below in Fig 4.12) shows, however, nearly *unchanging initial concentration* values to later decrease uniformly down. This is because as BH10 is located at the far end of the groundwater flow course through the wellfield, initially, it is less sensitive to any fluoride added at the influx boundaries. Before any fluoride reaches BH10, the initial fluoride available would get transported with the flowing groundwater to dilute it. A similar pattern is observed for borehole BH16 shown in Fig 4.13 where fluoride concentration commence decreasing at the early periods of prediction time (before 20^{th} month) indicating, at this prediction time, near-influx-boundary borehole of the wellfield (BH16) releases solute at a faster pace (because

it is far from the no-flow boundaries) than BH10 which is nearer to the no-flow boundaries.

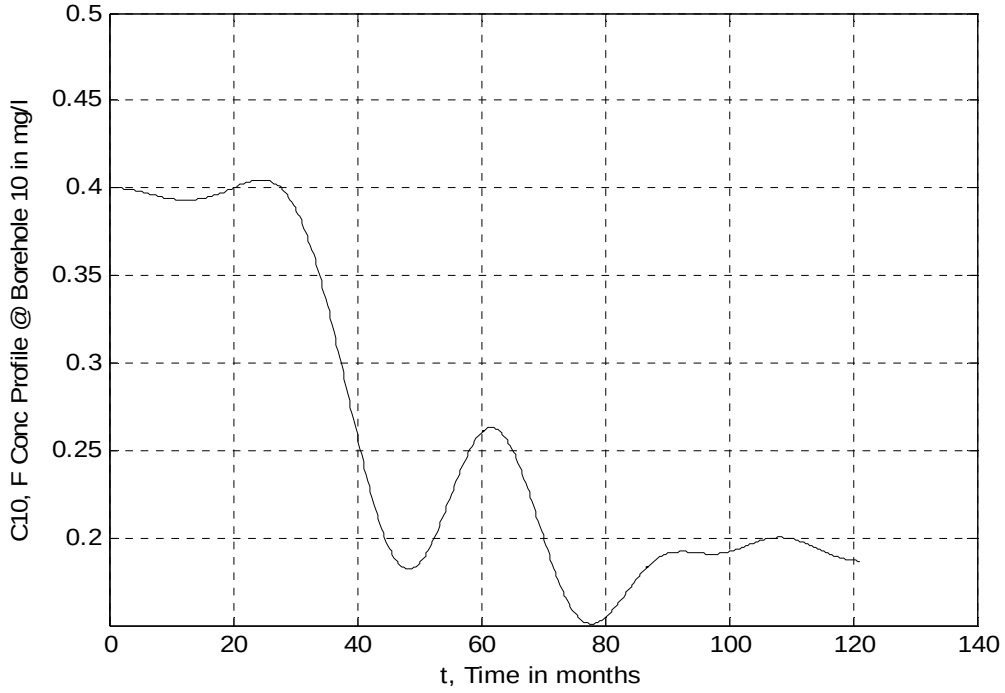

Fig 4.12 Fluoride Breakthrough Curve for Borehole BH10

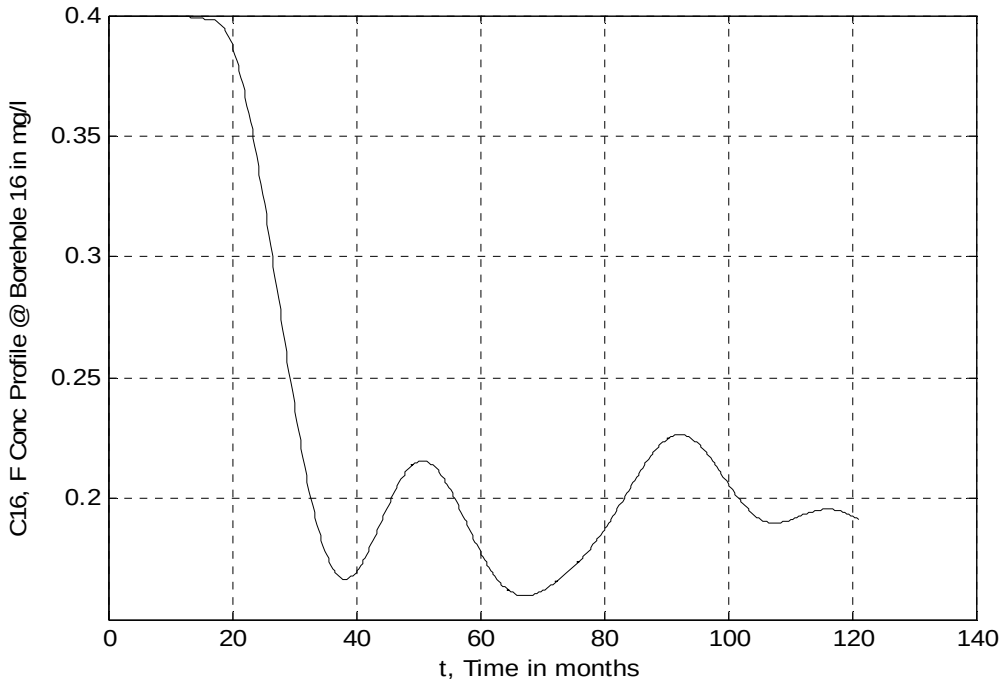

Fig 4.13 Fluoride Breakthrough Curve for Borehole BH16

A different pattern of fluoride variation is observed when we look at Fig 4.14 below for borehole BH22 – a borehole near the western influx boundary. Since this borehole is nearer to the western wellfield boundary, initially fluoride concentration gets increased to around 0.5 mg/l before it appears to have a net release of solute, after which the solute moves away with the flowing groundwater through advection to decrease it's concentration in this borehole as there is no further addition of solute through the wellfield influx boundaries.

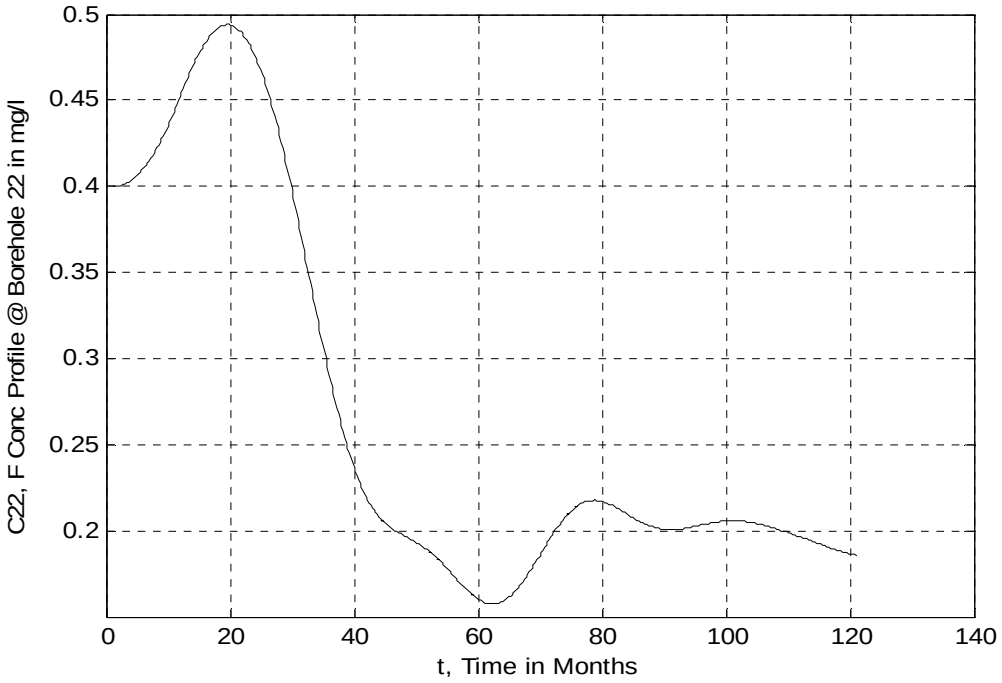

Fig 4.14 Fluoride Breakthrough Curve for Borehole BH22

Referring to Fig 4.15 below for fluoride breakthrough curve of borehole BH25 reveals similar pattern as that of BH22 except that initially the fluoride level commences decreasing from a higher value (around 0.62 mg/l). This is attributed to the fact that BH25 is nearer to the influx boundaries than BH22 and obviously it is immediately contaminated with fluoride to attain a higher peak fluoride concentration to latter start decreasing as the fluoride is transported via advection & dispersion.

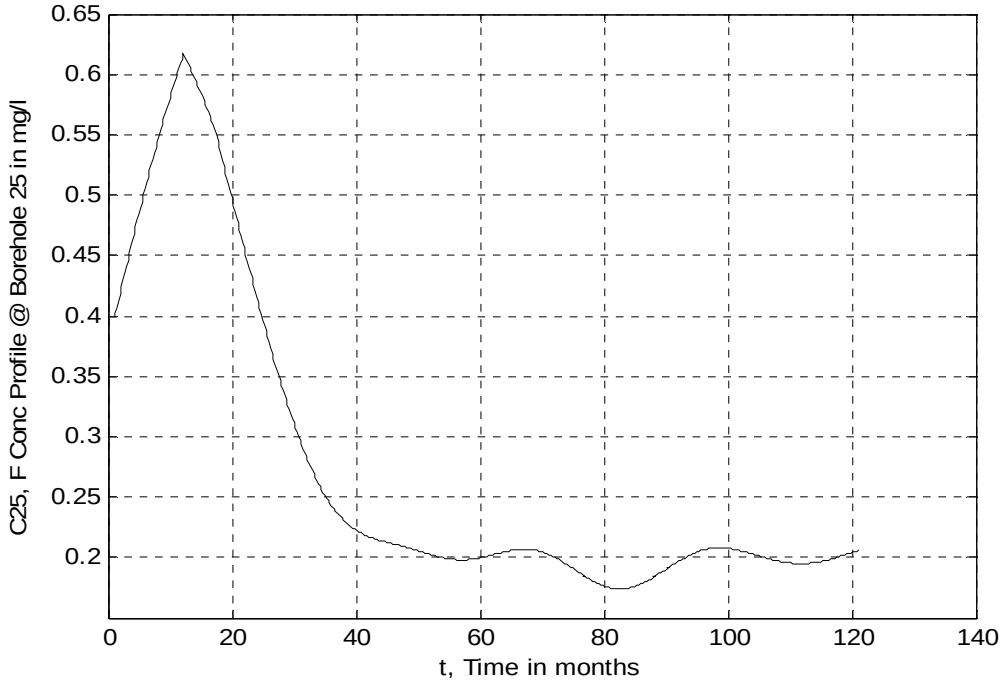

Fig 4.15 Fluoride Breakthrough Curve for Borehole BH25

The simulation results discussed above in sections 4.1 & 4.2 show that while chloride concentrations in the wellfield get increased; fluoride, however, is getting decreasing through out all of the boreholes in the wellfield. This is in agreement with the actual observed pattern of solute load of the wellfield revealing chloride is being introduced in to the wellfield by one or more mechanisms somewhere in the vicinity of the akaki river catchment (ARC) while chloride is not.

The breakthrough curves detailed above (both for chloride & fluoride) have the potential to indicate possible contamination of the wellfield by enabling us to observe at the concentration values each borehole has attained through out the simulation period. If the values, for instance, top the WHO standard levels of drinking water aesthetic quality, then the borehole is possibly said to be in threat of contamination and immediate groundwater quality monitoring measures are to be taken-yet this was not the case, to be later concluded in chapter five.

5. Conclusions & Suggestions

5.1 Conclusions

Groundwater is the subsurface water system preferred for use as drinking water than surface water since it is not as much liable to contamination than the latter for it has its own natural cleaning mechanism in the underground geologic structures. Yet, in cities like Addis Ababa where no proper solid & liquid waste management are available, it can be subjected to severe contamination. As a result, *indication of the degree of contamination of a groundwater system before its use for various purposes should be made by available tools* and numerical modeling of contaminants, using appropriate package, is one of the best methods for a groundwater system of a given area.

Analysis of chloride simulation results of the wellfield boreholes in previous chapter (chapter four) showed that the wellfield is adequately safe in view of chloride contamination. Under normal conditions, the maximum chloride ion concentration of the wellfield throughout the prediction period is found to be around 18 mg/l near borehole BH06 which is situated on the northern eastern boundary of the wellfield. It is worth mentioning that this borehole is located at a potentially contamination source where liquid & solid industrial effluents from upstream of this boundary (Kality & Akaki towns) are introduced in to the system.

The fact that chloride is being introduced in to the wellfield needs due attention as to how & where exactly it is generated inside the akaki river catchment. Fluoride, on the contrary, is getting decreasing since its human induced sources are rare unless natural fluoride release via infiltration in to the sub-surface system occur.

In general, those boreholes nearest to the northern & western solute influx boundaries attain higher chloride concentrations at the early periods of prediction while those located farther get ‘contaminated’ in a relatively longer prediction time. Thus, if any chloride ‘contamination’ is observed in the water quality monitoring wells, immediate attention should be given to the boreholes nearer to the influx boundaries.

The wellfield, with respect to fluoride, is not as equally safe as that for chloride contamination in that peak fluoride values of *0.62 mg/l* are predicted in most boreholes. Since the WHO standard value for fluoride in water is *1.5 mg/l*, the boreholes need due attention through the water quality monitoring wells. Incase any accidental fluoride release in to the wellfield occurs, proper *defluorization* treatment measures should be taken as *trace increase in fluoride is harmful to humans skeletal system*.

Yet, there are no treatment plants for the akaki groundwater field (The thesis assignee was told by AAWSA staff member about this) because it has been assumed that the wellfield is free from any contamination throughout its operation phase. Meanwhile, more alarming fluoride levels are predicted at the earlier periods of prediction than at latter periods because, as mentioned earlier, after the initial fluoride is introduced in to the study area there are no further fluoride sources to account for any increase.

Since most of the boreholes in the wellfield are expected to operate until 2020 (Akaki wellfield groundwater modeling, 2000), the solute transport modeling was made as much as possible to cover up to this time span. Thus, no immediate threat of contamination with respect to both species (F^- & Cl^-) will occur in the wellfield unless accidental contaminant release from the upstream towns of akaki & kaliti or from the near-by Addis-Debrezeit road occurs.

During the study of this thesis work it has been found that historical data used for model calibration were inadequate. Past data was found only for three boreholes in AAWSA archives; BH06, BH07 & BH22. For a solute transport modeling to have accurate results, extensive historical data of most of the boreholes should be available both for calibration & verification. This was the major drawback during this study and any discrepancy between the computed & observed solute concentrations are attributed to this.

5.2 Suggestions

This thesis work focuses on conservative solute transport modeling of akaki wellfield and it is not to be used as a means for accurately predicting non-reactive contaminant concentrations, rather *it is aimed at helping decision making on pollution threat faced by the indiscriminate discharge of solid & liquid wastes from the city located upstream of the wellfield*. That is, whenever conservative solute concentrations are predicted as increasing or exceeds the limit above the WHO standard values, immediate water quality monitoring tests followed by decision making by a panel of experts as to whether no-action or mitigation or else remediation measure is to be taken.

As its name implies, this study details only on two special anions (chloride & fluoride) that are conservative in nature. Most groundwater contaminants are, however, reactive in nature and further study encompassing the reactive constituents of groundwater should be made to address the full contamination threat to the wellfield. Reactive pollutants observed in the wellfield (though not above the permissible levels) include nitrite, nitrate, ammonia, phosphates, sulphate, bicarbonates and carbonates. Therefore, *a wider scope study of reactive solute transport modeling of the wellfield should be carried out by relevant organizations particularly by AAWSA.* Yet, *AAWSA has not conducted any solute transport modeling of the wellfield till now*. In view of the fact that the wellfield has an operation phase until 2020, an immediate action is needed to address the problem posed by these pollutants before the end of the operation phase.

References

1. Adinew A. (1999). *Water Supply Upgrading Projects: Their Potential Impact*. Addis Ababa: Author.
2. Chnmiao Z., & Gordon D. (2002). *Applied Contaminant Transport Modeling*. New York: Wiley Inter-science
3. Edward M., & Bruce R. (1999). *Coal Combustion By-products & Contaminant Transport in Groundwater.* Illinois: Inc. Brookfield, WI.
4. Getahun W. and Adinew A. (1999). *Integrated Development for Water Supply & Sanitation:Waste Water Management in Addis Ababa. Addis Ababa*: Authors.
5. Gideon T., Lisa C. and Pannie E. *Groundwater pollution: Are we monitoring appropriate parameters?* Fredericton: University of New Brunswick.
6. Jacques D., (1999). *The Handbook of Groundwater Engineering*. N.W Boca Raton: CRC Press LLC
7. John H. and Curtis D. (1999). *Numerical Methods Using MATLAB, 3rd Edition*. New jersey: Prentice Hall.
8. John H. and Curtis D. (2004). *Numerical Methods Using MATLAB, 4th Edition*. New jersey: Prentice Hall.
9. J. P. Zublena., Maurice G. and Mary B. **(**2004). *Health Effects of Groundwater Pollutants.* North Carolina: North Carolina Agricultural Extension Office.
10. Kebede T., Solomon W., Shiferaw L. & Abebe G. (2005). *Groundwater Management Using Groundwater Modeling: Case Study on Akaki Groundwater Model*. Addis Ababa: Authors.

11. Mohan, S & Muthukumaran, M. (2004). *Modeling of Pollutant Transport in Ground Water*.

12. Samuel M., Taddese W., Richard D. and Luc M. (2004). *Simultaneous Determination of Trace Elements in Tinishu Akaki River Water Sample, Ethiopia.* Addis Ababa: Addis Ababa University.

13. S. A. Mirbagheri. (2004). *Modeling contaminant transport in soil column and ground water pollution control*. Shiraz: Shiraz University.

14. Shaheen & Peaker Limited, (2007). *Groundwater Flow and Contaminant Transport Model.* Toronto: Author.

15. Shiferaw L., Abebe G., Kebede T., and Solomon W. (2004). *Groundwater Management Using Groundwater Modeling: Case study on Akaki Wellfield.* Addis Ababa.

16. Stephen G. and Randall R. (2000). *Contaminant Transport in Fractured Media: Models for Decision Makers.* Oklahoma: Robert S. Kerr Environmental Research Laboratory, Ada.

17. Tamiru A., Dagnachew L., Tenalem A., Yirga T., Solomon W., and Nuri M. (2005). *Assessment of Pollution Status and Groundwater Vulnerability Mapping of the Addis Ababa Water Supply Aquifers, Ethiopia*. Addis Ababa: AAWSA.

18. Thomas, H. (2003). *Groundwater Pollution & Quality*. California: Reagents of the University of California.

19. Vaclovas, T. (2002). *Research of Leachate, Surface, and Ground Water Pollution*. Šiauliai: Šiauliai University.

20. Yirga T. (2004). *Groundwater Modeling: A Case Study on Volcanic Water Supply Aquifer /Akaki Wellfield/ of the City of Addis Ababa. Addis Ababa:* Author.

21. Yirga T. (2000). *Modeling of Akaki Wellfield Final Report*. Addis Ababa: AAWSA.

22. Yong, S. C., & Ahmed, H. (1999). *Groundwater and Surface Water Pollution.* New Jersey: CRC Press LLC.

23. Yuji M., *Application of Geographic Information System (GIS) for Groundwater Resource Management*. *Practical Experience from Groundwater Development & Water Supply Training Center*. Addis Ababa: AG Consult, Consulting Hydrogeologists& Engineers.

```
clc
clear all
% Fully Explicit Method for Fluoride Model Calibration
format short
%Varying Input Strings
disp('Enter the Porosity of the Aquifers in AWF, n');
n=input('n = ');
disp('Enter the Longitudinal Dispersivity, L (m)');
L=input('L = ');
disp('Enter the Transversal Dispersivity, T (m)');
T=input('T = ');
disp('Enter the Hydraulic Conductivity of the AWF Aquifer, K (m/month)');
K=input('K = ');
%Discretization Scheme, Groundwater Velocity & Dispersion Coefficients
Lx=4000; Ly=3000; tmax=120; dx=500; dy=500; dt=0.25; Hx=-0.00033;
Hy=0.000652; vx=(-K/n)*Hx; vy=(-K/n)*Hy; v=sqrt(vx^2+vy^2);
Dx=(L*(vx^2/v))+(T*(vy^2/v));Dy=(L*(vy^2/v))+(T*(vx^2/v));
%Stability Criterion
if (dt > 1/((abs(vx)/dx)+(abs(vy)/dy))) | (dt > 0.5/((Dx/dx^2)+(Dy/dy^2)))
      warning('The Method is not stable',...
       'Try another values of dt, dx or dy');
      return
else
nx = (Lx/dx)+1;
ny = (Ly/dy)+1;
nt = (tmax/dt)+1;

   disp('The method is stable; MATLAB now calculates the nodal concentrations @ each
time step');
```

```
%Generating the Matrix C of Fluoride Concentration
   C=zeros(nx,ny,nt);
%Initial Fluoride Concentration Values for Interior Nodes(Based on AWF Solute Data)
   for i=2:nx-1
      for j=2:ny-1
         C(1,j,1)=0.51;C(i,1,1)=0.51;C(i,j,1)=0.51;C(nx,j,1)=0.51;C(i,ny,1)=0.4;
      end
   end
%Initial Fluoride Concentration Values for Corner Nodes
  C(1,1,1)=0.5*(C(1,2,1)+C(2,1,1));
  C(nx,1,1)=0.5*(C(nx,2,1)+C(nx-1,1,1));
  C(1,ny,1)=0.5*(C(1,ny-1,1)+C(2,ny,1));
  C(nx,ny,1)=0.5*(C(nx,ny-1,1)+C(nx-1,ny,1));
 %Time Iteration Loop
 for k=2:nt
    for i=2:nx-1
     for j=2:ny-1
%Describing Fluoride Concentration @ the Four Boundaries
C(1,j,2:74)=0.85;C(1,j,75)=0.49;C(1,j,76:77)=0.66;C(1,j,78)=0.29;C(1,j,79)=0.66;C(1,j,80:121)=0.51;
C(nx,j,k)=C(nx,j,k-1)+(-vx*dt/(2*dx)).*(C(nx,j,k-1)-C(nx-1,j,k-1))+(-vy*dt/2*dy)).*(C(nx,j+1,k-1)-C(nx,j-
1,k-1))+(dt*Dx/dx^2).*(C(nx,j,k-1)-2.*C(nx,j,k-1)+C(nx-1,j,k-1))+(dt*Dy/dy^2).*(C(nx,j+1,k-1)-
2.*C(nx,j,k-1)+C(nx,j-1,k-1));
C(i,1,k)=C(i,1,k-1)+(-vx*dt/(2*dx)).*(C(i+1,1,k-1)-C(i-1,1,k-1))+(-vy*dt/(2*dy)).*(C(i,2,k-1)-C(i,1,k-
1))+(dt*Dx/dx^2).*(C(i+1,1,k-1)-2.*C(i,1,k-1)+C(i-1,1,k-1))+(dt*Dy/dy^2).*(C(i,2,k-1)-2.*C(i,1,k-
1)+C(i,1,k-1));
C(i,ny,2:72)=0.75;C(i,ny,73:74)=0.61;C(i,ny,75)=0.49;C(i,ny,76:77)=0.38;C(i,ny,78)=0.31;C(i,ny,79)=0.4;
C(i,ny,80:84)=0.55;C(i,ny,85:121)=0.4;
%Describing Fluoride Concentration @ the Interior Nodes
C(i,j,k)=C(i,j,k-1)+(-vx*dt/(2*dx)).*(C(i+1,j,k-1)-C(i-1,j,k-1))+(-vy*dt/(2*dy)).*(C(i,j+1,k-1)-
C(i,j-1,k-1))+(dt*Dx/dx^2).*(C(i+1,j,k-1)-2.*C(i,j,k-1)+C(i-1,j,k-1))+(dt*Dy/dy^2).*(C(i,j+1,k-
1)-2.*C(i,j,k-1)+C(i,j-1,k-1));
     end
    end
```

```
%Describing Fluoride Concentration @ the four corner nodes of the AWF study area
  C(1,1,k)=0.5*(C(1,2,k)+C(2,1,k));
  C(nx,1,k)=0.5*(C(nx,2,k)+C(nx-1,1,k));
  C(1,ny,k)=0.5*(C(1,ny-1,k)+C(2,ny,k));
  C(nx,ny,k)=0.5*(C(nx,ny-1,k)+C(nx-1,ny,k));


 Max=(nx-2)*(ny-2);
 for i=1:Max
   error(i)=1;
 end
 error;
 count=0;
 tol =1E-06;
 %Count Iteration Loop
 while error>tol
   for i=2:nx-1
      for j=2:ny-1
Cnew(1,j,2:74)=0.85;Cnew(1,j,75)=0.49;Cnew(1,j,76:77)=0.66;Cnew(1,j,78)=0.29;Cnew(1,j,79)=0.66;Cnew(1,j,80:121)=0.51;
 Cnew(nx,j,k)=C(nx,j,k-1)+(-v_x*dt/(2*dx)).*(C(nx,j,k-1)-C(nx-1,j,k-1))+(-v_y*dt/2*dy)).*(C(nx,j+1,k-1)-C(nx,j-1,k-1))+(dt*Dx/dx^2).*(C(nx,j,k-1)-2.*C(nx,j,k-1)+C(nx-1,j,k-1))+(dt*Dy/dy^2).*(C(nx,j+1,k-1)-2.*C(nx,j,k-1)+C(nx,j-1,k-1));
Cnew(i,1,k)=C(i,1,k-1)+(-v_x*dt/(2*dx)).*(C(i+1,1,k-1)-C(i-1,1,k-1))+(-v_y*dt/(2*dy)).*(C(i,2,k-1)-C(i,1,k-1))+(dt*Dx/dx^2).*(C(i+1,1,k-1)-2.*C(i,1,k-1)+C(i-1,1,k-1))+(dt*Dy/dy^2).*(C(i,2,k-1)-2.*C(i,1,k-1)+C(i,1,k-1));
Cnew(i,ny,2:72)=0.75;Cnew(i,ny,73:74)=0.61;Cnew(i,ny,75)=0.49;Cnew(i,ny,76:77)=0.38;Cnew(i,ny,78)=0.31;Cnew(i,ny,79)=0.4;Cnew(i,ny,80:84)=0.55;Cnew(i,ny,85:121)=0.4;
Cnew(i,j,k)=C(i,j,k-1)+(-v_x*dt/(2*dx)).*(C(i+1,j,k-1)-C(i-1,j,k-1))+(-v_y*dt/(2*dy)).*(C(i,j+1,k-1)-C(i,j-1,k-1))+(dt*Dx/dx^2).*(C(i+1,j,k-1)-2.*C(i,j,k-1)+C(i-1,j,k-1))+(dt*Dy/dy^2).*(C(i,j+1,k-1)-2.*C(i,j,k-1)+C(i,j-1,k-1));
      end
   end
   Cnew(1,1,k)=0.5*(C(1,2,k)+C(2,1,k));
```

```
    Cnew(nx,1,k)=0.5*(C(nx,2,k)+C(nx-1,1,k));
    Cnew(1,ny,k)=0.5*(C(1,ny-1,k)+C(2,ny,k));
    Cnew(nx,ny,k)=0.5*(C(nx,ny-1,k)+C(nx-1,ny,k));

    for i=2:nx-1
        for j=2:ny-1
            error=abs((Cnew(i,j,k)-C(i,j,k))./Cnew(i,j,k));
            count=count+1;
            C(i,j,k)=Cnew(i,j,k);
        end
    end
    Cnew;
  end
 end
end

format short
 Cnew
%Sketching the Spatial Concentration Distribution of Fluoride @ the end of June 07
figure (1)
X=[0:dx:Lx];
Y=[0:dy:Ly];
D=Cnew(:,:,nt);Cend=D'
surf(X,Y,Cend)
colormap hsv
colorbar
xlabel('X, East Length of the AWF in m')
ylabel('Y, North Length of the AWF in m')
zlabel('Cend, Conc in mg/l')
title('Concentration profile @ the end of June 2007')
```

```
clc
clear all
% Fully Explicit Method for Fluoride Prediction
format short
%Varying Input Strings
disp('Enter the Porosity of the Aquifers in AWF, n');
n=input('n = ');
disp('Enter the Longitudinal Dispersivity, L (m)');
L=input('L = ');
disp('Enter the Transversal Dispersivity, T (m)');
T=input('T = ');
disp('Enter the Hydraulic Conductivity of the AWF Aquifer, K (m/month)');
K=input('K = ');
%Discretization Scheme, Groundwater Velocity & Dispersion Coefficients
Lx=4000; Ly=3000; tmax=120; dx=500; dy=500; dt=0.25; Hx=-0.00033;
Hy=0.000652; vx=(-K/n)*Hx; vy=(-K/n)*Hy; v=sqrt(vx^2+vy^2);
Dx=(L*(vx^2/v))+(T*(vy^2/v));Dy=(L*(vy^2/v))+(T*(vx^2/v));
%Stability Criterion
if (dt > 1/((abs(vx)/dx)+(abs(vy)/dy))) | (dt > 0.5/((Dx/dx^2)+(Dy/dy^2)))
   warning('The Method is not stable',...
      'Try another values of dt, dx or dy');
   return
else
nx = (Lx/dx)+1;
ny = (Ly/dy)+1;
nt = (tmax/dt)+1;
   disp('The method is stable; MATLAB now calculates the nodal concentrations @ each
time step');
%Generating the Matrix C of Fluoride Concentration
   C=zeros(nx,ny,nt);
   %Initial Fluoride Concentration Values for Interior Nodes in June 07
```

```
   for i=2:nx-1
      for j=2:ny-1
        C(1,j,1)=0.51;C(i,1,1)=0.37;C(i,j,1)=0.4;C(nx,j,1)=0.25;C(i,ny,1)=0.4;
      end
   end
%Initial Fluoride Concentration Values for Corner Nodes in June 07
  C(1,1,1)=0.5*(C(1,2,1)+C(2,1,1));
  C(nx,1,1)=0.5*(C(nx,2,1)+C(nx-1,1,1));
  C(1,ny,1)=0.5*(C(1,ny-1,1)+C(2,ny,1));
  C(nx,ny,1)=0.5*(C(nx,ny-1,1)+C(nx-1,ny,1));
 for k=2:nt
    for i=2:nx-1
     for j=2:ny-1
%Describing Fluoride Concentration @ the Four Boundaries
      C(1,j,2:45)=0.82;C(1,j,46:65)=0.34;C(1,j,66:481)=0.2;
      C(nx,j,k)=C(nx,j,k-1)+(-vx*dt/(2*dx)).*(C(nx,j,k-1)-C(nx-1,j,k-1))+(-
vy*dt/(2*dy)).*(C(nx,j+1,k-1)-C(nx,j-1,k-1))+(dt*Dx/dx^2).*(C(nx,j,k-1)-2.*C(nx,j,k-
1)+C(nx-1,j,k-1))+(dt*Dy/dy^2).*(C(nx,j+1,k-1)-2.*C(nx,j,k-1)+C(nx,j-1,k-1));
      C(i,1,k)=C(i,1,k-1)+(-vx*dt/(2*dx)).*(C(i+1,1,k-1)-C(i-1,1,k-1))+(-
vy*dt/(2*dy)).*(C(i,2,k-1)-C(i,1,k-1))+(dt*Dx/dx^2).*(C(i+1,1,k-1)-2.*C(i,1,k-1)+C(i-
1,1,k-1))+(dt*Dy/dy^2).*(C(i,2,k-1)-2.*C(i,1,k-1)+C(i,1,k-1));
      C(i,ny,2:65)=0.4;C(i,ny,66:481)=0.19;
%Describing Fluoride Concentration @ the Interior Nodes
      C(i,j,k)=C(i,j,k-1)+(-vx*dt/(2*dx)).*(C(i+1,j,k-1)-C(i-1,j,k-1))+(-
vy*dt/(2*dy)).*(C(i,j+1,k-1)-C(i,j-1,k-1))+(dt*Dx/dx^2).*(C(i+1,j,k-1)-2.*C(i,j,k-1)+C(i-
1,j,k-1))+(dt*Dy/dy^2).*(C(i,j+1,k-1)-2.*C(i,j,k-1)+C(i,j-1,k-1));
     end
    end
%Describing Fluoride Concentration @ the four corner nodes of the AWF study area
  C(1,1,k)=0.5*(C(1,2,k)+C(2,1,k));
  C(nx,1,k)=0.5*(C(nx,2,k)+C(nx-1,1,k));
```

```
  C(1,ny,k)=0.5*(C(1,ny-1,k)+C(2,ny,k));
  C(nx,ny,k)=0.5*(C(nx,ny-1,k)+C(nx-1,ny,k));
 end
end

format short
C
%F Conc Verifications for Boreholes BH07, BH10, BH16, BH20, BH22 & BH25
disp('C(:,:,9)');C(:,:,9),disp('C(:,:,29)');C(:,:,29),disp('C(:,:,45)');C(:,:,45),
disp('C(:,:,65)');C(:,:,65),disp('C(:,:,77)');C(:,:,77),disp('C(:,:,101)');C(:,:,101),

%Sketching the Spatial Concentration Distribution of Fluoride @ the end of June 17
figure (1)
X=[0:dx:Lx];
Y=[0:dy:Ly];
D=C(:,:,nt);Cend=D'
surf(X,Y,Cend)
colormap hsv
colorbar
xlabel('X, East Length of the AWF in m')
ylabel('Y, North Length of the AWF in m')
zlabel('Cend, Conc in mg/l')
title('Concentration profile @ the end of June 2017')

%Plotting Fluoride Concentration of Selected Boreholes Vs Calibration Time
figure (2)
%t=1:dt:nt
for t=1:nt
%C07=C(6,4,:)
   time(t)=((t-1)/4)+1;
   C07(t)=C(7,5,t);
```

```
end
plot(time,C07);
grid on
xlabel('t, Time in months')
ylabel('C07, F Conc Profile @ Borehole 07 in mg/l')

figure (3)
%t=1:dt:nt
for t=1:nt
%C10=C(6,3,:)
   time(t)=((t-1)/4)+1;
   C10(t)=C(6,3,t);
end
plot(time,C10);
grid on
xlabel('t, Time in months')
ylabel('C10, F Conc Profile @ Borehole 10 in mg/l')

figure (4)
%t=1:dt:nt
for t=1:nt
%C16=C(5,5,:)
   time(t)=((t-1)/4)+1;
   C16(t)=C(5,5,t);
end
plot(time,C16);
grid on
xlabel('t, Time in months')
ylabel('C16, F Conc Profile @ Borehole 16 in mg/l')
```

```
figure (5)
%t=1:dt:nt
for t=1:nt
%C20=C(4,5,:)
   time(t)=((t-1)/4)+1;
   C20(t)=C(4,5,t);
end
plot(time,C20);
grid on
xlabel('t, Time in months')
ylabel('C20, F Conc Profile @ Borehole 20 in mg/l')

figure (6)
%t=1:dt:nt
for t=1:nt
   time(t)=((t-1)/4)+1;
   C22(t)=C(3,3,t);
end
plot(time,C22);
grid on
xlabel('t, Time in Months')
ylabel('C22, F Conc Profile @ Borehole 22 in mg/l')

figure (7)
%t=1:dt:nt
for t=1:nt
%C25=C(2,3,:)
   time(t)=((t-1)/4)+1;
   C25(t)=C(2,3,t);
end
plot(time,C25);
```

```
grid on
xlabel('t, Time in months')
ylabel('C25, F Conc Profile @ Borehole 25 in mg/l')

figure (8)
%t=1:dt:nt
for t=1:nt

   time(t)=((t-1)/4)+1;
   C07(t)=C(7,5,t);C10(t)=C(6,3,t);C16(t)=C(5,5,t);
end
plot(time,C07,time,C10,time,C16);
grid on
xlabel('t, Time in Months')
ylabel('C, F Conc Profile @ Selected Boreholes in mg/l')

figure (9)
%t=1:dt:nt
for t=1:nt

   time(t)=((t-1)/4)+1;
   C20(t)=C(4,5,t);C22(t)=C(3,3,t);C25(t)=C(2,3,t);
end
plot(time,C20,time,C22,time,C25);
grid on
xlabel('t, Time in Months')
ylabel('C, F Conc Profile @ Selected Boreholes in mg/l')
```

BH - 07 Raw Water Quality Monitoring					
General Information			**Major Cations**	Unit	Jun.20-22, 97
Date of Sampling			NH_3, Ammonia	mg/l	0.182
Date of Analysis		Jun.20-22, 97	Na, Sodium	mg/l	
Laboratory		AAWSA	K, Potassium	mg/l	
			Ca, Calcium	mg/l	69.6
Phys-Chem. Parameters	Unit		Mg, Magnisium	mg/l	15.36
Temperature	^oC	21	Fe, Iron	mg/l	0.012
Turbidity	FTU	Nil	Mn, Manganese	mg/l	0.042
Color	Pt.Co.units	Nil	Al, Almunium	mg/l	
Oder		Non-object.	Cu, Copper	mg/l	nil
Taste		Non-object.	Cr, Chromium	mg/l	Nil
PH		8.3	**MajorAnions**		
TDS	mg/l	313	Cl, Chloride	mg/l	2
Conductivity	µS/cm	456	NO_2, Nitrite	mg/l	0.031
Dissolved O_2	mg/l	6.5	NO_3, Nitrate	mg/l	21
Dissolved CO_2	mg/l	nil	F, Flouride	mg/l	0.51
Silica, SiO_2	mg/l	51	HCO_3, Bicarbonate	mg/l	
Hydrogen Sulfide, H_2S	mg/l		CO_3, Carbonate	mg/l	
Total hardness as $CaCO_3$	mg/l	244	SO_4, Sulfate	mg/l	2.2
Calcium hardness as $CaCO_3$	mg/l	174	PO_4, Phosphate	mg/l	0.186
Magnisium hardness as $CaCO_3$	mg/l	64			
Total Alkalinity as $CaCO_3$	mg/l	238			
Bicarbonate Alkalinity as $CaCO_3$	mg/l	238			
Carbonate Alkalinity as $CaCO_3$	mg/l	Nil			
Hydroxide Alkalinity as $CaCO_3$	mg/l	Nil			

Source: AAWSA

X	Y	Z, water level meter aml	Akaki Phase II BH No.	BH owner/location Name
473600	1001013	2522	1	American Embassy-1
473700	1001012	2528	2	American Embassy-2
474300	1001005	2478	7	French Embassy
466200	1001008	2539	8	Tikur Abay Shoe Factory
467200	1001017	2482	9	Glass and bottle factory
468400	1001016	2554	10	Anbessa Transport
466600	1001003	2477	11	Women's Rehabilitation Center
468300	1001003	2484	12	General Winget School
468800	1001007	2522	13	Ethio-Marble Industry-1
468900	1001007	2468	14	Ethio-Marble Industry-2
469900	1001000	2518	15	St. Poulos Hospital
471400	997400	2417	16	Meskerem Soft Drinks
474000	999400	2460	18	Total Sidist Kilo
473300	999300	2464	22	Total Sidist Kilo
480400	998500	2425	25	Total Sidist Kilo
476100	998300	2420	28	Total Sidist Kilo
474200	997400	2409	31	Total Sidist Kilo
471300	998200	2429	34	Total Sidist Kilo
469800	996300	2349	36	Total Sidist Kilo
470000	996400	2336	37	Coca Cola Factory-1
470000	996400	2337	38	Coca Cola Factory-2
469900	996000	2326	39	Awash Winery
470100	996100	2322	40	Building College
469800	996200	2345	41	Civil Aviation
479200	996700	2248	43	Ethio- Plastic Factory
473800	996600	2363	47	Hilton Hotel
473400	996400	2350	48	National Palace-1
473400	996300	2352	49	National Palace-2
473100	996400	2340	50	Filwooha Hotel-1
473300	996100	2342	53	Ghion Hotel-1
473300	996200	2334	54	Ghion Hotel-2
473300	996300	2283	55	Ghion Hotel-3
473400	995800	2334	56	St. Joseph's School
472900	995900	2334	58	Stadium Total
472500	996300	2320	62	Ras Hotel
471700	995900	2329	65	Technical School
471600	995800	2326	66	Addis Abeba Brewery-1
471500	995900	2328	67	Addis Abeba Brewery-2
471400	995800	2333	68	Addis Abeba Brewery-3
471400	996000	2322	69	Addis Abeba Brewery-4
471500	996000	2326	70	Addis Abeba Brewery-5
471500	996000	2322	71	Addis Abeba Brewery-6
471500	995800	2329	72	Addis Abeba Brewery-7
471300	995800	2337	73	Addis Abeba Brewery-8
471800	995500	2324	79	Ministry of Mines
471300	995400	2330	80	Defence Inustry-1
471300	995600	2335	81	Defence Inustry-2
471300	994800	2301	82	Cigarette Factory
470900	994800	2303	83	AAWSA Near Cigarette Factory
471700	995100	2313	84	SEDE(plant-A) - 1
471700	995000	2309	85	SEDE(plant-A) - 2
471700	994900	2310	86	SEDE(plant-A) - 3

X	Y	Z, water level meter aml	Akaki Phase II BH No.	BH owner/location Name
469700	994500	2325	87	Former Golf Club
469300	995500	2331	88	Old Airport (Army)
471700	986600	2194	90	Hana Mariam-2
471300	996200	2334	93	Hana Mariam-2
466300	993100	2270	98	Hope Enterprise-2
471704.7	973385.9	2019.3	99	Dewara Gua NWR
465800	992600	2245	100	Repi Soap Factory
467200	993600	2282	101	Voice of Revolutionary Ethiopia
468000	993200	2298	102	ALERT-1 Gate Well
468100	993100	2270	103	ALERT-2 West Well
468100	993200	2280	104	ALERT-3 East Well
471000	993800	2232	105	Progress/Edget Cotton Factory
471200	993700	2277	106	Anbessa/Walya Transport (Diabaco)
473000	992700	2181	108	Abay Mesk Soft Drinks-1(Pepsi Cola)
473100	992600	2254	109	Abay Mesk Soft Drinks-2 (pepsi Cola)
473500	992900	2157	110	Misrak Flour and oil Mills-1
472900	992500	2190	111	Misrak Flour and oil Mills-2
474300	993300	2199	112	Telecommunications Ware House
474300	992700	2292	113	Army Camp Construction
473200	992400	2258	115	United Oil Mills-1
473200	992400	2247	116	United Oil Mills-2
473100	991800	2224	117	Cement Factory-1
473100	991900	2167	118	Cement Factory-2
471400	991000	2214	128	Gofa Sefer Army Camp
473800	989900	2225	129	Adey Abebe Cotton Mill-1
473700	990000	2195	130	Adey Abebe Cotton Mill-2
473800	990200	2174	132	Ethiopia Thread Factory
473500	987900	2186	134	Awash Tannery-1
473600	988300	2184	135	Awash Tannery-2
474100	989300	2186	137	Kokeb Flour and Pasta Factory
473900	989000	2175	138	Addis Tyre Factory-1
473900	989000	2181	139	Addis Tyre Factory-2
474000	989100	2207	140	SEDE(Plant B)-1
474100	989000	2185	141	SEDE(Plant B)-2
475000	987800	2124	142	National Road Transport Corp
472400	989100	2193	143	Ethio- Pickling and Tanning Factory, near Behere Tsige
473500	987600	2155	144	Ethio-Meat Concentrete Factory
473300	987300	2145	146	WWDA Ware house
475000	985800	2125	149	AAWSA Kality Well
473900	985100	2157	150	Military Food Service Kitchen
475335.6	980717.3	2051.94	153	Meher Fiber Factory-1
476369	981717.3	2053.74	156	Akaki Indo-Europian Textiles-3
481507.4	976221	2005.27	157	Akaki Dairy Farm
482400	983000	2184.7	160	Kality Airforce-1
476400	984800	2118	161	Kality Airforce-2
474800	984700	2140.41	162	Galetti Project
477446.3	978851.2	2020.24	166	Akaki Metal Products/Sabean Utility Factory-4
477232.6	978999.8	2021.14	167	Akaki Metal Products/Sabean Utility Factory-1
475300	983800	2122	173	Kality Military Camp-1
475300	984000	2110	174	Kality Military Camp-2
475200	999200	2401	176	Minilik Hospital
472500	998700	2451	181	St. George's Cathedral

Source:

X	Y	Z, water level meter aml	Akaki Phase II BH No.	BH owner/location Name
472400	998500	2445	183	Private Well
472500	996600	2353	189	Ministry of Public Works Office
471800	994800	2312	203	AAWSA-1 Near Defence Industry
472700	996500	2537	206	Ministry of Defence
474800	994800	2312	209	AAWSA-2 Near Defence Industry
470500	994500	2278	210	Old Airpor-2
466900	1001005	2497	211	Gulele Glass-Factory-3
471400	995900	2328	213	Addis Beer-9
478462.8	977721.6	2020.47	215	NMWC Spare Parts & Hand Tools Factory-1
478462.8	977506.2	2020.62	230	NMWC Spare Parts & Hand Tools Factory-2
477608.9	978689.7	2019.6	216	NMWC Pump Factory
474225	982650	2104.8	217	Kality Metal Products Factory
455500	985200	2149	223	Meta Abo Brewery
464300	990600	2276	226	Darge - Suq, WSSA
479819.8	977155.6	2018.47	227	Sidamo Awash Village
473600	1001013	2535	228	American Embassy-3
473000	992700	2268	229	Abay Mesk Soft Drinks-3/pepsi cola factory
476427	980749.4	2053.33	231/1	Ethiopian Iron And Steel Faoundry BH-1
476430	980669.2	2052.95	231/2	Ethiopian Iron And Steel Faoundry BH-2
476520.6	980710.5	2053.446	232	Ethiopian Iron And Steel Faoundry BH-3
489200	1001025	2424	235	Legetafo-Nigata, Sendafa
463600	988200	2253	236	Gen. Gebre Kebede, Alemgena
462500	987000	2217	237	Highway N. 1, Alemgena
461900	974300	2082	238	Bisrate Wengel, Boneya
451900	983000	2100	239	Ato Abebe Dima, Sebeta
457700	1001008	2608	241	Tatek Tor Sefer-2
457000	1001005	2609	242	Tatek Tor Sefer-3
457500	1001005	2573	243	Tatek Tor Sefer-4
456900	1001012	2615	244	Tatek Tor Sefer-5
457400	1001013	2616	245	Tatek Tor Sefer-6
473000	992700	2182	246	Abay Mesk Soft Drinks-4/pepsi cola factory
475800	998600	2410	247	Kokebe Thebah school
488600	1001027	2454	248	Water III Testwell-B1
464000	997000	2429	249	Water III Testwell-B2
463700	988500	2261	250	Water III Testwell-B3
486200	1001042	2440	251	Water III Testwell-B4
481200	980000	2139	252	Water III Testwell-B5
470800	982900	2095.77	253	Water III Testwell-B6
473566	978610	2040.325	254	Water III Testwell-B7
487300	995300	2262	255	Water III Testwell-B8
481600	982900	2174.9	256	Water III Testwell-B9
461500	1001023	2548	257	Water III Testwell-B10
466200	988800	2246	258	Water III Testwell-B11
466400	987600	2234.5	259	Water III Testwell-B12
481200	980000	2141.9	260	Water III Testwell-T1
481600	982900	2175.3	261	Water III Testwell-T5
479400	981400	2130.7	262	Water III Testwell-13
480900	978800	2040.4	263	Water III Testwell-14
479400	981400	2130.7	264	Water III Testwell-T2
479340	981400	2130.6	265	Akaki Water Supply Test Well EP-1
481600	982850	2170.5	266	Akaki Water Supply Test Well EP-2
479740	981400	2130.5	267	Akaki Water Supply Test Well EP-3

X	Y	Z, water level meter aml	Akaki Phase II BH No.	BH owner/location Name
473069	979881	2051.6	268	Water III Testwell-B15
473108	979851	2051.27	269	Water III Testwell-T4
477972	974859	2019.6	270	Water III Borehole BH01
478399	975589	2019.7	271	Water III Borehole BH03
480517	977974	2028.7	272	Water III Borehole BH03a
478713	974977	2019.7	273	Water III Borehole BH3b
477992	975552	2019.2	274	Water III Borehole BH04
476574	975607	2019.5	275	Water III Borehole BH05b
479696	976936	2019.6	276	Water III Borehole BH06
479405	976735	2019.4	277	Water III Borehole BH07
479061	976370	2019.4	278	Water III Borehole BH08
479246	977104	2019.3	279	Water III Borehole BH09
479058	976020	2019.6	280	Water III Borehole BH10
478780	977307	2019.5	281	Water III Borehole BH11
478808	976867	2019.2	282	Water III Borehole BH12
478580	976051	2019.6	284	Water III Borehole BH14
478347	976752	2019.6	285	Water III Borehole BH16
478199	976361	2019.5	286	Water III Borehole BH17
478154	975966	2019.6	287	Water III Borehole BH18
478019	977482	2019.5	288	Water III Borehole BH19
477945	976985	2019.5	289	Water III Borehole BH20
477856	976402	2019.4	290	Water III Borehole BH21
477651	975923	2019.6	291	Water III Borehole BH22
477477	977216	2020.6	292	Water III Borehole BH23
477330	976793	2018.6	293	Water III Borehole BH24
477162	976038	2019.7	294	Water III Borehole BH25-2
477181	975680	2019.6	295	Water III Borehole BH26
476454	976951	2019.7	296	Water III monitoring well 01b
476523	976374	2019.4	297	Water III monitoring well 02
476972	976152	2018.4	298	Water III monitoring well 03
477185	975729	2019.6	299	Water III monitoring well 04
479942	977322	2025.43	300	Akaki Water Supply Well EP-4
478450	979950	2044.2	301	Akaki Water Supply Well EP-5
479526	977468	2022.35	302	Akaki Water Supply Well EP-6
479021	977596	2018.47	303	Akaki Water Supply Well EP-7
478998	977937	2018.03	304	Akaki Water Supply Well EP-8
472870	980925	2054	305	Kality EELPA
477900	982875	2110	306	Akaki Kebele 06 Kilento
478775	983133	2141	307	Akaki Kebele 06 Kilento
482480	976133	2076.733	309	Atlas Resort Hotel, Dalota
486006	974882	1958.8	310	Teshome Augna PLC, Dalota
485745	973864	1960	312	Dalota Keta
487992	972679	1875.58	311	Arena Dukem
481825	966272	1831.6	314	Dimtu Peasant's Village
484486	970026	1832.39	315	Oda Nabe Peasants village
475300	985080	2120	317	Kality Food Factory BH-1
475430	984955	2118	318	Kality Food Factory BH-2
488391	961066	1792	322	Dire clinic borehole
481241	958830	1782	323	Chelaba Silasie Borehole
483292	961700	1767	326	Shoki-1 village borehole
488517	966191	1805	327	Wajitu village old borehole (BH1)
488673	966156	1805	328	Wajitu village borehole (BH2)

Source:

X	Y	Z, water level meter aml	Akaki Phase II BH No.	BH owner/location Name
496138	977670	1977	329	Yerer meka Peasants village
494127	977806	2007	330	Korke peasants village
496697	974436	1875	331	Buti peasants village-BH1 old borehole
496705	974857	1870	332	Buti peasants village-BH2
499160	1009646	2533	371	Romina Dairy farm Sendafa
499700	1008450	2516	333	Merdia
493250	1012115	2561	334	Dire dam
496147	967674	1860	335	Debre-Zeit Flour and Pasta Factory BH1
496385	967764	1860	336	Debre-Zeit Flour and Pasta Factory BH2
473350	1002550	2615	338	Kuskuam St. Peter Hospital BH2
500576	974180	1870	340	Debrezeit Water Supply and Sewerage Authority BH1
501529	974064	1870	341	Debrezeit Water Supply and Sewerage Authority BH2
500903	973662	1870	342	Debrezeit Water Supply and Sewerage Authority BH3
501003	974094	1870	343	Debrezeit Water Supply and Sewerage Authority BH4
501081	974632	1870	344	Debrezeit Water Supply and Sewerage Authority BH5
500615	974742	1870	345	Debrezeit Water Supply and Sewerage Authority BH6
490331	968384	1805	346	Dukem East Africa Ethipia Plc. Factory
496270	967022	1860	348	DebreZeit steel rolling mill BH-1
475856	956602	1800	353	Sera Village
484190	998500	2434.98	355	AAWSA, Kotebe Kara
485925	1000975	2474.41	356	Day light Legedad
486000	1001115	2472.2	357	Gedera 2 Legedad
491300	1004800	2455.58	359	Legedadi, Community borehole
481700	999150	2469.42	360	Kotebe, Selam Vocational School
481650	997725	2363.21	361	Kotebe, Selam Childeren's Village
466175	1001800	2534.4	363	Asco, Black Lion Shoe Factory
465900	1002875	2584.25	364	Sansuzi, AAWSA
476750	995800	2289	372	St. Gabriel Hospital
479450	996115	2326	373	International Livestock Research Center (ILRI)
466440	1001760	2542	378	San Francisco, Asco
467150	992150	2246	387	Abune Yosef School, Alert
468650	995450	2304	397	D.H. Geda, Augusta
468650	999800	2393	398	Bingham Academy, Kolfe
464500	1003150	2584	401	Mohamed Abdo Borehole, Burayu
466550	1000150	2487	402	Micky Layland Children's Home
474600	995550	2254	403	Greece Community, Olympia Bole area
468625	996900	2330	404	Netherlands Embassy, Keranio area
468200	1001600	2532	405	Dire Tannery BH1, Gulele
468150	1001750	2585	406	Dire Tannery BH2, Gulele
469050	994450	2234	407	Ato Temesgen Chaka, Ketana Hulet area
468425	996350	2300	408	Korea Embassy, Ketana Hulet area
469280	993350	2275	409	Donbosco, Bisrate Gabriel area
468875	993750	2287	410	Hagbes PLC., Bisrate Gabriel area
470950	993300	2271	415	Indonesian Embassy, Vatican
467250	999800	2451	417	Apostlic, Tero, Kolfe
472700	999800	2476	420	Nigeria Embassy, Afinchober
476975	994500	2283	422	Bole Medihanialem Church BH2
492143	1004643	2420	R	Head in rivers
491570	1001143	2360	R	Head in rivers
486700	988500	2200	R	Head in rivers
460929	1001143	2580	R	Head in rivers
467000	997929	2340	R	Head in rivers

Source:

X	Y	Z, water level meter aml	Akaki Phase II BH No.	BH owner/location Name
467857	996714	2320	R	Head in rivers
474000	989000	2160	R	Head in rivers
472600	990250	2200	R	Head in rivers
468100	993500	2280	R	Head in rivers
473500	993500	2300	R	Head in rivers
477000	981000	2050	R	Head in rivers
470000	966300	1900	R	Head in rivers
488400	989900	2220	R	Head in rivers
483000	988700	2180	R	Head in rivers
488500	988400	2210	R	Head in rivers
480550	987800	2160	R	Head in rivers
478000	988700	2140	R	Head in rivers
476500	988050	2120	R	Head in rivers
475980	987750	2100	R	Head in rivers
506600	998300	2460	R	Head in rivers
475000	1003000	2600	R	Head in rivers
474300	1001400	2500	R	Head in rivers
460000	1004600	2600	R	Head in rivers
457600	1002800	2600	R	Head in rivers
456400	998600	2600	R	Head in rivers
458100	998100	2600	R	Head in rivers
469500	1002100	2600	R	Head in rivers
475000	1003000	2600	R	Head in rivers
490800	1014300	2600	R	Head in rivers
502800	1013800	2600	R	Head in rivers
504000	1005800	2500	R	Head in rivers
510600	1007300	2500	R	Head in rivers
492700	1009500	2500	R	Head in rivers
464400	1001000	2500	R	Head in rivers
466200	999100	2400	R	Head in rivers
489600	998500	2300	R	Head in rivers
482200	995100	2300	R	Head in rivers
489600	992600	2260	R	Head in rivers
474800	990600	2200	R	Head in rivers
482700	989700	2200	R	Head in rivers
484300	989800	2200	R	Head in rivers
495500	1002300	2400	R	Head in rivers
497500	995000	2400	R	Head in rivers
491600	1003700	2400	R	Head in rivers
491700	993100	2300	R	Head in rivers

Source:

Well Name given during drilling	Grid UTM E longitude X	Grid UTM N latitude Y	Water level Depth mBG (m.BGL)	Depth (m)	Diameter drilling (mm)	Diameter casing (mm) 25.4	Screen position (m)	Screen type	Screen Lithology	Depth (m.BGL)	Thickness (m)	Remarks
Area A												
B3	463700	988500	19.5	130	0to36m 381mm, 36to130m 250mm	152.4	49 to 72 & 84 to 107	uPVC	Weathered trachyite and weathered vesicular basalt	49 to 72 & 84 to 107	46	
B11	466200	988800	-0.6	100	0 to 15.3m 381mm, 15.3 to100m 250mm	152.4	20 to 6o	uPVC	Weathered trachyite	18 to 50	32	
B12	466400	987600	18.3	125	0 to 42 m 381mm, 42 to125m 250mm	152.4		uPVC	Weathered trachyite	68 to 86	18	
T3	464400	987600	20	93	1 to 42 m 381mm, 42 to93m 250mm	203	34 to 45 & 68 to 85	uPVC	Weathered trachyite	30 to 42 & 70 to 78	20	
Area B						1 inch : 25.4 mm						
B5A (Seureca)	481,200	980,000	11.5	150	0.0	0.0	11 to 50 62 to 74 96 to 102 125 to147	PVC	Scoria, and sand	12to50, 125 to 150	63	
T1 (Seureca)	481,200	980,000	8.9	173			161.8 to 167.5 127.8 to 150.5		Weathered scoria	161.8-167.5	5.7	
T5 (Seureca)	481,600	982,900	37.3	120	0to16m 381, 16to40m 300, 40to120m 254	203.2	46to52, 58to64, 72to114	PVC	Weathered basalt / Fractured Fresh basalt with minor scoria	77to113m	36	
B9 (Seureca)	481,600	982,900	35.1	120	0to23m 381 23to120m 203	open	casing up to 44 m, open hole below		Fractured basalt	41 to 67 m, 69-73 m	27	
B13 (Seureca)	479,400	981,400	2.7	100	0.0	0.0	19.6 to 54.1	PVC	Vesicular basalt, Weathered scoria and Weathered vesicular basalt	14 to 25,25 to 36, 36 to 55	41	
B14 (Seureca)	480,900	978,800	86.0	160	0.0	0.0	119.8 to 154.3	PVC	Basalt fissures	119.8 to 154.3	34.5	
T2 (Seureca)	479,400	981,400	2.8	74	254.0	152.4	16 to 52	steel	Heavily fractured vesicular basalt	16 to 52	36	
EP-1	479,340	981,400	1.48	108.7	0to4 635 4to20m 508 20to71m 381 71to108m 254	0to71m 305, 71to108m 152.4	28to46m , 53to108m 152.5	steel	Fractured fresh an weathered visicular basalt with minor scoria cones	30to36m,78to81 m, 87to93m	25	This well is located 55m an 76m west of B13 and T2 respectively.
EP-2	481,600	982,850	34.4	136	0to144 m 482.6 14to69m 381 69to136m 254	0to 69.9m 254, 69.9to 136m 152.4	51.4 to 57.4, 84.6to91.6m, 99.3to128.6	steel	fractured vesicular basalt	34to52m, 80to87m, 95to130m	50	This well is located 455m an 77m south of B9 and T5 respectively.
EP-3	479,740	981,400	4.94	126		0 to 79 m 304.8 79 to 120 m 152.4	30 to 36, 42 to 48 m, 55 to 73 m, 92 to 100 m		Vesicular & Weathered basalt	see the screen position	38	
EP-5	478,450	979,950	55.82	102	0 to 6 m 381 mm 6 to 102 m 254 mm	177.8	60 to 72 m, 79 to 97 m.	PVC 7	Red and dark scoria	60 to 92 m	32	
Area C												
B6 (Seureca)	470,800	982,900	+0.56	114	0.0	open	open hole	open hole	Weathered and fractured basalt	50 to 62 78 to 81 83 to 84	16	
B7 (Seureca)	473,800	978,400	22.48	122	380 to 24 m 203.2 from 24 to 122 m	0	31 to 48 62 to 77	PVC	Scoria	63 to 78	15	
B15 (Seureca)	473,200	979,800	6.32	113	381 to 65 m 203.2 from 65 to 113 m	0	62 to 113	PVC	Scoria and weathered basalts	62 to 64 85 to 90 95 to 111	23	
T4 (Seureca)	473,200	979,800	7.6	103	0.0	0	74 to 99	PVC	Scoria	82 to 91	9	
Area D												
BH01	**477,972.857**	**974,859.574**	58.5	133	609.6 to 24.8 444.5 from 24.8 to 90 m 304.8 from 90 to 133 m	355.6 from- 0.85 to 90 m 203 from 90 m to 133 m	69.05 to 80.65 and 94.03 to 111.43	Steel casings/Johnson's stainless steel screen	Scoria and fractured basalt	78 to 90 and 90 to 105	27	
BH02	**478,399.737**	**975,589.689**	52.6	122	609.6 to 27.8 444.5 from 27.8 to 90 m 304.8 from 90 to 122 m	355.6 from -0.7 to 90 m 203 from 90 m to 122 m	63.85 to 75.45 and 90.54 to 107.97	Steel casings/Johnson's stainless steel screen	Scoria	62 to 76 and 102 to 110	22	
BH-03a (Abandoned)	**480,517.697**	**977,974.648**	-	169.53	609.6 from 0 to 1 & 444.5 from 1 to 116 m 304.8 from 116 to 170.5 m	355.6 from 0 to 106 m 203.2 from 106 m to 160.4 m	70.93 to 82.53 and 132.13 to 155.33	Steel casings/Johnson's stainless steel screen	Scoria	59.5 to 95.5, 110 to 120, 133 to 141, 147 to 165.	72	The *aquifers depth* are chosen from the E log curve/lithological log. The permeabilities of the formations are bad.
BH-03b	**478,713.309**	**974,977.481**	63.11	130	609.6 0 to 24 444.5 from 24 to 90 m 304.8 from 90 to 130 m	355.6 from -0.7 to 90 m 203.2 from 90 m to 130 m	63.85 to 75.45 and 101.06 to 119	Steel casings/Johnson's stainless steel screen	Scoria/massive basalt & Scoria/weathered volcanic rock	64-75 and 112-117	16	The aquifers depth are chosen from the E-log curve/lithological log. The loc. of water aquifers (pump test
BH-04	**477,992.754**	**975,552.803**	**47.9**	125.83	609.6 0 to 1.9 from 1.9 to 90 m 444.5 from 90 to 132 m 304.8	355.6 from -0.7 to 90 m 203.2 from 90 m to 132 m	355.6 from 61.5 to 76.7m 203.2 from 96.6m to 119.8m	Steel casings/Johnson's stainless steel screen	Scoria/Scoriaceous basalt/weathered and fractured basalt	63 to 78m and 104 and115m	26	
BH-05a (Abandoned)	**479,762.535**	**977,855.751**	about 50m	168.9	609.6 0 to 7.3 from 7.3 to 168.9m 228.6	No casing	-	-	Fractured basalt, Scoria an Beaked volcanic rock	60 to 66.5m, 105 to108m, 121.5 to 130, 139 to 148, 152 to 165m	39	Due to low yiel it was abanone as dry well
		975,607.028			609.6 0 to 28.5 from 28.5 to 90m 444.5, from 90m to 142	355.6 from -0.85 to 90 m 203.2 from 90 m to	75.26 to 88.86 and	Steel casings/Johnson's stainless steel	Scoria/Scoriaceous basalt/weathered and	See litholog, SP		

Well Name given during drilling	Grid UTM E longitude X	Grid UTM N latitude Y	Water level Depth mBG (m.BGL)	Depth (m)	Diameter drilling (mm)	Diameter casing (mm) 25.4	Screen position (m)	Screen type	Screen Lithology	Depth (m.BGL)	Thickness (m)	Remarks
BH-05b	**476,574.831**		48.85	142	304.8	133 m	90.54 to 107.94	screen	fractured basalt	and R log		
BH-06	**479,696.660**	**976,936.535**	*67.82*	145.53	609.6 0 to 6.8 from 6.8 to 105.92m 444.5, from105.92m to 145.3 304.8	355.6 from-0.3 to 97.55 m 203.2 from 97.55 m to 136.11 m	75.03 to 80.83 and 110.68 to 133.88	Steel casings/Johnson's stainless steel screen	Scoria/Scoriaceous basalt	75.03 to 82.5m, 103.7 to143.5	47.3	
BH-07	**479,405.708**	**976,735.015**	**67.42**	151	609.6 0 to 6 from 6 to 97m 444.5, from 97m to 151m 304.8	355.6 from-0.62 to 96.7m 203.2 from 96.7m to 150.5m	79.18 to 84.98 and 124.27 to 147.47	Steel casings/Johnson's stainless steel screen	Scoria/Scoriaceous basalt/weathered and fractured basalt	70 to 88.5m, 1114.5 to118.5, 121.5 to 150	51	
BH-08	**479,061.557**	**976,370.799**	67.2	144.18	609.6 0 to 15.4 from 15.4 to 103m 444.5, from 103m to 144.18m 304.8	355.6 from 0.00 to 102.32m 203.2 from 102.32m to 143.68m	83.87 to 95.47 and 112.15 to 141.15m	Steel casings/Johnson's stainless steel screen	Scoria/Scoriaceous basalt/weathered and fractured basalt	70m to 94m, 110.5 to 125, 135 to 141	45	
BH-09	**479,246.528**	**977,104.643**	58.7	146.38	609.6 0 to 14.2 from 14.2 to 90m 444.5, from 90m to 146.38m 304.8	355.6 from -0.26 to 89.7m 203.2 from 89.7m to 145.5m	78.61 to 84.41 and 113.97 to 142.97m	Steel casings/Johnson's stainless steel screen	Scoria/Scoriaceous basalt/weathered and fractured basalt	76.61m to 84.41m, 113.97 to 142.97	34.8	
BH-10	**479,058.958**	**976,020.107**	72.3	130	609mm 0 to 7m from 7 to 92m 444.5, from 92m to 130m 304.8	355.6 from -0.7 to 92m 203.2 from 92m to 129m	76.4 to 88 and 93.47 to 122.47m	Steel casings/Johnson's stainless steel screen	Scoria/Scoriaceous basalt/weathered and fractured basalt	75m to 110m, 117 to 125	43	
BH-11-2	**478,780.537**	**977,307.579**	61.14	138	609mm.0 to 28.1m from 28.1m to 86m 444.5, from 86m to 138m 304.8	355.6 from -0.75 to 83m 203.2 from 83m to 137m	66.12 to 77.72 and 96.04 to 130.84m	Steel casings/Johnson's stainless steel screen	Scoria/Scoriaceous basalt/weathered and fractured basalt	64.5m to 84.5m, 103 to 106, 111.5 to 134	45.5	
BH-12	**478,808.328**	**976,867.470**	51.53	152.4	609mm.0 to 9.2m from 9.2m to 95m 444.5, from 95m to 152.4m 304.8	355.6 from -0.91 to 94.7m 203.2 from 94.7m to 151.8m	53 to 82.33 and 126.27 to 149.47m	Steel casings/Johnson's stainless steel screen	Scoria/Scoriaceous basalt/weathered and fractured basalt	54m to 82m, 104 to 106, 117.5 to 122.5, 127.5 to 132, 139.5 to 149.5	49.5	
BH-13	**478,694.864**	**976,490.552**	**51.17**	149	609mm.0 to 17.5m from 17.5m to 100m 444.5, from 100m to 149m 304.8	355.6 from -0.30 to 70.41m 203.2 from 70.41m to 118.71m	47.26 to 58.86 and 92.87 to 116.18m	Steel casings/Johnson's stainless steel screen	Scoria/Scoriaceousbasalt/weathered and fractured basalt , tuff	37.5m to 57.5m, 78 to 102, 116 to 148m	76	The water level in this well is strange and probably there is problem with the well
BH-14	**478,580.608**	**976,051.679**	59.18	130	609mm.0 to 10m from 10m to 105m 444.5, from 105m to 130m 304.8	355.6 from -0.81 to 104.4m 203.2 from 104.4m to 128.46m	78.53 to 90.13 and 110.53 to 122.13m	Steel casings/Johnson's stainless steel screen	Scoria/Scoriaceous basalt/weathered and fractured basalt	65m to 70m, 75 to 105, 109 to 115m, 124 to 126m	43	
BH-16	**478,347.234**	**976,752.673**	**47.98**	148.56	609mm.0 to 20.02m from 20.02m to 92m 444.5, from 92m to 148.56m 304.8	355.6 from -0.76 to 92m 203.2 from92m to 148.26m	78.27 to 84.04 and 92.53 to 114.73m	Steel casings/Johnson's stainless steel screen	Scoria/Scoriaceous basalt/weathered and fractured basalt	71.5m to 74m, 81 to 84, 92.5 to 106m, 110 to 119m, 124 to 148m	52	
BH-17	**478,199.176**	**976,361.674**	45.94	144.18	609mm.0 to 15.4m from 15.4m to 103m 444.5, from 103m to 144.18m 304.8	355.6 from 0.0 to 94m 203.2 from 94m to 141.5m	77.4 to 89m and 108.47 to 137.47m	Steel casings/Johnson's stainless steel screen	Scoria/Scoriaceous basalt/weathered and fractured basalt	68m to 89m, 117 to 119, 126 to 137m	34	
BH-18	**478,154.375**	**975,966.371**	54.08	140	609mm.0 to 19.4m from 19.4m to 106m 444.5, from 106m to 140m 304.8	355.6 from 0.0 to 106m 203.2 from 106m to 140m	82.6 to 100m and 108.47 to 137.47m	Steel casings/Johnson's stainless steel screen	Scoria/Scoriaceous basalt/weathered and fractured basalt	64m to 106m, 113 to 118, 126 to 128m, 136 to 138m	51	
BH-19	**478,019.429**	**977,482.170**	51.45	150.15	609mm.0 to 19m from 19m to 93m 444.5, from 93m to 150.15m 304.8	355.6 from -0.75 to 93m 203.2 from 93m to 150m	71.94 to 83.54m and 103.4 to 144m	Steel casings/Johnson's stainless steel screen	Scoria/Scoriaceous basalt/weathered and fractured basalt	57m to 61m, 67 to 70, 73 to 76m, 78 to 85, 95 to 106, 112 to 128, 130 to 144	58	
BH-20	**477,945.037**	**976,985.086**	**50.05**	148.6	609mm.0 to 18.5m from 18.5m to 93m 444.5, from 93m to 148.6m 304.8	355.6 from -0.75 to 93m 203.2 from 93m to 148m	73.22 to 84.82m and 101.34 to 141.94m	Steel casings/Johnson's stainless steel screen	Scoria/Scoriaceous basalt/weathered and fractured basalt	75m to 82m, 94 to 121, 126 to 148m	56	
BH-21	**477,856.365**	**976,402.405**	44.68	151	609mm. 0 to 11.5m from 11.5m to 93m 444.5, from 93m to 151m 304.8	355.6 from -0.75 to 92.7m 203.2 from 92.7m to 150m	71.07 to 88.47m and 108.13 to 125m, 134.34 to 146.49m	Steel casings/Johnson's stainless steel screen	Scoria/Scoriaceous basalt/weathered and fractured basalt	76m to 88m, 99 to 100, 105 to 106m, 111 to 113m, 119 to 125m, 132 to 150m	40	
BH-22	**477,651.572**	**975,923.577**	**47.9**	142	609mm. 0 to 11.1m from 11.1m to 93m 444.5, from 93m to 142m 304.8	355.6 from -0.80 to 80m 203.2 from 80m to 141m	58.6 to 76m, 95.87 to 107.47m, 109.4 to 121m, 125.87 to 137.47m	Steel casings/Johnson's stainless steel screen	Scoria/Scoriaceous basalt/weathered and fractured basalt	58.6m to 76m, 95 to 107, 113 to 117m, 124 to 138m	47	

Well Name given during drilling	Grid UTM E longitude X	Grid UTM N latitude Y	Water level Depth mBG (m.BGL)	Depth (m)	Diameter drilling (mm)	Diameter casing (mm) 25.4	Screen position (m)	Screen type	Screen Lithology	Depth (m.BGL)	Thickness (m)	Remarks
BH-23	**477,477.480**	**977,216.975**	**45.02**	145	609mm. 0 to 14.8m from 14.8m to 92.5m 444.5, from 92.5m to 145m 304.8	355.6 from -0.80 to 92.1m 203.2 from 92.1m to 144.5m	68.91 to 80.51m, 103.64 to 138.44m	Steel casings/Johnson's stainless steel screen	Scoria/Scoriaceous basalt/weathered and fractured basalt	51 to 70m, 86 to 89, 96 to 108m, 113 to 130m	51	
BH-24	**477,330.427**	**976,793.113**	**42.92**	130	609mm. 0 to 14.8m from 14.8m to 90m 444.5, from 90m to 130m 304.8	355.6 from -0.80 to 90m 203.2 from 90m to 130m	62.96 to 74.56m, 100.73 to 123.93m	Steel casings/Johnson's stainless steel screen	Scoria/Scoriaceous basalt/weathered and fractured basalt	59 to 75m, 97.5 to 104m, 113 to 119m	28	
BH-25-2	**477,162.775**	**976,038.564**	**41.92**	135	609mm. 0 to 11.1m from 11.1m to 90m 444.5, from 90m to 135m 304.8	355.6 from -0.83 to 89.3m 203.2 from 89.3m to 134m	80 to 85.8m, 94.67 to 129.47m	Steel casings/Johnson's stainless steel screen	Scoria/Scoriaceous basalt/weathered and fractured basalt	80 to 95m, 99 to 132m	48	
BH-26	**477,181.545**	**975,680.606**	**50.95**	116.68	609mm. 0 to 12.5m from 12.5m to 85m 444.5, from 85m to 116.68m 304.8	355.6 from -0.69 to 81.78m 203.2 from 81.78m to 113.21m	57.48 to 69.08m, 85.35 to 108.55m	Steel casings/Johnson's stainless steel screen	Scoria/Scoriaceous basalt/weathered and fractured basalt	60 to 72m, 78 to 82m, 93 to 112m	33	
MW01A	**476,451.224**	**976,951.337**		-								Observation well 1 abandoned
MW01B	**476,454.104**	**976,951.735**	42.6	129	304.8mm. 0 to 10.5m from 10.5m to129m 254mm	152.4	80 to 86m, 104 to 128m	uPVC	Tuff and Scoria			
MW02	**476,523.053**	**976,374.826**	36.15	60	304.8mm. 0 to 6m from 6m to129m 254mm	152.4	39 to 51	uPVC	Scoria			
MW03	**476,972.320**	**976,152.504**	41	120	304.8mm. 0 to 6m, from 6m to 66m 254mm, from 66m to 120m 203.2mm	152.4	46 to 58m, 64 to 100m	uPVC	Scoria//weathered and fractured basalt			
MW04	**477,185.550**	**975,729.161**	47	114	304.8mm. 0 to 6m from 6m to114m 254mm	152.4	34 to 46m, 64 to 70m, and 82 to 94	uPVC	Scoria//weathered and fractured basalt			
EP-4	479,942.431	977,322.013	64.44	120	482.6 mm. 0 to 4.65 m, from 4.65 to 120 m 381 mm.	254	75 to 91 m, 96 to 114 m	Steel	Dark and red Scoria	64 to 118 m	54	
EP-6	479,526.295	977,468.339	71.7	129	609.6 mm. 0 to 11.5 m, from 11.5 to 97m 444.5 mm, from 97 to 129 m 317.5 mm.	355.6 mm. 0 to 97 m, from97 to 129 203.2 mm.	85 to 97m,114 to 127 m	Stainless steel Johnson screens	-	-	-	-
EP-7	479021.149	977596.019	66.12	126	609.6 mm. 0 to 11.5 m, from 11.5 to 97m 444.5 mm, from 97 to 129 m 317.5 mm.	355.6 mm. 0 to 96.84 m, from 96.84 to 125.6 203.2 mm.	99.07 to 122.67 m.	Stainless steel Johnson screens	Scoria		-	-
EP-8	478,998.569	977,937.935	73.48	130	609.6 mm. 0 to 12 m, from 12 to 97m 444.5 mm, from 97 to 130 m 317.5 mm.	355.6 mm. 0 to 96.20 m, from 96.84 to 128.3 203.2 mm.	86 to 92m,96 to 102m, and 110 to 127	stainless stell well screens	Scoria/ and fractured basalt	86 to 130	44	
Low yield areas												
B1	488600	1001027	15	125	0to24m 381mm, 24 to125m 250mm	152	26 to 49m,95 to 112	uPVC	ignimbrite & basalt	26 to 49 & 95 to 112	40	
B2	464000	997000	50.7	100	0to2m 300mm, 2 to100m 250mm	Open hole			Fissured basalt			
B8	487300	995300	22	120	0 to 67m 381mm, 67 to120m 250mm	152	62 to 74 & 102 to 118	uPVC	Weathered rhyolite	67 to 118	51	Very low yield less than 0.5 l/s
B4	486200	1001042	10	100	0 to 1.7m 300mm, 1.7 to100m 200mm	152	13 to 31 & 65 to 71 & 82 to 94	uPVC	Weathered basalt	10 to 28 & 83 to 94	29	low yield 2 l/s
B10	461500	1001023	82	110	1 to 8m 300mm, 8 to100m 200mm	152	52 to 64 & 75 to 85	uPVC	Weathered basalt & ignimbrite	52 to 64 & 75 to 85	22	low yield 2 l/s

Suereca Code	AAWSA Code	Akaki groundwater Phase II	Well Location name	X	Y	Water level (m) aMSL	Transmissivity (m2/day)	Transmissivity (m2/S)
9		9	Glass and bottle factory	467200	1001017	2482	2.7	3.13E-05
43	4	43	Ethio- Plastic Factory	479200	996700	2248	1.18	1.37E-05
47		47	Hilton Hotel	473800	996600	2363	4	4.63E-05
73		73	Addis Abeba Brewery-8	471300	995800	2337	3347	3.87E-02
90		90	Hana Mariam-2	471700	986600	2194	0.4	4.63E-06
91		91	Anbessa Transport (Shegole)	471200	995700		0.26	3.01E-06
106	119	106	Anbessa Transport (Diabaco)	471200	993700	2277	0.26	3.01E-06
130		130	Adey Abebe Cotton Mill-2	473700	990000	2195	5	5.79E-05
142		142	National Road Transport Corp	475000	987800	2124	1.45	1.68E-05
144		144	Ethio-Meat Concentrete Factory	473500	987600	2155	25.57	2.96E-04
145		145	Ethio-Spice Extraction	473300	987700		25.7472	2.98E-04
146		146	WWDA Ware house	473300	987300	2145	3.7	4.28E-05
152		152	Meher Fiber Factory-1	475662.3	980783.8		23	2.66E-04
162		162	Galetti Project	474800	984700	2140.41	32	3.70E-04
166		166	Akaki Metal Products Factory-4	477446.3	978851.2	2020.24	20.04	2.32E-04
167		167	Akaki Metal Products Factory-1	477232.6	978999.8	2021.14	45.27	5.24E-04
173		173	Kality Military Camp-1	475300	983800	2122	49.77	5.76E-04
174		174	Kality Military Camp-2	475300	984000	2110	22.29	2.58E-04
203		203	AAWSA-1 Near Defence Industry	471800	994800	2312	28.5	3.30E-04
204		204	Military Orphanage				1.5	1.74E-05
205		205	Awash Winnery-2				5760	6.67E-02
206		206	Ministry of Defence	472700	996500	2537	0.7	8.10E-06
210		210	Old Airpor-2	470500	994500	2278	32.7	3.78E-04
211		211	Gulele Glass-Factory-3	466900	1001005	2497	1.3	1.50E-05
215/1		215	NMWC Spare Parts & Hand Tools Factory-1	478462.8	977721.59	2020.47	6099.84	7.06E-02
216		216	NMWC Pump Factory	477608.9	978689.7	2019.6	52.96	6.13E-04
217		217	Kality Metal Products Factory	474225	982650	2104.8	2.76	3.19E-05
219		219	Artificial Insemination	475300	983800		30.4	3.52E-04
223		223	Meta Abo Brewery	455500	985200	2149	9.9	1.15E-04
227		227	Sidamo Awash Village	479819.84	977155.55	2018.47	7900	9.14E-02
229		229	Abay Mesk Soft Drinks-3	473000	992700	2268	150.5	1.74E-03
231/1		231/1	Ethiopian Iron And Steel Faoundry	476427	980749.4	2053.33	75.3	8.72E-04
231/2		231/2	Ethiopian Iron And Steel Faoundry	476430	980669.2	2052.95	109	1.26E-03

Source:
BCEOM SUERECA Joint Venture in association with Tropics Consulting Engineers PLC.

Suereca Code	AAWSA Code	Akaki groundwater Phase II	Well Location name	X	Y	Water level (m) aMSL	Transmissivity (m2/day)	Transmissivity (m2/S)
242	233	242	Tatek Tor Sefer-3	457000	1001005	2609	44.9	5.20E-04
244		244	Tatek Tor Sefer-5	456900	1001012	2615	16.4	1.90E-04
246		246	Abay Mesk Soft Drinks-4	473000	992700	2182	34.6	4.00E-04
248		248	Water III Testwell-B1	488600	1001027	2454	5	5.79E-05
249		249	Water III Testwell-B2	464000	997000	2429	0.5	5.79E-06
250		250	Water III Testwell-B3	463700	988500	2261	95	1.10E-03
251		251	Water III Testwell-B4	486200	1001042	2440	4	4.63E-05
252		252	Water III Testwell-B5	481200	980000	2139	18	2.08E-04
253		253	Water III Testwell-B6	470800	982900	2095.77	19	2.20E-04
254		254	Water III Testwell-B7	473566	978610	2040.325	95	1.10E-03
255		255	Water III Testwell-B8	487300	995300	2262	7	8.10E-05
256		256	Water III Testwell-B9	481600	982900	2174.9	820	9.49E-03
257		257	Water III Testwell-B10	461500	1001023	2548	5	5.79E-05
		258	Water III Testwell-B11	466200	988800	2246	11	1.27E-04
		259	Water III Testwell-B12	466400	987600	2234.5	70	8.10E-04
		260	Water III Testwell-T1	481200	980000	2141.9	33	3.82E-04
		261	Water III Testwell-T5	481600	982900	2175.3	50	5.79E-04
		262	Water III Testwell-B13	479400	981400	2130.7	550	6.37E-03
		263	Water III Testwell-B14	480900	978800	2040.4	210	2.43E-03
		264	Water III Testwell-T2	479400	981400	2130.7	520	6.02E-03
		265	Akaki Water Supply Test Well EP-1	479340	981400	2130.6	478	5.53E-03
		267	Akaki Water Supply Test Well EP-3	479740	981400	2130.5	317.4552	3.67E-03
		268	Water III Testwell-B15	473069	979881	2051.6	30	3.47E-04
		269	Water III Testwell-T4	473108	979851	2051.27	117	1.35E-03
		270	Water III Borehole BH03b	478713	974977	2019.7	15552	1.80E-01
		274	Water III Borehole BH04	477992	975552	2019.2	9100.8	1.05E-01
		275	Water III Borehole BH05b	476574	975607	2019.5	11923.2	1.38E-01
		276	Water III Borehole BH06	479696	976936	2019.6	105408	1.22E+00
		277	Water III Borehole BH07	479405	976735	2019.4	43700	5.06E-01
		278	Water III Borehole BH08	479061	976370	2019.4	49600	5.74E-01
		282	Water III Borehole BH12	478808	976867	2019.2	28100	3.25E-01
		284	Water III Borehole BH14	478580	976051	2019.6	25600	2.96E-01
		286	Water III Borehole BH17	478199	976361	2019.5	55738	6.45E-01

Source:
BCEOM SUERECA Joint Venture in association with Tropics Consulting Engineers PLC.

Suereca Code	AAWSA Code	Akaki groundwater Phase II	Well Location name	X	Y	Water level (m) aMSL	Transmissivity (m2/day)	Transmissivity (m2/S)
		289	Water III Borehole BH20	477945	976985	2019.5	2272.32	2.63E-02
		292	Water III Borehole BH23	477477	977216	2020.6	10791.36	1.25E-01
		293	Water III Borehole BH24	477330	976793	2018.6	4631.04	5.36E-02
		294	Water III Borehole BH25-2	477162	976038	2019.7	43372.8	5.02E-01
		295	Water III Borehole BH26	477181	975680	2019.6	98800	1.14E+00
		300	Akaki Water Supply Test Well EP-4	479942	977322	2025.43	2480.914286	2.87E-02
		301	Akaki Water Supply Test Well EP-5	478450	979950	2044.2	5287.68	6.12E-02
		302	Akaki Water Supply Test Well EP-6	479526	977468	2022.35	1833.84	2.12E-02
		304	Akaki Water Supply Test Well EP-8	478998	977937	2018.03	2995.2	3.47E-02
		311	Arena Dukem	487992	972679	1875.58	86.4	1.00E-03
		317	Kality Food Factory BH-1	475300	985080	2120	158.5	1.83E-03
		318	Kality Food Factory BH-2	475430	984955	2118	381.888	4.42E-03
		323	Chelaba Silasie Borehole	481241	958830	1782	153	1.77E-03
		325	Shoki-1 village borehole	483292	961700	1767	61	7.06E-04

Source:

Declaration

I, the under signed, declare that this thesis is my own work and that all sources of material used for the thesis have been dully acknowledged.

Name: Jemal Seid

Signature: _____

Place and date of submission,

Nov., 2009, Addis Ababa.